The Role of eIF4E/4E-BP2-dependent Translation in Epileptic Seizure

Danning Lou

Department of Biochemistry

McGill University, Montreal

2022

A thesis submitted to McGill University in partial fulfillment of the requirements of the degree Master of Science

Table of Contents

List of Abbreviations

Numerical	4E-BP	Eukaryotic translation initiation factor 4E-binding protein
	5’ UTR	5’ untranslated region
A	AD	Alzheimer’s disease
	ADP	Adenosine diphosphate
	AED	Antiepileptic drug
	Akt	Protein kinase B
	AMP	Adenosine monophosphate
	AMPK	AMP-activated serine/threonine kinase
	A-site	Aminoacyl site
	ASD	Autism spectrum disorder
	ATP	Adenosine triphosphate
C	Ca^{2+}	Calcium ion
	CA1	Cornu Ammonis 1
	CAMKII	Ca^{2+}/calmodulin-dependent protein kinase II
	cKO	Conditional knockout
	CNS	Central nervous system
	CT	Computed tomography
D	DAPI	4′,6-diamidino-2-phenylindole
	DEPTOR	DEP domain-containing mTOR-interacting protein
	DEPDC5	DEP domain-containing protein 5
	DG	Dentate gyrus
	DNA	Deoxyribonucleic acid
E	E	Excitation
	EEG	Electroencephalogram
	eEF1A	Eukaryotic translation elongation factor 1A
	eEF2	Eukaryotic translation elongation factor 2
	eIF1	Eukaryotic translation initiation factor 1
	eIF1A	Eukaryotic translation initiation factor 1A
	eIF2	Eukaryotic translation initiation factor 2
	eIF2B	Eukaryotic translation initiation factor 2B
	eIF2α	Eukaryotic translation initiation factor 2 alpha subunit
	eIF3	Eukaryotic translation initiation factor 3
	eIF4A	Eukaryotic translation initiation factor 4A
	eIF4E	Eukaryotic translation initiation factor 4E
	eIF4F	Eukaryotic translation initiation factor 4F
	eIF4G	Eukaryotic translation initiation factor 4G
	eIF5	Eukaryotic translation initiation factor 5
	eRF1	Eukaryotic translation releasing factor 1

	eRF3	Eukaryotic translation releasing factor 3
	ERK	Extracellular-signal regulated kinase
	eNSC	Embryonic neural stem cells
F	FCD	Focal cortical dysplasia
	FXS	Fragile X syndrome
G	GABA	ɣ-Aminobutyric acid
	GAD	Glutamate decarboxylase
	GAP	GTPase-activating protein
	GATOR	GAP activity towards rags complex
	GβL	Mammalian lethal with SEC13 protein 8
	GDP	Guanosine diphosphate
	GFAP	Glial-fibrillary acidic protein
	GPCR	G-protein coupled receptors
	GTP	Guanosine triphosphate
I	I	Inhibition
	IP	Intraperitoneal
J	JAK	Janus kinase
K	KA	Kainic acid
	KO	Knockout
L	LKB1	Liver kinase B1
	LTD	Long-term depression
	LTP	Long-term potentiation
M	MAPK	MAP-kinase Mitogen-activated protein kinase
	Met-tRNA$_i^{Met}$	Initiator tRNA
	MLST8	Mammalian lethal with SEC13 protein 8
	MRI	Magnetic resonance imaging
	mRNA	Messenger RNA
	mTOR	Mechanistic target of rapamycin
	mTORC1/2	Mechanistic target of rapamycin complex 1/2
N	NSC	Neural stem cell
	Nkx2.1	NK2 homeobox 1/thyroid transcription factor 1
	NPC	Neural progenitor cell

	NPRL2/3	Nitrogen permease regulator protein 2 and 3
O	ORF	Open reading frame
P	PABP	Poly(A)-binding protein
	PCR	Polymerase chain reaction
	PD	Parkinson's disease
	PDK1	Phosphoinositide-dependent kinase 1
	PI3K	Phosphatidylinositol 3-kinase
	PIC	Preinitiation complex
	PNN	Perineuronal net
	PRAS40	Proline-rich AKT1 substrate of 40 kDa
	P-site	Peptidyl site
	PSD95	Postsynaptic density protein 95
	PTEN	Phosphatase and tensin homolog
	PTZ	Pentylenetetrazol
	PVALB	Parvalbumin
R	Raptor	Regulatory-associated protein of mTOR
	Rheb	Ras homolog enriched in the brain
	RNA	Ribonucleic acid
	RTK	Receptor tyrosine kinase
S	S6	p70-S6
	S6K	p70-S6 kinase
	SEM	Standard error of mean
	shRNA	Short hairpin RNA
	SNAP25	Synaptosomal-associated protein 25kDA
	SST	Somatostatin
	STAT	Signal transducer and activator of transcription
T	TAC	Transit-amplifying cell
	TBI	Traumatic brain injuries
	TC	Ternary complex
	TLE	Temporal lobe epilepsy
	TOR	Target of rapamycin
	tRNA	Transfer RNA
	TSC1/2	Tuberous Sclerosis Complex 1/2
V	VGAT	Vesicular GABA transporter
	VIP	Vasoactive intestinal peptide

W	WFA	Wisteria floribunda agglutinin
	WHO	World Health Organization
	WT	Wild type

List of Figures

List of Tables

Abstract

In the central nervous system (CNS), gene expression is tightly controlled spatiotemporally for proper brain development and homeostasis. The mammalian/mechanistic target of rapamycin complex 1 (mTORC1) is a major nexus that integrates upstream cellular and environmental signals to regulate cellular processes such as protein synthesis by targeting the eukaryotic translation initiation factor 4E-binding proteins (4E-BPs). Upon phosphorylation (or inactivation) by mTOR, 4E-BPs release eukaryotic translation initiation factor 4E (eIF4E), allowing it to initiate cap-dependent translation of messenger RNAs (mRNAs). Mutations that lead to hyperactivate mTORC1 signaling are commonly associated with the pathophysiology of epilepsy in both human patients and animal models.

However, the specific 4E-BP paralog and the neuronal subtype mediating the epileptogenic effect of mTORC1-dependent translation need to be uncovered. Moreover, the mechanistic link between mTORC1 and neuronal circuitry in the development of epilepsy needs to be investigated to understand the disease progression. There are three 4E-BP homologs in the mammalian brain, 4E-BP1, 4E-BP2, and 4E-BP3. Therefore, we first used triple knockout mice in which all three paralogs of 4E-BPs were deleted (*Eif4Ebp*$^{-/-/-}$) and induced seizures using three different dosages of pentylenetetrazol (PTZ) (50, 60, and 70 mg/kg). We found that 70 mg/kg of PTZ exhibited a significantly earlier onset towards generalized seizure, increased cumulative duration of seizure episodes, and higher mortality rates in *Eif4Ebp*$^{-/-/-}$ mice. Next, to identify the 4E-BP paralog which mediates this effect, we induced seizures in mice lacking 4E-BP1 (*Eif4Ebp1*$^{-/-}$) or 4E-BP2 paralog (*Eif4Ebp2*$^{-/-}$) (4E-BP3 is not detected in the brain) and observed that the loss of 4E-BP2, but not 4E-BP1, lowered the threshold to PTZ- and kainic acid (KA)-induced seizure in mice. Next, to identify the neuronal type in which 4E-BP2 deletion lowered the seizure threshold, we generated mouse lines with conditional knockout of 4E-BP2 in the excitatory or inhibitory neuron. We observed that the sensitivity to PTZ-induction was increased in mice lacking 4E-BP2 in inhibitory neurons but not excitatory neurons. We further dissected the subtypes of inhibitory neurons in which 4E-BP2 deletion promotes epileptic seizures, and we found that the deletion of 4E-BP2 in parvalbumin (PVALB^{+}) neurons (cKO^{Pvalb}), but not somatostatin (SST^{+}) or vasoactive intestinal protein (VIP^{+}) neurons, resulted in increased susceptibility to PTZ- and KA-induced seizures. Then to confirm the essential role of PVALB^{+} neurons in epilepsy, we generated mice carrying a human *PIK3CA* hyperactivation mutation selectively in PVALB^{+}

neurons (*Pik3ca*$^{H1047R\text{-}Pvalb}$). PI3K protein is located upstream in the mTORC1 signaling pathway, and its activation triggers the serial activation of downstream proteins and eventually mTOR. We observed an increased seizure severity in those mutant mice upon PTZ-induction. Next, we examined phenotypic changes at cellular and tissue levels between wild type, cKO^{Pvalb}, and *Pik3ca*$^{H1047R\text{-}Pvalb}$ mice. Perineuronal net (PNN) is a characteristic extracellular matrix expressed in mature PVALB^{+} neurons to regulate synapse formation and protect cells from oxidative stress. We detected a concomitant reduction of the PVALB^{+} neuron population and increased PNN density in the CA1 region of the hippocampus in cKO^{Pvalb} and *Pik3ca*$^{H1047R\text{-}Pvalb}$ mutants. Furthermore, in these mice, we found alterations in the expressions of synaptic markers in the hippocampus due to 4E-BP2 deletion or *PIK3CA* hyperactivation in PVALB^{+} neurons. These changes could account for the shift in excitatory/inhibitory (E/I) balance that ultimately leads to the epileptogenesis and propagation of seizures.

Collectively, our study demonstrates that the increased mTORC1 activity in 4E-BP2 knockout mice, particularly in PVALB^{+} neurons, contributes to the pathophysiology of epilepsy. These results highlight the importance of eIF4E-dependent translation as a potential therapeutic target in the treatment of epilepsy.

Résumé

Dans le système nerveux central (SNC), l'expression des gènes est étroitement contrôlée spatio-temporellement pour un développement cérébral et une homéostasie appropriés. La cible mammifère/mécaniste du complexe de rapamycine 1 (mTORC1) est un lien majeur qui intègre les signaux cellulaires et environnementaux en amont pour réguler les processus cellulaires tels que la synthèse des protéines, en ciblant les protéines eucaryotes du facteur d'initiation de la traduction 4E (4E-BP). Lors de la phosphorylation (ou de l'inactivation) par mTOR, les 4E-BP libèrent le facteur d'initiation de la traduction eucaryote 4E (eIF4E), lui permettant d'initier la traduction dépendante de la coiffe des ARN messagers (ARNm). Les mutations qui conduisent à l'hyperactivation de la signalisation mTORC1 sont couramment associées à la physiopathologie de l'épilepsie chez les patients humains et les modèles animaux.

Cependant, le paralogue spécifique de 4E-BP et le sous-type neuronal médiant l'effet épileptogène de la traduction dépendante de mTORC1 doivent être découverts. De plus, le lien mécaniste entre mTORC1 et les circuits neuronaux dans le développement de l'épilepsie doivent être étudiés pour comprendre la progression de la maladie. Il existe trois homologues de 4E-BP dans le cerveau des mammifères, 4E-BP1, 4E-BP2 et 4E-BP3. Par conséquent, nous avons d'abord utilisé des souris triple knock-out dans lesquelles les trois paralogues de 4E-BP sont supprimés (*Eif4Ebp*$^{-/-/-}$) et induit des convulsions en utilisant trois dosages différents de pentylènetétrazole (PTZ) (50, 60 et 70 mg/kg). Nous avons constaté que 70 mg/kg de PTZ présentaient un début significativement plus précoce vers la crise généralisée, une augmentation de la durée cumulée des épisodes de convulsions et des taux de mortalité plus élevés chez les souris *Eif4Ebp*$^{-/-/-}$. Ensuite, pour identifier le paralogue de 4E-BP qui médie cet effet, nous avons induit des crises chez des souris dépourvues du paralogue 4E-BP1 (*Eif4Ebp1*$^{-/-}$) ou 4E-BP2 (*Eif4Ebp2*$^{-/-}$) (4E-BP3 n'est pas détecté dans le cerveau) et avons observé que la perte de 4E-BP2, mais pas de 4E-BP1, abaissait le seuil des crises induites par le PTZ et l'acide kaïnique (KA) chez la souris. Puis, pour identifier le type neuronal dans lequel la suppression de 4E-BP2 a abaissé le seuil épileptogène, nous avons généré des lignées de souris avec un knock-out conditionnel de 4E-BP2 dans le neurone excitateur ou inhibiteur. Nous avons observé que la sensibilité à l'induction PTZ était augmentée chez les souris dépourvues de 4E-BP2 dans les neurones inhibiteurs mais pas dans les neurones excitateurs. Nous avons ensuite disséqué les sous-types de neurones inhibiteurs

dans lesquels la délétion de 4E-BP2 favorise les crises d'épilepsie, et avons constaté que la délétion de 4E-BP2 dans les neurones à parvalbumine (PVALB^{+}) (cKO^{Pvalb}), mais pas chez celle liée à la somatostatine (SST^{+}) ou à la protéine intestinale vasoactive (VIP^{+}), a entraîné une sensibilité accrue aux crises induites par le PTZ et le KA. Puis pour confirmer le rôle essentiel des neurones PVALB^{+} dans l'épilepsie, nous avons généré des souris porteuses d'une mutation d'hyperactivation *PIK3CA* humaine sélectivement dans les neurones PVALB^{+} (*Pik3ca*$^{H1047R\text{-}Pvalb}$). La protéine PI3K est située en amont dans la voie de signalisation mTORC1, et son activation déclenche la stimulation en série de protéines en aval et éventuellement de mTOR. Nous avons observé une sévérité accrue des crises chez ces souris lors de l'induction au PTZ. Ensuite, nous avons examiné les changements phénotypiques aux niveaux cellulaire et tissulaire entre les souris de type sauvage, cKO^{Pvalb} et *Pik3ca*$^{H1047R\text{-}Pvalb}$. Le réseau périneuronal (PNN) est une matrice extracellulaire caractéristique exprimée dans les neurones PVALB^{+} matures pour réguler la formation des synapses et protéger les cellules du stress oxydatif. Nous avons détecté une réduction concomitante de la population de neurones PVALB^{+} et une augmentation de la densité du PNN dans la région CA1 de l'hippocampe chez les mutants cKO^{Pvalb} et *Pik3ca*$^{H1047R\text{-}Pvalb}$. De plus, chez ces souris, nous avons trouvé des altérations de l'expression des marqueurs synaptiques dans l'hippocampe dues à la délétion de 4E-BP2 ou à l'hyperactivation de *PIK3CA* dans les neurones PVALB^{+}. Ces changements pourraient expliquer la transition d'équilibre excitateur/inhibiteur (E/I) qui conduit finalement à l'épileptogenèse et à la propagation des crises.

Collectivement, notre étude démontre que l'activité accrue de mTORC1 chez les souris knock-out 4E-BP2, en particulier dans les neurones PVALB^{+}, contribue à la physiopathologie de l'épilepsie. Ces résultats soulignent l'importance de la traduction dépendante de eIF4E comme cible thérapeutique potentielle dans le traitement de l'épilepsie.

Acknowledgments

I would like to express my sincere gratitude to my supervisor, Dr. Nahum Sonenberg, for his consistent guidance and support throughout my master's degree. I would like to thank Dr. Arkady Khoutorsky and my advisors in my research advisory committee, Dr. Maria Vera Ugalde, Dr. Mark Brandon, and Dr. Wayne Sossin, for their precious comments and advice on my project.

I want to thank my mentors, Dr. Vijendra Sharma and Dr. Rapita Sood, for their guidance and support and for loving me as part of the family. It is my most tremendous honor to learn different experimental techniques from both and be part of the team dedicated to this project.

I would also like to thank Dr. Junghyun Choi for her patience, skills, and her support, which have been a source of motivation for me. It has been a great experience working with her. Warm thanks to Tzu-Yu Hung and Yelin Han for being my best friends and coworkers, who always stood by my side throughout my master's education. I also want to thank Xinjie Yeow, who helped me through the emotionally most challenging time. I would also like to thank every member of Dr. Nahum Sonenberg's lab, especially Ms. Isabelle Harvey, Ms. Eva Migon, Dr. Peng Wang, and two recent volunteers, Xinzhu Guo and Junshen Wang.

Importantly, I want to express my love and gratitude to my parents back in China for recognizing my ability, supporting my decisions, and always encouraging me to love and be curious about the world.

I am genuinely grateful for everything that happened and everyone who came into my life over the past two years.

CHAPTER 1: Introduction

Literature review

1.1 Epilepsy

1.1.1 Overview of epilepsy

According to a report from the World Health Organization (WHO) in 2019, the incidence rate of epilepsy worldwide was approximately 0.6 % (50 million patients), with nearly 80% of the cases diagnosed in low- and middle-income countries (Who, 2019). Within Canada the prevalence of epilepsy was around 40.4 per 1,000 population, and about 75% of the patients were diagnosed with the disease before the age of 30, as reported in the 2012 Canadian Community Health Survey (Gilmour *et al.*, 2016). Known risk factors for developing epilepsy include brain traumas, injuries, infections, genetic mutations, and other neurological conditions (Walsh *et al.*, 2017).

Epilepsy is characterized by recurrent and unprovoked seizures caused by the abnormally hypersynchronous firing of a group of neurons which leads to an imbalance of inhibition (I) and excitation (E) in neuronal networks (Chang and Lowenstein, 2003; Barker-Haliski and White, 2015). Depending on the brain regions affected by seizures, epilepsy can be categorized into generalized or focal epilepsy (Berg and Millichap, 2013). In generalized epilepsy, abnormal electrical discharges occur throughout the whole cortex, while in focal epilepsy, seizure activity is restricted to one specific area of the brain (Stafstrom and Carmant, 2015). Genetic factors are more likely to be involved in generalized epilepsy, whereas focal epilepsy is more prominent in brain traumas (American Association of Neurological Surgeons).

Neurological comorbidities such as depression, migraine, and stroke are commonly present in epileptic patients (Gilmour *et al.*, 2016; Keezer *et al.*, 2016). Individuals are evaluated for epilepsy diagnosis after having at least two spontaneous seizures (Stafstrom and Carmant, 2015). Patients often show abnormal brain electrical activities in electroencephalogram (EEG) recordings (Benbadis, 2009). Diagnostic tests also include computed tomography (CT) scans and magnetic resonance imaging (MRI), looking for brain lesions and abnormalities, and blood tests looking for signs of inflammation and genetic factors (Nunes *et al.*, 2012).

Post-mortem studies in patients with the sudden unexpected death of epilepsy (SUDEP) showed severe cerebral and pulmonary edema along with neuronal loss and gliosis (Antoniuk *et al.*, 2001; Yu *et al.*, 2019). Some histopathological characteristics in human epileptic brains include rewiring of the hippocampal neuronal circuitry evidenced by loss of neurons and changes in neuronal connectivities, and elevated glial cells' proliferation rate and their activity in the site of lesion (De Lanerolle *et al.*, 2012).

Treatments of epilepsy include taking antiepileptic drugs (AEDs) and having brain surgeries to remove the affected brain areas (Shorvon *et al.*, 2015). AEDs aim to control neuronal electrical activities by either modulating functions of ion channels, enhancing γ-aminobutyric acid- (GABA) mediated inhibition, or inhibiting glutamate-mediated excitation (Rogawski and Loscher, 2004; Stafstrom and Carmant, 2015). Around 60-70% of newly treated patients with currently available AEDs show satisfactory seizure control (Schmidt, 2009). Surgical treatment is an option for medically intractable epilepsies (Engel, 2008). Candidates for epilepsy surgeries are carefully evaluated prior to the surgery, for example, whether their epileptogenic regions can be precisely located and whether the resection of the lesion would affect essential brain functions (Noachtar and Borggraefe, 2009). According to an epidemiological study in 2018, regardless of the surgery type, patients live a seizure-free life for 8.4 years post-surgery. (Mohan *et al.*, 2018). Even with the currently available treatment methods, some patients still suffer from side effects and limited seizure control (Jacobs *et al.*, 2001). Therefore, a more comprehensive understanding of the pathology of epilepsy and its progression is required to provide epilepsy patients with better care.

1.1.2 Pathophysiology of epilepsy

The molecular and cellular pathophysiological processes through which the brain develops epilepsy is known as epileptogenesis (Devinsky *et al.*, 2018). The generation of a seizure is described by the term ictogenesis (Blauwblomme *et al.*, 2014). The initiating alterations in epileptogenesis, which lead to an E/I imbalance in the brain, could be either acquired or genetic or a combination of both factors (Goldberg and Coulter, 2013; Stafstrom and Carmant, 2015).

Brain tumors, brain infections, and strokes are the most common acquired factors in seizure pathologies (Goldberg and Coulter, 2013). These injuries in the central nervous system

(CNS) could directly cause neuronal cell deaths (Choi, 1988). On the other hand, injuries could cause an elevation in extracellular glutamate concentration, with a concomitant increase in intracellular calcium ion (Ca^{2+}) level, which would over-stimulate the Ca^{2+} signaling in the surviving neurons (Choi, 1988; Delorenzo *et al.*, 2005). Therefore, neurons that survived injuries would undergo permanent alterations in their physiological functions, leading to large-scale synaptic reorganizations (Pitkanen and Sutula, 2002; Delorenzo *et al.*, 2005).

Genetic epilepsy accounts for around 30% of all diagnosed cases, in which epilepsy is caused primarily by genetic factors (Berkovic *et al.*, 2006). However, many epilepsy cases possess a complex of acquired and genetic bases that contribute to the perturbation of the neuronal circuitry (Helbig *et al.*, 2008; Pandolfo, 2011; Stafstrom and Carmant, 2015). According to Wang *et al.*, genes associated with epilepsy can be divided into several categories (Wang *et al.*, 2017). There are "epilepsy genes" whose mutations are directly related to epilepsy or cause diseases in which epilepsy is the predominant symptom (Wang *et al.*, 2017). These genes encode ion channels, including sodium channels and GABA receptors, whose mutations would directly lead to neuronal network hyperexcitability (Armijo *et al.*, 2005; Wang *et al.*, 2017; Oyrer *et al.*, 2018). Another primary class of genes is neurodevelopment-associated, which mainly encode enzymes or enzyme modulators, whose mutations could result in cortical maldevelopment and defective neuronal network (Wang *et al.*, 2017). Such genes include Tuberose Sclerosis Complex 1/2 and doublecortin, etc. (Leventer *et al.*, 2008; Bozzi *et al.*, 2012; Wang *et al.*, 2017). Previous genetic studies have revealed more complex disease mechanisms in genetic epilepsy, as usually more than one gene is mutated (Poduri and Lowenstein, 2011).

It has also been proposed that the pathologies in both acquired and genetic epilepsies might converge at some point involving changes in large-scale molecular signaling pathways, such as the mechanistic/mammalian target of rapamycin (mTOR) pathway, MAP-kinase Mitogen-activated protein kinase/extracellular-signal-regulated kinase (MAPK/ERK) pathway and Janus Kinase/Signal Transducer and Activator of transcription (JAK/STAT) pathway (Goldberg and Coulter, 2013; Meng *et al.*, 2013; Gautam *et al.*, 2021). These molecular signaling pathways regulate essential biological processes, including transcription, translation, cell growth and survival, and inflammatory response. (Laplante and Sabatini, 2009; Harrison, 2012; Sun *et al.*, 2015). They are essential for normal brain development and

function, and their dysfunction is implicated in many neurological conditions, including epilepsy (Nicolas *et al.*, 2013; Takei and Nawa, 2014; Bockaert and Marin, 2015; Albert-Gasco *et al.*, 2020). Studies on molecular mechanisms underlying epileptogenesis are in urgent need as they will enhance our understanding of the progression of epilepsy and will provide a foundation for developing new therapeutics for treatment.

1.1.3 Epilepsy and seizure models

The development and use of animal models for epilepsy allow us to study and comprehend the complex mechanisms driving epileptogenesis and seizure initiation (Kandratavicius *et al.*, 2014). Methods commonly used to induce seizures in animal models include chemoconvulsants, electrical stimulation, thermal and hypoxic insults to the brain, audiogenic induction and optogenetics, and brain traumatic injuries, as summarized and discussed by Kandratavicius *et al.* (Kandratavicius *et al.*, 2014). This section briefly reviews two commonly used models for acute seizures induced by chemoconvulsants which we chose to use in this study.

Pentylenetetrazol (PTZ) is widely used as a systematic chemoconvulsants and utilized in drug screening in animal models to compare the antiepileptic effects of AEDs (Fisher, 1989; Hansen *et al.*, 2004). PTZ functions as an antagonist to $GABA_A$ receptors, interacting at the picrotoxin-binding site (Ramanjaneyulu and Ticku, 1984; Hansen *et al.*, 2004). By binding to the $GABA_A$ receptor, it inhibits the chloride ion influx, preventing the repolarization of the cell membrane and, therefore, affects the endogenous inhibitory GABA signaling (Huang *et al.*, 2001; Hansen *et al.*, 2004). Systemic injection of PTZ in rodents elicits generalized seizures in a dose-dependent manner: a small dosage of PTZ produces absence seizures without convulsion, and a higher dosage of PTZ leads to acute convulsive seizures (Fisher, 1989; Luttjohann *et al.*, 2009). Serial injections at a small dosage (sub-convulsive) have been used as a chemical-induced kindling model of chronic epilepsy (Dhir, 2012; Shimada and Yamagata, 2018; Singh *et al.*, 2021).

Kainic acid (KA) is an excitatory amino acid and acts as a glutamate receptor agonist (Fisher, 1989; Kandratavicius *et al.*, 2014). Its mechanism of seizure induction is via activation of kainate receptors to increase Ca^{2+} conductance and cause sustained membrane depolarization and firing of neurons (Nadler *et al.*, 1978; Sperk *et al.*, 1983). Administration of KA, either

via intraperitoneal (IP) injection or intraventricular injection, preferentially targets neurons in the hippocampus (Nadler *et al.*, 1978; Fisher, 1989). Due to this advantage, KA is used as a reliable tool to study temporal lobe epilepsy (TLE), in which seizures usually start and cause damage to the hippocampus and surrounding area (Nadler, 1981; Levesque and Avoli, 2013; Kandratavicius *et al.*, 2014).

1.2 The mechanistic target of rapamycin

mTOR is crucial in maintaining normal brain homeostasis throughout development, from embryonic to postnatal stages (Takei and Nawa, 2014; Bockaert and Marin, 2015). It regulates crucial processes, including neurogenesis, cell migration and maturation, circuitry formation and synaptic plasticity, and apoptosis (Meng *et al.*, 2013; Bockaert and Marin, 2015; Switon *et al.*, 2017). Dysfunctional mTOR signaling is implicated in many neurological diseases such as autism spectrum disorder (ASD), Fragile X syndrome (FXS), Alzheimer's disease (AD), Parkinson's disease (PD), and epilepsy as well (Griffin *et al.*, 2005; Chu *et al.*, 2009; Sharma *et al.*, 2010; Zhou and Parada, 2012; Querfurth and Lee, 2021). mTOR hyperactivation is one of the underlying mechanisms that contribute to the E/I imbalance in the complex pathology of epilepsy (Gkogkas *et al.*, 2013; Meng *et al.*, 2013; Lasarge and Danzer, 2014). Inhibiting the mTOR signaling pathway has been proven to have anti-epileptogenic and antiseizure effects in both animal models and epilepsy patients (Ryther and Wong, 2012). The following chapters will be focused on mTOR, especially the mTORC1 signaling pathway, summarizing the basics of mTORC1, its role in CNS regarding health and diseases, and specifically the current knowledge about its implication in epilepsy.

1.2.1 Overview of mTOR

mTOR is a serine/threonine-protein kinase that forms two distinct protein complexes (mTORC1 and mTORC2) with different binding partners to regulate cellular growth and homeostasis (Saxton and Sabatini, 2017). Yeast TOR and its mammalian homolog mTOR were first discovered in the early 90's as the critical enzymes that mediate the antifungal activity of rapamycin (Brown *et al.*, 1994; Sabatini *et al.*, 1994). It was found that a small natural molecule could arrest fungi's cell cycle at the G1 phase (Magnuson *et al.*, 2012). This molecule, later named rapamycin, was proven to be immunosuppressive and antiproliferative via its direct interaction with TOR/mTOR (Seto, 2012). mTORC1 and mTORC2 are activated by different upstream signals (Magnuson *et al.*, 2012; Saxton and Sabatini, 2017). mTORC1 senses cellular nutrient and energy levels to control protein synthesis (Bond, 2016; Tan and Miyamoto, 2016). mTORC2, on the other hand, mainly responds to growth factors and is responsible for metabolism, and it also regulates the organization of the actin cytoskeleton (Oh and Jacinto, 2011) (Figure 1.1).

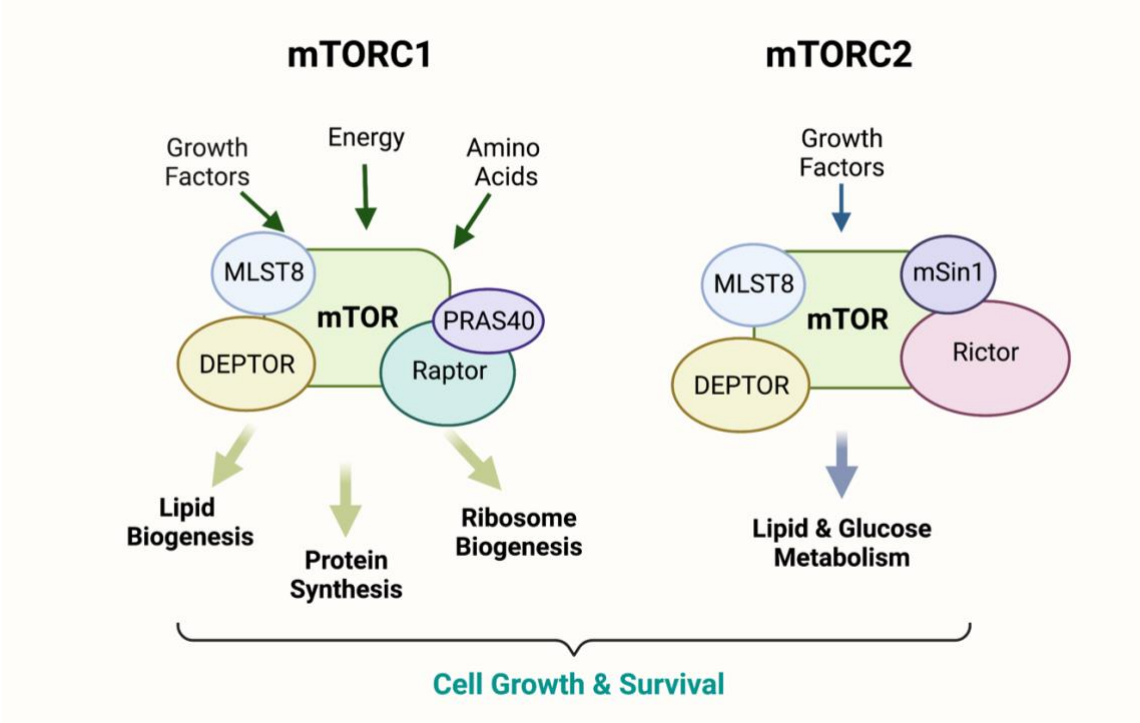

Figure 1. 1: Diagrammatic representation of mTORC1/2.
mTOR forms two distinct complexes of different components. mTORC1 and 2 respond to different cellular and extracellular signals to regulate cell growth and survival. Figure adapted from (Kim *et al.*, 2017). Created with BioRender.com

1.2.2 mTORC1

mTORC1 is a complex of five proteins, including mTOR, regulatory-associated protein of mTOR (Raptor), mammalian lethal with SEC13 protein 8 (MLST8, also known as GβL), proline-rich AKT1 substrate of 40 kDa (PRAS40), and DEP domain-containing mTOR-interacting protein (DEPTOR) (Kim *et al.*, 2002) (Figure 1.1). Raptor functions as a scaffolding protein for the recruitment of mTOR substrates eukaryotic translation initiation factor 4E-binding proteins (4E-BPs) and p70 ribosomal protein S6 kinases (S6Ks) (Oshiro *et al.*, 2004). GβL protein binds between Raptor and mTOR, stabilizes their interaction, and promotes mTOR kinase activity (Kim *et al.*, 2003). PRAS40 exerts a negative effect on mTORC1 signaling, and its phosphorylation by protein kinase B (Akt) results in its dissociation from mTORC1, allowing the recruitment of two substrates of mTORC1, 4E-BPs, and S6Ks, by Raptor (Wiza *et al.*, 2012). DEPTOR functions as a negative regulator in both mTORC1 and mTORC2 signaling pathways as it directly binds and inhibits the mTOR kinase activity (Peterson *et al.*, 2009).

1.2.3 Upstream of mTORC1

Three main mechanisms regulate the activity of the mTORC1 pathway in response to different upstream signals and strictly control the level of protein synthesis under different conditions (Crino, 2016). These mechanisms are the growth factor pathway, the energy-sensing pathway, and the amino acid sensing pathway (Crino, 2016). mTOR requires phosphorylation at Ser2448 via a positive feedback mechanism by S6K1 and autophosphorylation at Ser2481 to be fully activated for its kinase activity (Chiang and Abraham, 2005; Soliman *et al.*, 2010).

1.2.3.1 The growth factor pathway

In the growth factor pathway, phosphatidylinositol 3-kinases (PI3Ks) can be activated by receptor tyrosine kinases (RTKs) or G protein-coupled receptors (GPCRs) at the membrane, responding to hormones and growth factors (Nicholson and Anderson, 2002; New and Wong, 2007; Castellano and Downward, 2011). Activated PI3K triggers the lipid phosphorylation to produce a second messenger molecule, PI(3,4,5)P3, which causes protein Akt translocation from the cytosol to the plasma membrane (Fruman *et al.*, 1998; Cantley, 2002). Once at the membrane, Akt undergoes a conformational change, allowing phosphoinositide-dependent kinase 1 (PDK1) to phosphorylate Akt at its Thr308 position (Hemmings and Restuccia, 2015). Then partially active Akt is further phosphorylated at Ser473 by different kinases, including mTOR, via a positive feedback mechanism, into its fully activated form (Hemmings and Restuccia, 2015). Activated Akt then phosphorylates Tuberous Sclerosis Complex 2 (TSC2) protein at 2-5 sites and leads to the dissociation of TSC1/TSC2 dimer (Ma and Blenis, 2009). TSC2 is a GTPase-activating protein (GAP) for a guanosine triphosphate- (GTP-) binding protein called Ras homolog enriched in the brain (Rheb) (Ma and Blenis, 2009). Phosphorylated TSC2 can no longer activate Rheb-GTP to Rheb-guanosine diphosphate (GDP) (Ma and Blenis, 2009). Therefore, the active Rheb-GTP complex can activate the mTORC1 signaling pathway (Ma and Blenis, 2009; Mendoza *et al.*, 2011) (Figure 1.2).

1.2.3.2 The energy-sensing pathway

In the energy-sensing pathway, the cellular adenosine diphosphate/adenosine monophosphate (ADP/AMP) level is actively sensed by the AMP-activated serine/threonine kinase (AMPK) (Crino, 2016). When adenosine triphosphate (ATP) is consumed, and ATP level is low in the cell, ADP/AMP binds to AMPK to promote the phosphorylation of AMPKα by the liver

kinase B1 (LKB1) (Garza-Lombo *et al.*, 2018). Activated AMPK phosphorylates Raptor to suppress mTOR kinase activity and phosphorylates TSC2 on Ser1387 residue to enhance its GAP activity to deplete the pool of Rheb-GTP and thereby indirectly down-regulate mTORC1 activity (Inoki *et al.*, 2003; Gwinn *et al.*, 2008; Mihaylova and Shaw, 2011) (Figure 1.2).

1.2.3.3 The amino acid sensing pathway

Rab proteins (small GTPases) sense the enriched amino acid level in the amino acid sensing pathway, triggering the rapid translocation of mTORC1 from the cytoplasm to the lysosomal membrane where Rheb-GTP resides (Sancak *et al.*, 2008; Bar-Peled and Sabatini, 2014). This allows the physical contact between mTORC1 and Rheb-GTP and the subsequent activation of the mTOR kinase activity (Suzuki and Inoki, 2011). GAP activity towards rags complex (GATOR1, comprises of DEP domain-containing protein 5 (DEPDC5) and nitrogen permease regulator proteins 2 and 3 (NPRL2 and NPRL3)) is the primary regulator of this process (Crino, 2016). In normal physiological conditions, GATOR1 functions to inhibit the recruitment of the mTORC1 complex to the lysosomal membrane when the level of amino acid is low (Klofas *et al.*, 2020) (Figure 1.2).

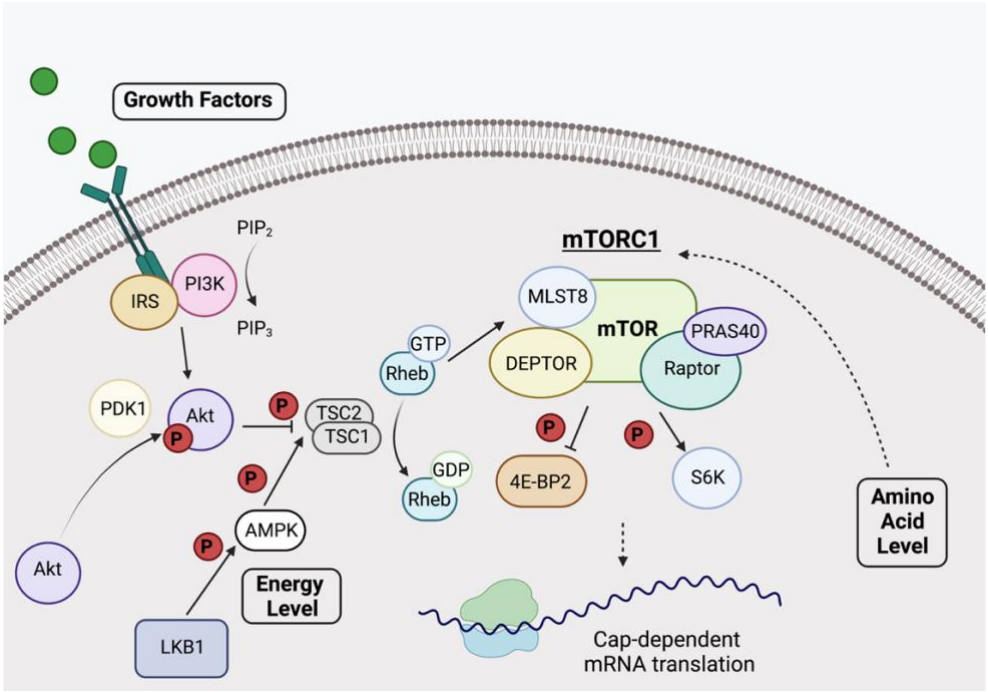

Figure 1. 2: Summary of three primary signaling pathways regulating mTORC1. mTOR in the mTORC1 complex can be regulated by growth factors, cellular energy levels, and the availability of amino acids. Adapted from (Crino, 2016). Created with BioRender.com

1.2.4 Downstream of mTORC1

Upon activation, mTOR in mTORC1 directly phosphorylates its downstream targets S6Ks and 4E-BPs (Crino, 2016). Both S6Ks and 4E-BPs are crucial in the initiation phase of messenger ribonucleic acid (mRNA) translation in eukaryotes, making mTORC1 a key node for regulating protein synthesis (Hay and Sonenberg, 2004).

1.2.4.1 S6 kinases

There are two variants of S6 kinases in mammalians: S6K1 and S6K2 (Sridharan and Basu, 2020). Phosphorylation of Thr389 on S6Ks by mTORC1 and Thr229 by phosphoinositide-dependent kinase 1 (PDK1) leads to the fully activated S6Ks (Yang *et al.*, 2014). S6Ks have several downstream targets involved in the translation machinery, including ribosomal protein S6, one of the 40S small ribosomal subunit components (Chauvin *et al.*, 2014).

1.2.4.2 4E-BPs

There are three isoforms of 4E-BPs (4E-BP1/2/3), with different distributions in the body (Banko *et al.*, 2005). Within the mammalian brain, 4E-BP2 is the most abundant isoform, and it is expressed and active in all regions of the CNS (Banko *et al.*, 2005; Bockaert and Marin, 2015). 4E-BPs are small repressors of mRNA translation that bind to eukaryotic translation initiation factor 4E (eIF4E) and prevent its interaction with the eukaryotic translation initiation factor 4G (eIF4G) (Hay and Sonenberg, 2004). eIF4E is a cap-binding protein that recognizes the 5' cap structure, and it is required for the translation of almost all mRNAs (Amorim *et al.*, 2018). Its interaction with eIF4G leads to the circularization of mRNA, and it also guides the entrance of ribosomes onto the mRNA template (Wells *et al.*, 1998) (Figure 1.3). When 4E-BPs are hypophosphorylated, eIF4E is sequestered, and the global mRNA translation level is kept low (Gingras *et al.*, 2001). When proper signals activate the mTORC1 pathway, mTOR phosphorylates 4E-BPs, and the affinity between eIF4E and 4E-BPs drops, freeing eIF4E to initiate the translation of most capped mRNAs (Gingras *et al.*, 2001).

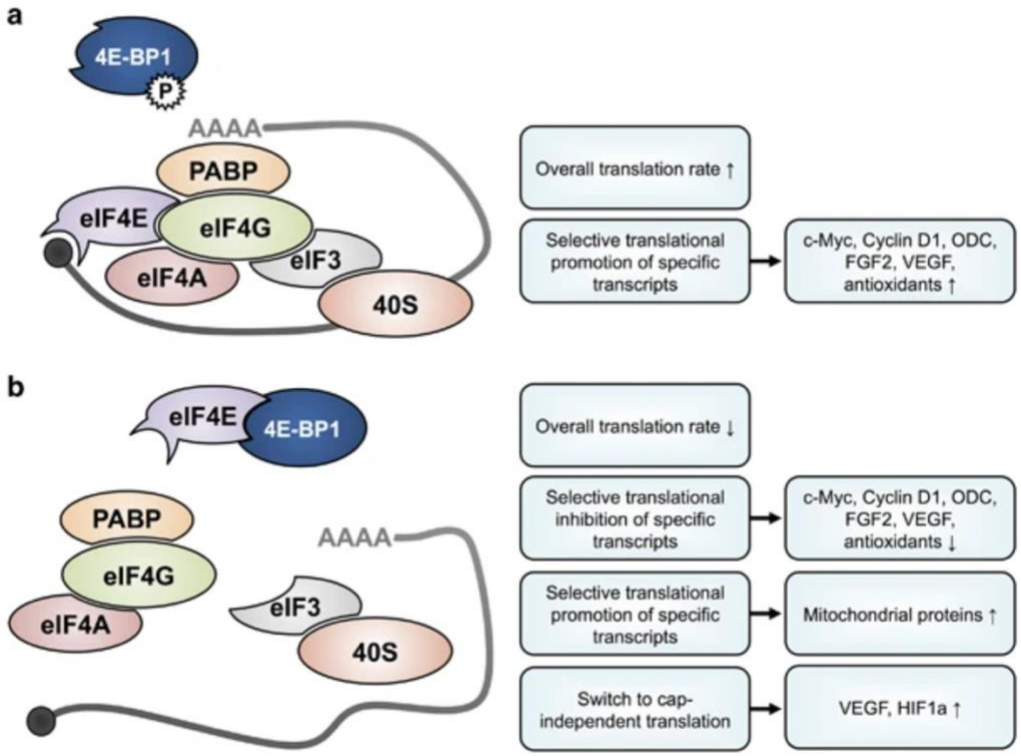

Figure 1. 3: Schematic illustration of 4E-BP regulating mRNA activation.
a) Phosphorylated 4E-BP releases eIF4E, allowing the formation of the eIF4F complex with circularization of mRNA. **b)** When 4E-BP is hypophosphorylated, it sequesters eIF4E and suppresses the cap-dependent mRNA translation initiation (Musa *et al.*, 2016).

1.2.5 Eukaryotic translation

The translation is the cellular process through which the protein-coding information in messenger RNAs (mRNAs) is decoded and translated into amino acid sequences that make up the functional polypeptides (Jishi *et al.*, 2021). mRNA translation takes place in the cytoplasm and consists of three major steps: initiation, elongation, and termination, among which the rate of translation is most tightly regulated at the initiation phase (Kapp and Lorsch, 2004; Hinnebusch and Lorsch, 2012; Baboo *et al.*, 2014). The nascent polypeptides are co-translationally folded into functional proteins, and then the proteins are brought to their sites of action (Waudby *et al.*, 2019).

1.2.5.1 Initiation of translation

Depending on the requirement of the 5’ cap structure on the mRNA for the translation to begin, the initiation step can be either cap-dependent (canonical) or cap-independent (non-canonical (Shirokikh and Preiss, 2018; Yang and Wang, 2019). In eukaryotes, the predominant pathway is cap-dependent translation initiation (Wang *et al.*, 2020).

In the canonical pathway, initiation starts with the formation of the ternary complex (TC), which is composed of the initiator transfer RNA (Met-tRNA$_i^{Met}$) and eukaryotic translation initiation factor 2 (eIF2) with a guanosine triphosphate (GTP) molecule attached, loaded by eIF2B (Sonenberg and Hinnebusch, 2009). A 43S preinitiation complex (43S PIC) is formed by assembling the 40S small ribosomal subunit and the TC with the translation initiation factors eIF1, eIF1A, and eIF3 (Pestova *et al.*, 2001). The initiation factor eIF4E recognizes the 5' cap structure on an mRNA molecule and binds to it as part of the eIF4F complex with two other components, eIF4A and eIF4G (Sonenberg and Hinnebusch, 2009; Amorim *et al.*, 2018). eIF4G, as a scaffolding protein, leads to the circularization of mRNA through the interaction with the poly(A)-binding proteins (PABPs) on the poly(A) tail at the 3' end of the mRNA (Prevot *et al.*, 2003).

Next, eIF4A hydrolyzes ATP molecules for energy to resolve mRNA secondary structures at the 5' untranslated region (5' UTR) (Andreou and Klostermeier, 2013). The interaction between eIF4G and eIF3 allows the recruitment of the 43S PIC onto the mRNA template (Lomakin and Steitz, 2013). Using energy generated from ATP hydrolysis, the 43S PIC scans through the 5' leader region of the mRNA till it reaches the start codon, usually AUG (Lomakin and Steitz, 2013). Met-tRNA$_i^{Met}$ on the ternary complex base-pairs with the AUG codon at the peptidyl site (P-site) of 40S small ribosomal subunit for start codon recognition (Kolitz and Lorsch, 2010).

When the proper start codon is reached, eIF5, which is a GAP for eIF2, will induce eIF2 to hydrolyze its attached GTP molecule, and this process triggers the dissociation of initiation factors from the 40S ribosomal subunit (Kimball, 1999). 60S large ribosomal subunit then binds to form the complete ribosome (80S), with the methionine on the Met-tRNA$_i^{Met}$ fitting in its P-site, and then the elongation phase of translation begins (Sonenberg and Hinnebusch, 2009). Figure 1.4 shows the schematic representation of eukaryotic translation initiation.

There are two major regulation sites at translation initiation to control the rate of protein synthesis (Sonenberg and Hinnebusch, 2009). The first one is through the phosphorylation of the alpha subunit of eIF2 (eIF2α), which determines the availability of eIF2 for the second-round ternary complex formation (Wek, 2018). The second one is by regulating the availability of eIF4E via the phosphorylation of 4E-BPs by mTORC1 (Nandagopal and Roux, 2015).

1.2.5.2 Elongation of translation

At the end of the initiation phase, the 80S ribosome, mRNA, and Met-tRNA$_i^{Met}$ are positioned in a way such that the aminoacyl site (A-site) of the ribosome is ready to accept the next aminoacyl-tRNA whose anticodon can be base-paired with the second codon on the mRNA's open reading frame (ORF) (Dever *et al.*, 2018). The aminoacyl-tRNA lies within a TC with the eukaryotic translation elongation factor 1A (eEF1A) and a GTP molecule (Stark *et al.*, 2002). When the proper codon and anticodon match, eEF1A hydrolyzes its GTP and inserts the aminoacyl-tRNA in the A-site of the ribosome (Dever *et al.*, 2018). eIF5A aids the corresponding peptide bond formation between the Met-tRNA$_i^{Met}$ and the aminoacyl-tRNA (Schuller *et al.*, 2017). Moreover, the eukaryotic translation elongation factor 2 (eEF2) hydrolyzes its GTP to catalyze mRNA translocation by one codon and the tRNAs into the P and E sites, leaving itself in the A site (Kaul *et al.*, 2011). eEF2-GDP then leaves the complex and is prepared for the next cycle (Kaul *et al.*, 2011). The next codon on the mRNA is now present in the A site and available for the anti-codon base-pairing (Dever *et al.*, 2018).

1.2.5.3 Termination of translation

When a stop codon on the mRNA and the corresponding aminoacyl-tRNA reach the A site of the ribosome, eukaryotic releasing factor 1 (eRF1) recognizes the codon and triggers the release of the nascent polypeptide from the ribosome, and eukaryotic releasing factor 3 (eRF3) hydrolyzes its GTP to help the release (Alkalaeva *et al.*, 2006; Hellen, 2018) (Figure 1.4).

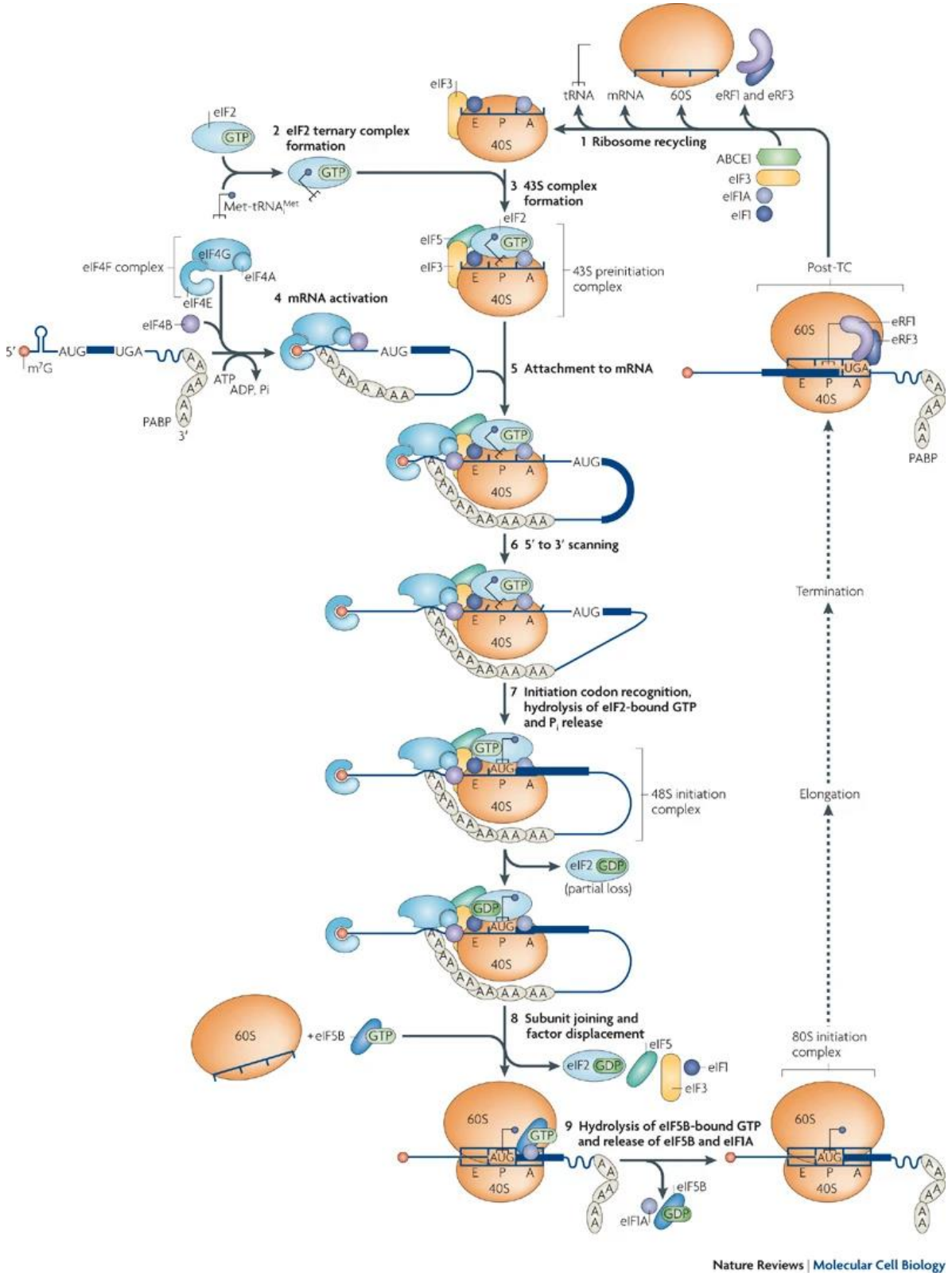

Figure 1. 4: The Cap-dependent (canonical) initiation of eukaryotic mRNA translation. In brief, canonical initiation starts with forming a ternary complex and activating mRNA by translation initiation factors. Then a 43S preinitiation complex (43S PIC) forms, followed by its scanning through the 5' UTR till it recognizes the AUG start codon and forms 48S PIC. Next, the large ribosomal subunit is recruited to form the complete ribosome and proceeds to the elongation phase (Jackson *et al.*, 2010).

1.3 mTORC1 signaling pathway in the brain

The mTORC1 signaling pathway is critical in maintaining normal brain physiology, and it regulates neurogenesis, cell migration, axonal and dendritic growth, and synaptic plasticity, among other processes. (Switon *et al.*, 2017). This section reviews some of the critical functions of the mTORC1 signaling in normal brain function.

1.3.1 Neural stem cell homeostasis and neurogenesis

mTORC1 signaling in CNS development has been extensively studied (Takei and Nawa, 2014). Neurogenesis at both embryonic and postnatal stages is known to be regulated by the mTORC1 pathway, as neural stem cells' (NSCs') maintenance and proliferation require proper signaling, such as nutrient levels and growth factors, through Akt/mTOR (Switon *et al.*, 2017; Licausi and Hartman, 2018). Conditional knockout (cKO) of Raptor in mTORC1 in embryonic neural stem cells (eNSCs) in mice resulted in fewer mature neurons (Cloetta *et al.*, 2013). Ex vivo study showed that inhibiting mTOR kinase activity by rapamycin impairs eNSCs' self-renewal capability (Magri *et al.*, 2011). Transgenic mice expressing hyperactive mTORC1 in the forebrain at the embryonic stage showed severe apoptosis of neural progenitor cells and had prominent cortical atrophy (Kassai *et al.*, 2014). In young mice, activation of mTORC1 in NSCs favors differentiation instead of self-renewal (Mahoney *et al.*, 2016). Postnatal deactivation of mTORC1 in NSCs residing at the lateral ventricle using a short hairpin RNA (shRNA) against Rheb significantly reduced the population of newborn neurons (Hartman *et al.*, 2013). In addition to this, mTORC1 hyperactivation by expressing constitutively active Rheb at the lateral ventricle drove NSCs to terminally differentiate into transit-amplifying cells (TACs), which later would give rise to neuroblasts (Hartman *et al.*, 2013).

1.3.2 Axonal myelination and regeneration

mTORC1 signaling pathway tightly controls axonal myelination and regeneration via its direct effectors, eIF4E-BPs and S6Ks. (Gong *et al.*, 2015). Raptor has been shown to positively regulate axonal myelination in mouse models (Wahl *et al.*, 2014). Higher levels of phosphorylated mTOR (at Ser2448) and phosphorylated S6K were observed in axons of injured neurons, with high spatiotemporal specificity (Terenzio *et al.*, 2018). mTORC1, but not mTORC2, was explicitly required for axonal regeneration through the PI3K/Akt/mTOR signaling pathway (Miao *et al.*, 2016).

1.3.3 Long-term potentiation and depression

The requirement of mTORC1 signaling-dependent protein synthesis for the formation of long-term potentiation (LTP) and long-term depression (LTD) at the site of synapses has been extensively studied in many animal models (Huber *et al.*, 2001; Tang and Schuman, 2002). When S6K1/2 is knocked-out, long-term memory is drastically affected (Antion, Hou, *et al.*, 2008; Antion, Merhav, *et al.*, 2008). 4E-BP2 knockout (KO) mice have been shown to display severe defects in the formation of hippocampus-dependent late LTP (L-LTP), even though they presented a lower threshold of eliciting L-LTP (Banko *et al.*, 2005; Hoeffer and Klann, 2010).

1.4 mTORC1 signaling pathway in epilepsy

Mutations that lead to mTORC1 hyperactivation in the brain are associated with various brain disorders (Costa-Mattioli and Monteggia, 2013). For example, loss of the phosphatase and tensin homolog (PTEN), a negative regulator of the mTOR signaling pathway, contributes to ASD (Zhou and Parada, 2012). In the brains of patients with AD, abnormally high p-Akt (Ser 473) and p-p70S6K (Thr389) levels have been observed, which indicate a higher activity of mTORC1 (Griffin *et al.*, 2005; Querfurth and Lee, 2021). Inhibiting mTORC1 by rapamycin promotes the autophagy pathway and enhances the clearance of β-Amyloid deposited in extracellular space in mouse models (Boland *et al.*, 2008). It has also been shown that there is an upregulated mTOR activity in the brain of patients with PD (Chu *et al.*, 2009). The role of the mTORC1 signaling pathway in epilepsy and epileptogenesis has also been extensively studied (Meng *et al.*, 2013). This chapter reviews some existing evidence of the implication of the mTORC1 signaling in epilepsy.

PI3K lies upstream in the growth factor pathway, activating the subsequent mTORC1 signaling (Sanchez-Alegria *et al.*, 2018). Several activating mutations of PI3K have been identified in patients with epileptogenic cortical malformations (Lee *et al.*, 2012; Jansen *et al.*, 2015). Molecular analysis for common variants of PI3K using polymerase chain reaction (PCR) was recently suggested to be an effective diagnostic tool for epileptic patients with cortical dysplasia (Pirozzi *et al.*, 2021). Mouse models carrying activating mutant alleles of *Pik3ca* (*H1047R* and *E545K*) in neuronal progenitors developed various brain disorders seen in human patients, including epilepsy (Roy *et al.*, 2015).

PTEN, a PI(3,4,5)P_3 phosphatase, functions against the action of PI3K and, therefore, is a negative regulator of the PI3K/Akt/mTORC1 signaling pathway (Endersby and Baker, 2008). Somatic mutations of PTEN have been reported in patients with cortical dysplasia and spontaneous seizure (Elia *et al.*, 2012; Marchese *et al.*, 2014; Koboldt *et al.*, 2021). Mice with the conditional deletion of PTEN in the brain developed spontaneous seizure episodes at the early adult stage (Backman *et al.*, 2001).

TSC1/2 is one of the most well-characterized epilepsy genes and is named after the autosomal dominant disease tuberous sclerosis (Ryther and Wong, 2012). It functions as a negative regulator of the mTORC1 signaling pathway (Huang and Manning, 2008). Inactivation mutations of TSC1/2 lead to widespread tumorigenesis in different organs, and

the disease TSC is one of the most common causes of epilepsy (Franz *et al.*, 2010; Lasarge and Danzer, 2014). Somatic mutations of TSC1/2 that result in hyperactive mTORC1 have been reported in patients with focal cortical dysplasia, the primary genetic cause of focal epilepsy (Lim *et al.*, 2017). Besides, truncating mutations have also been found in some patients with intractable epilepsy (Liu *et al.*, 2020). A mouse model with neuronal loss of TSC1 showed dysplastic hippocampal neurons with extremely high mTOR kinase activity and delayed myelination, and these mice often had spontaneous seizures (Meikle *et al.*, 2007). Mice with cKO of TSC2 in glial-fibrillary acidic protein (GFAP)-positive cells exhibited severer neurological phenotypes compared to TSC1 cKO mice, as seizures with earlier onsets and higher frequencies were observed (Zeng *et al.*, 2011).

Rheb, in its GTP-bounded state, is a direct activator of mTORC1 activity (Heard *et al.*, 2014). Recent studies have revealed several brain somatic activating mutations of Rheb in patients with brain dysplasia and refractory epilepsy (Reijnders *et al.*, 2017; Salinas *et al.*, 2019; Zhao *et al.*, 2019). In mice, the expression of a constitutively active form of Rheb in neurons from embryonic development resulted in dysregulated maturation of neurons and spontaneous seizures (Nguyen *et al.*, 2019).

Another upstream negative regulator of mTORC1 activity is the GATOR1 complex, and its major component, DEPDC5, has been found mutated (loss-of-function) in many cases of familial focal epilepsies (Dibbens *et al.*, 2013; Baulac *et al.*, 2015; Anderson, 2018). After deleting DEPDC5 in their embryonic stage, transgenic mice had severe developmental defects and premature and sudden death (Hughes *et al.*, 2017). DEPDC5 cKO in excitatory neuron lineage in early development resulted in macrocephaly, premature death, and spontaneous seizure in mice, and the inhibition of mTORC1 activity using rapamycin was sufficient to suppress seizure and improve overall survival (Klofas *et al.*, 2020). Mutations in the other two components of the GATOR1 complex, NPRL2, and NPRL3, also contribute to the disease progression in familial focal epilepsy, emphasizing the importance of GATOR1 in the disease (Ricos *et al.*, 2016).

In patients with focal cortical dysplasia (FCD), drug-resistant epilepsy is often a major complication, and brain somatic activating mutations of mTOR protein itself has been frequently detected in blood-brain paired deoxyribonucleic acid (DNA) samples and dysplastic tissues (Lim *et al.*, 2015; Moller *et al.*, 2016; Hanai *et al.*, 2017; Guerrini *et al.*,

2021). FCD brains exhibit abnormal GABA signaling networks, and therefore there is an increased risk of epileptogenesis (Moloney *et al.*, 2021). Tissue samples from FCD patients showed histological evidence of the hyperactivated mTORC1 signaling pathway (Moller *et al.*, 2016; Hanai *et al.*, 2017). In mice expressing activating mutants of mTOR, administration of rapamycin was sufficient to suppress abnormal neurological phenotypes and reduce epileptic seizures (Lim *et al.*, 2015).

Apart from familial epilepsies and epilepsies triggered by de novo mutations, elevated mTOR kinase activity has also been found in acquired epilepsies, as in the cases of traumatic brain injuries (TBI) and hypoxic-ischemic brain injuries (Meng *et al.*, 2013; Ostendorf and Wong, 2015). The initial mTORC1 activation in response to the injury is neuroprotective because it prevents excessive neuronal apoptosis and promotes angiogenesis and axonal regeneration (Chen *et al.*, 2012; Don *et al.*, 2012). However, importantly, the time window for which mTORC1 signaling remains active requires strict regulation for not being epileptogenic because the upregulation of mTORC1 activity may result in aberrant neurogenesis and neuronal activity structural changes (Parent *et al.*, 1997; Lasarge and Danzer, 2014).

Previous studies have revealed that translational dysregulations, due to mutations in many of the mTORC1 upstream regulators and the mTORC1 itself, contribute to epileptogenesis (Cho, 2011; Pernice *et al.*, 2016; Moloney *et al.*, 2021). However, the precise molecular and cellular mechanisms by which mTORC1-dependent translation drives neuronal hyperexcitability and eventually epilepsy require further investigation (Moloney *et al.*, 2021). It is essential to determine which of the 4E-BPs, as a crucial translational regulator directly downstream of mTORC1, is mostly implicated in epileptogenesis. Moreover, it is also essential to uncover the specific neuronal subtype mediating the effect of mTORC1-dependent translation in this disease.

CHAPTER 2: Hypothesis and aims

Hypothesis:

4E-BP2-dependent translation in parvalbumin-expressing interneurons affects the threshold of epileptic seizures.

Aims:

1. Chapter 3: To determine which 4E-BP isoform is implicated in epileptogenesis.
2. Chapter 4: To determine which neuronal subtype mediates the effect of enhanced mTORC1 activity in epileptogenesis.
3. Chapter 5: To identify the hippocampal phenotypic changes associated with cell-type-specific activation of mTORC1.

CHAPTER 3: Investigating the Implication of 4E-BP Isoform in Epileptogenesis

3.1 Introduction

The mTORC1 signaling pathway is an essential molecular pathway that regulates protein synthesis, cell growth, homeostasis, and apoptosis (Laplante and Sabatini, 2009; Saxton and Sabatini, 2017). Because it is malfunctioning and often manifests in diseases, the activity of mTORC1 requires strict regulation (Dazert and Hall, 2011). It has been established that dysregulated neuronal mTORC1 pathway is one of the pathologic mechanisms which drive epileptogenesis and seizure progression (Russo *et al.*, 2012; Meng *et al.*, 2013). Moreover, the connections between proteins upstream of mTORC1 and epilepsy have been extensively studied (Russo *et al.*, 2012). However, it remains unclear how the mTORC1-dependent translation plays an important role in epileptogenesis. Since downstream of mTORC1, there are three isoforms of 4E-BP that control the rate of mRNA translation, we set out to determine the contribution of each isoform to the disease.

3.2 Experimental Aims

The main aim of this thesis is to study the neuronal cell-type-specific contribution of mTORC1-dependent translation in epilepsy. We first ask if three isoforms of 4E-BPs regulate seizure threshold differentially using epileptic mouse models. By injecting different concentrations of PTZ into 4E-BP triple-knockout mice, we examined the general functions of 4E-BPs in epileptogenesis and optimized the dosage to be used in the following experiments. Using 4E-BP1 knockout and 4E-BP2 knockout mice, we investigated the implication of each 4E-BP isoform in epileptogenesis.

3.3 Results and Conclusions

Before presenting the results and discussion of the data, Figure 3.1 illustrates the schematic representation of the timeline of seizure induction and video recording of the mice.

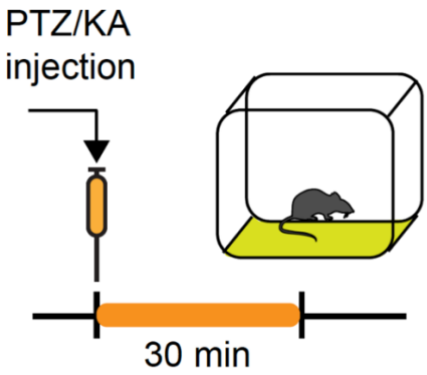

Figure 3. 1: Schematic representation of the timeline of seizure induction and videorecording of the mice.
Mice were injected I.P. with PTZ of 50, 60, and 70 mg/kg or KA of 10, 20, and 30 mg/kg. Mice were monitored for 30 minutes post-injection. Seizure behaviors of the injected mice were scored: onset of the first seizure and cumulative seizure duration, and the percentage of the mice that survived were recorded (Sharma *et al.*, 2021).

3.3.1 *Eif4ebp1/2/3* triple knockout mice showed increased susceptibility to PTZ-induced seizure

To examine the general function of 4E-BPs in epilepsy, we subjected mice lacking all three isoforms of 4E-BP (*Eif4ebp*$^{-/-/-}$) (Figure 3.2 A) to IP injection of different dosages of PTZ (50, 60, and 70 mg/kg).When 70 mg/kg of PTZ were administrated, *Eif4ebp*$^{-/-/-}$ mice showed significant earlier onset of seizures (*Eif4ebp*$^{-/-/-}$ mice, 2.91 ± 0.45; *Eif4ebp*$^{+/+/+}$ mice, 7.01 ± 0.75; mean [time in minutes] ± SEM; $t_{17.95} = 4.659$, $P = 0.0006$, $n = 12, 12$; Figure 3.2 B), increased cumulative duration of seizure (111.73 ± 20.5% compared to wild-type (WT), $t_{21.44} = 4.249$, $P = 0.001$, $n = 12, 12$; Figure 3.2 C), and increased mortality rate (*Eif4ebp*$^{-/-/-}$ mice, 75%; *Eif4ebp*$^{+/+/+}$ mice, 25%; $n = 12, 12$; Figure 3.2 D-F). These data suggest that the genetic deletion of 4E-BPs leads to lowered threshold to PTZ-induced seizure and increased seizure severity.

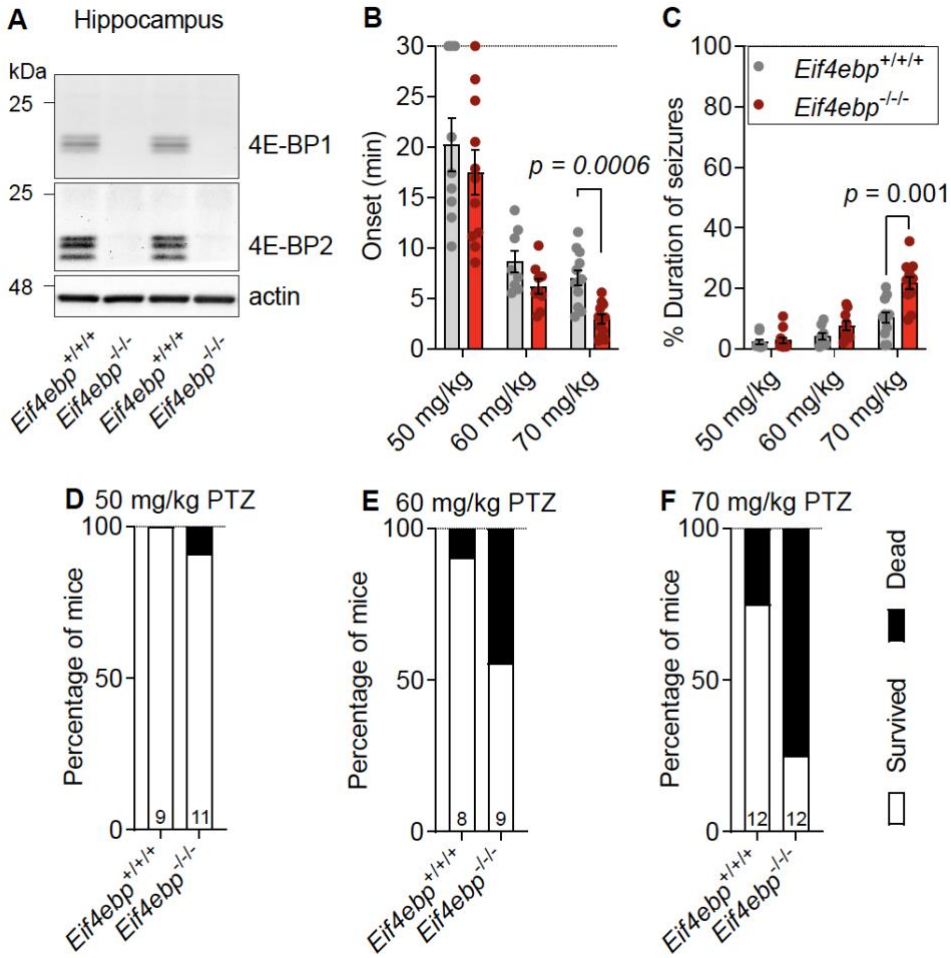

Figure 3. 2: Global knockout of *Eif4ebp1/2/3* increased susceptibility to PTZ-induced seizure.

A) Representative western blot of hippocampal tissue from Eif4ebp1/2/3 triple knockout (*Eif4ebp*$^{-/-/-}$) mice. Fresh hippocampi from *Eif4ebp*$^{-/-/-}$ and WT mice were taken and homogenized, followed by western blotting for 4E-BP1, 4E-BP2, and 4E-BP3, respectively (around 15-20 kDa). β-actin was used as a loading control at 42 kDa. The upper panel shows the ablation of 4E-BP1, and the middle panel shows the ablation of 4E-BP2 in *Eif4ebp*$^{-/-/-}$ mice (4E-BP3 was not detected in the brain). **B)** Onset of the first PTZ-induced seizure at different PTZ concentrations: 50, 60, 70 mg/kg. (Sidak's multiple comparisons test) **C)** Cumulative percentage duration of seizure in response to different dosages of PTZ. (Sidak's multiple comparisons test) **D-F)** Percentage of *Eif4ebp*$^{-/-/-}$ and WT control mice survived seizure within 30 minutes post-PTZ injection at different dosages: 50, 60, 70 mg/kg. A two-tailed unpaired t-test with Welch's correction was used to compare the two groups. Quantitative data with mean ± standard errors of the mean (SEM) are shown (Sharma *et al.*, 2021).

3.3.2 *Eif4ebp2* KO mice showed increased sensitivity to PTZ-induced seizure

To confirm the role of 4E-BPs in epileptogenesis, we questioned which 4E-BP isoform had a more critical impact in mediating PTZ-induced seizures. To answer this question, we examined the severity of PTZ-induced seizure in both 4E-BP1 knockout (*Eif4ebp1*$^{-/-}$) and 4E-BP2 knockout (*Eif4ebp2*$^{-/-}$) mice (Figure 3.3 A, E), by measuring the response to 70 mg/kg of

PTZ in both groups. Genetic deletion of 4E-BP1 in mice did not elicit a significant alteration in mortality rate, the onset of the first seizure, or the total seizure duration compared to WT control mice (*Eif4ebp1*$^{-/-}$: seizure onset: $t_{16.69}$ = 1.186, P = 0.252, n = 10, 12; cumulative duration: $t_{19.35}$ = 1.594, P = 0.127, n = 10, 12; Figure 3.3 B-D). Whereas *Eif4ebp2*$^{-/-}$ mice showed a significant increase in the mortality rate (*Eif4ebp2*$^{-/-}$ mice, 88.24%; *Eif4ebp2*$^{+/+}$ mice, 15%; Figure 3.3 F), a substantial reduction in seizure latency (52.12 ± 4.83%; $t_{17.54}$ = 4.674, P = 2.02 × 10^{-4}, n = 13, 18; Figure 3.3 G) and an increase in the cumulative duration of the seizure (91.8 ± 23.42%; $t_{24.37}$ = 3.915, P = 6 × 10^{-4}, n = 13, 17; Figure 3.3 H), compared to WT control mice. These observations conclude that 4E-BP2, but not 4E-BP1, has a vital role in determining the susceptibility to PTZ-induced seizures.

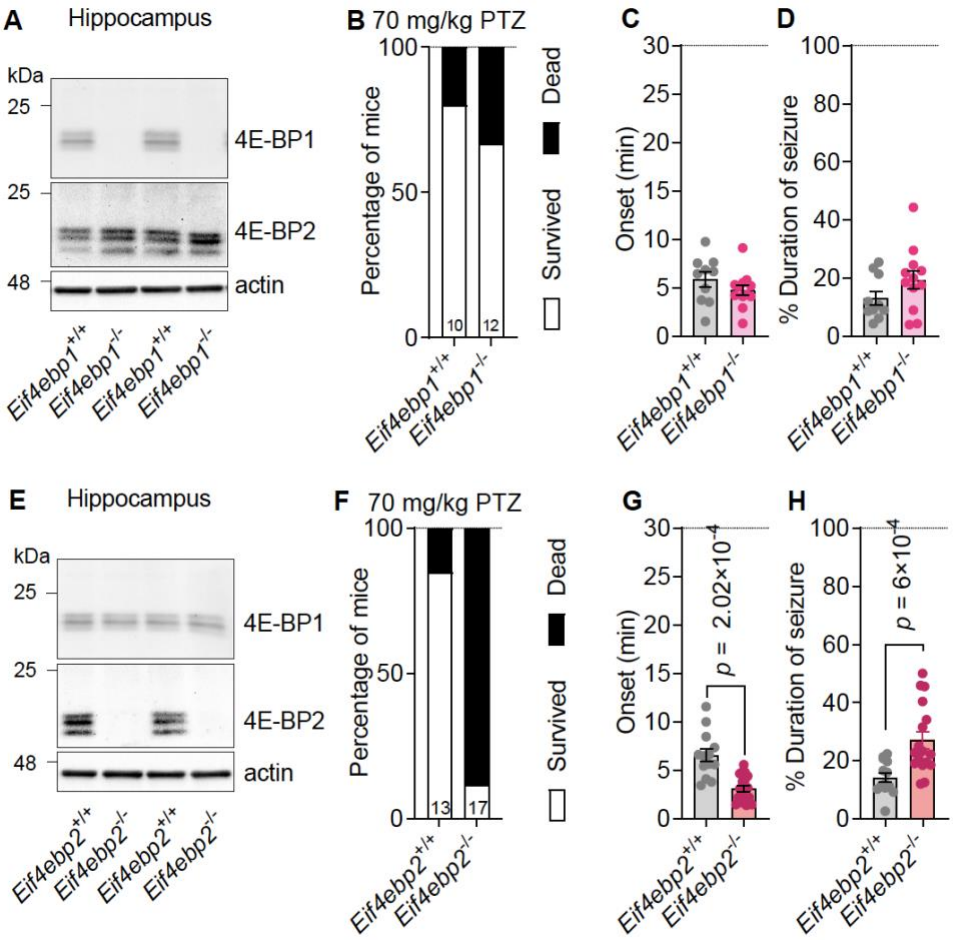

Figure 3. 3: *Eif4ebp2* KO mice showed increased sensitivity to PTZ-induced seizure.
A) Representative western blot of hippocampal tissue from Eif4ebp1 KO (*Eif4ebp1*$^{-/-}$) mice. Fresh hippocampi from *Eif4ebp1*$^{-/-}$ and WT mice were taken and homogenized, followed by western blotting for 4E-BP1 and 4E-BP2 (around 15-20 kDa). β-actin was used as a loading control at 42 kDa. **B-D)** *Eif4ebp1*$^{-/-}$ and WT control mice had similar mortality rates, first seizure onset, and cumulative seizures duration when given 70 mg/kg of PTZ. **E)** Representative western blot of hippocampal tissue from *Eif4ebp2* KO (*Eif4ebp2*$^{-/-}$) mice. Fresh hippocampi from *Eif4ebp2*$^{-/-}$ and WT mice were taken and homogenized, followed by western blotting for 4E-BP1 and 4E-BP2 (around 15-20 kDa). β-actin was used as a loading control at 42 kDa. **F-H)** The deletion of *Eif4ebp2* in mice leads to a higher mortality rate, a reduction of seizure onset, and a longer cumulative duration of seizures in response to 70 mg/kg of PTZ. A two-tailed unpaired t-test with Welch's correction was used to compare the two groups. Quantitative data with mean ± SEM are shown (Sharma *et al.*, 2021).

Overall, in this section, we confirmed the essential role of 4E-BPs in an epileptic seizure. Moreover secondly, we showed that the 4E-BP2 isoform is more implicated in regulating the seizure threshold in the PTZ-induced seizure model.

CHAPTER 4: Investigating the Cell Type-Specific Contribution of Enhanced mTORC1 Signaling in Epileptogenesis

4.1 Introduction

Neurons in the brain are classified based on their intrinsic functions and morphologies, and two major groups of cortical neurons are excitatory neurons and inhibitory interneurons, depending on the types of neurotransmitters they release (Levinson and El-Husseini, 2005). While excitatory neurons release excitatory neurotransmitters such as glutamate and acetylcholine to increase the likelihood of the recipient neurons to fire an action potential, inhibitory interneurons utilize inhibitory neurotransmitters such as γ-aminobutyric acid (GABA) to suppress the activity of the recipient neurons (Zhou and Danbolt, 2014; Lim *et al.*, 2018). Because inhibitory interneurons possess a widely diversified in their shapes, connectivities, and characteristic peptide markers, they are further divided into subtypes, including somatostatin- (SST-), parvalbumin- (PVALB-), vasoactive intestinal peptide- (VIP-) expressing neurons, and others (Kepecs and Fishell, 2014; Tremblay *et al.*, 2016; Lim *et al.*, 2018). Evidence suggests that populations of neurons are differentially affected by seizures (Houser, 2014; Pfisterer *et al.*, 2020). However, it is not clear whether translational deregulation in a different subset of neurons has different impacts on epileptogenesis.

4.2 Experimental Aims

To further delineate the role of the mTORC1 signaling pathway in epileptogenesis, and given that we have shown 4E-BP2 is implicated neuronal isoform in the disease, we next examined whether there is a neuronal cell type-specific contribution of enhanced mTORC1 activity in promoting epileptogenesis, by generating mice with cell type-specific conditional knockout of 4E-BP2 and subjecting them to PTZ-induction of seizure.

4.3 Results and Conclusions

4.3.1 Conditional knockout of *Eif4ebp2* in inhibitory interneurons affects seizure response to PTZ induction

To determine the neuronal subpopulations through which 4E-BP2 affects seizure susceptibility, we generated neuronal cell-type-specific conditional 4E-BP2 knockout mice, as shown in the schematic design in Figure 3.4.

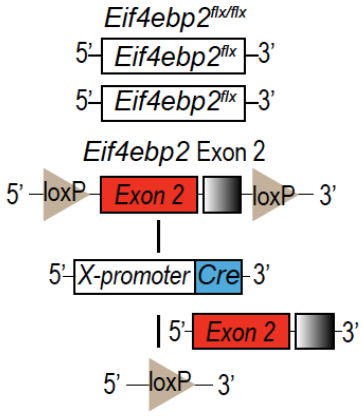

Figure 4. 1: Genetic design for the cell type-specific conditional knockout of 4E-BP2. The exon 2 of the *Eif4ebp2* gene is flanked by the LoxP sites. After crossing *Eif4Ebp2*$^{flx/flx}$ mice with mice expressing Cre recombinase under different cell type-specific promoters, the exon 2 of the *Eif4ebp2* gene is deleted upon Cre expression in different cell types (Sharma *et al.*, 2021).

To examine the effect of conditional knockout of 4E-BP2 in excitatory neurons, we first generated excitatory neuron-specific conditional knockout mice, *Eif4Ebp2*$^{flx/flx}$*; Emx1-Cre*$^{+}$ (cKO^{Emx1}) for 4E-BP2 ablation at early development (embryonic day E12.5) and *Eif4Ebp2*$^{flx/flx}$*; Camk2α-Cre*$^{+}$ (cKO^{Camk2α}) for 4E-BP2 ablation during postnatal developmental stage respectively. Immunohistochemical co-staining of 4E-BP2 and CAMK2α, a hippocampal pyramidal neuron marker (excitatory), confirmed the deletion of 4E-BP2 in hippocampal excitatory neurons in both cKO^{Emx1} and cKO^{Camk2α} mice (cKO^{Emx1}, $t_{6.239} = 9.023$, $P = 8.3 \times 10^{-5}$, $n = 5, 6$; cKO^{Camk2α}, $t_{9.924} = 10.30$, $P = 1.3 \times 10^{-6}$, $n = 6, 6$, Figure 3.5 A and E). Mutant and WT control mice were intraperitoneally injected with 70 mg/kg of PTZ to study the effect of excitatory neuron-specific deletion of 4E-BP2 in epileptogenesis. Similar seizure behavior were observed between cKO^{Emx1} and *Eif4Ebp2*$^{+/+}$*; Emx1-Cre*$^{+}$ (WT^{Emx1}) mice, and cKO^{Camk2α} and *Eif4Ebp2*$^{+/+}$*; Camk2α-Cre*$^{+}$ (WT^{Camk2α}) mice. Comparing to each corresponding control group, both mutant groups showed similar seizure parameters (mortality rates, seizure onset and cumulative duration of seizures) (cKO^{Emx1}: seizure onset: $t_{29.65} = 0.275$, $P = 0.785$, $n = 17, 15$; cumulative duration: $t_{26.01} = 1.154$, $P = 0.259$, $n = 17, 15$, Figure 3.5 B-D; cKO^{Camk2α}: seizure onset: $t_{23.77} = 0.623$, $P = 0.54$, $n = 17, 15$; cumulative duration: $t_{19.22} = 0.716$, $P = 0.483$, $n = 17, 15$, Figure 3.5 F-H). We concluded from these results that the deletion of 4E-BP2 in excitatory neurons does not exacerbate epileptogenesis in the PTZ-induced model.

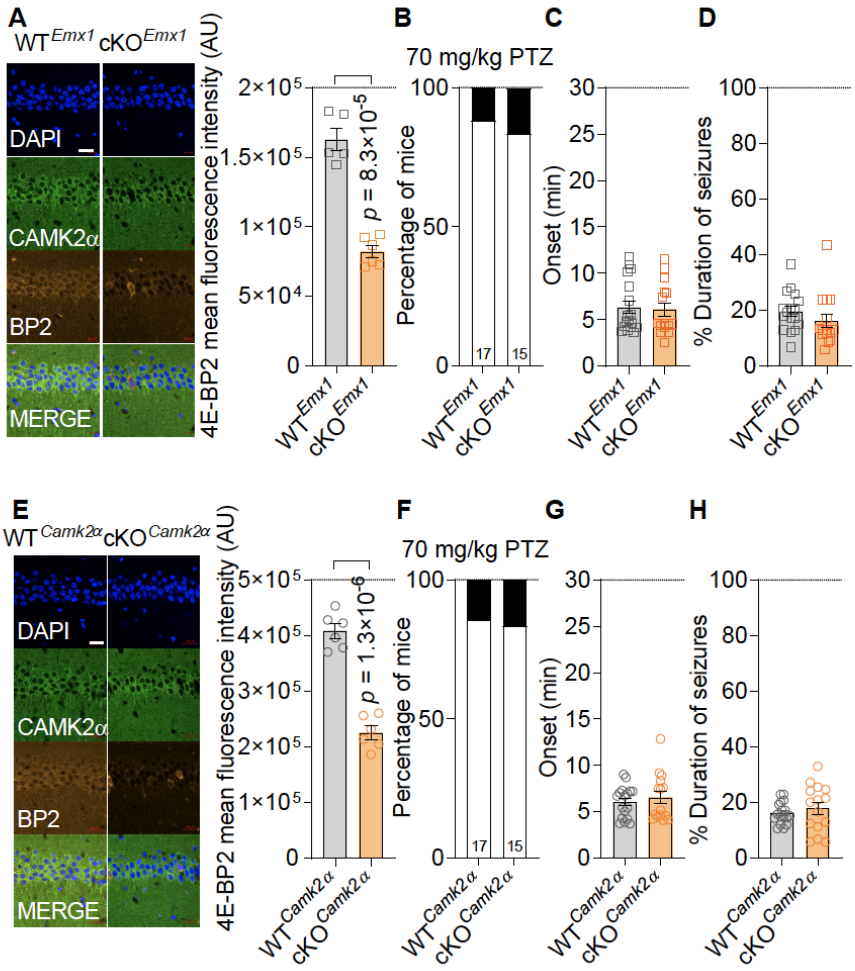

Figure 4. 2: Ablation of *Eif4Ebp2* in excitatory neurons does not affect susceptibility to PTZ-induced seizure.

A) Representative immunohistochemical co-staining of 4E-BP2 and CAMK2α in the CA1 region of the hippocampus of *Eif4Ebp2*$^{flx/flx}$*; Emx1-Cre*$^{+}$ mice. After perfusion, brain tissues were fixed and cut into 40 µm sections. Sections were incubated in blocking buffer followed by immunostaining of 4E-BP2 (1:400) and CAMK2α (1:1000). DAPI (1:5000) was used to visualize cell nuclei. The pyramidal cell layer of the hippocampal CA1 region was used for immunofluorescence imaging and quantification. Quantitative analyses of 4E-BP2 mean fluorescence intensity are shown in the right panel. **B-D)** Mortality rates, seizure onsets, and cumulative duration of seizure of cKO^{Emx1} and WT^{Emx1} mice during 30 minutes after being injected with 70 mg/kg of PTZ. **E)** Representative immunohistochemical co-staining of 4E-BP2 and CAMK2α in the CA1 region of the hippocampus of *Eif4Ebp2*$^{flx/flx}$*; Camk2α-Cre*$^{+}$ mice. After perfusion, brain tissues were fixed and cut into 40 µm sections. Sections were incubated in blocking buffer followed by immunostaining of 4E-BP2 and CAMK2α. DAPI was used to visualize cell nuclei. Quantitative analyses of 4E-BP2 mean fluorescence intensity are shown in the right panel. **F-H)** Mortality rates, seizure onsets, and cumulative duration of seizure of cKO^{Camk2α} and WT^{Camk2α} mice during 30 minutes after being injected with 70 mg/kg of PTZ. Scale bar = 20 µm. A two-tailed unpaired test with Welch's correction was used to compare the two groups. Quantitative data with mean ± SEM are shown (Sharma *et al.*, 2021).

In parallel, to study the effect of conditional deletion of 4E-BP2 in GABAergic inhibitory neurons at different developmental stage in epileptogenesis, *Eif4Ebp2*$^{flx/flx}$ mice were crossed with mice expressing Cre recombinase under the control of *Nkx2.1* promoter (*Nkx2.1-Cre*$^{+}$) for 4E-BP2 ablation in inhibitory neurons at E10.5, or under Gad2 promoter (*Gad2-Cre*$^{+}$) for 4E-BP2 deletion from postnatal day 6 (P6). Immunofluorescent co-labeling of 4E-BP2 and Gad67, a glutamate decarboxylase as a marker for inhibitory interneurons, verified the deletion of 4E-BP2 in both *Eif4Ebp2*$^{flx/flx}$*; Nkx2.1-Cre*$^{+}$ (cKO$^{Nkx2.1}$) and *Eif4Ebp2*$^{flx/flx}$*; Gad2-Cre*$^{+}$ (cKO^{Gad2}) mice (*cKO*$^{Nkx2.1}$, $t_{14.2} = 12.27$, $P < 0.0001$, $n = 12, 14$; *cKO*^{Gad2}, $t_{7.597} = 7.782$, $P = 7 \times 10^{-5}$, $n = 6, 5$; Figure 3.6 A and E). After injected with 70 mg/kg of PTZ, *cKO*$^{Nkx2.1}$ mice showed a significant increase of PTZ-induced seizure mortality rates (Figure 3.6 B), an earlier onset of first seizure ($t_{13.84} = 4.82$, $P = 2.82 \times 10^{-4}$, $n = 10, 11$, Figure 3.6 C), and an increase in the cumulative duration of epileptic seizure ($t_{14.09} = 3.68$, $P = 2.48 \times 10^{-3}$, $n = 10, 11$, Figure 3.6 D), as compared to *Eif4Ebp2*$^{+/+}$*; Nkx2.1-Cre*$^{+}$ (WT$^{Nkx2.1}$) mice. Postnatal deletion of 4E-BP2 in inhibitory neuron (cKO^{Gad2}) also resulted in a rise in mortality rate (Figure 3.6 F), a reduced latency to first seizure ($t_{15.03} = 4.168$, $P = 8.2 \times 10^{-4}$, $n = 13, 14$, Figure 3.6 G), and a prolonged duration of total seizure events ($t_{20.28} = 3.671$, $P = 1.5 \times 10^{-3}$, $n = 13, 14$, Figure 3.6 H). Taken together, these results demonstrate that the deletion of 4E-BP2 in inhibitory interneuron from both embryonic and postnatal development enhances PTZ-induced seizure severity.

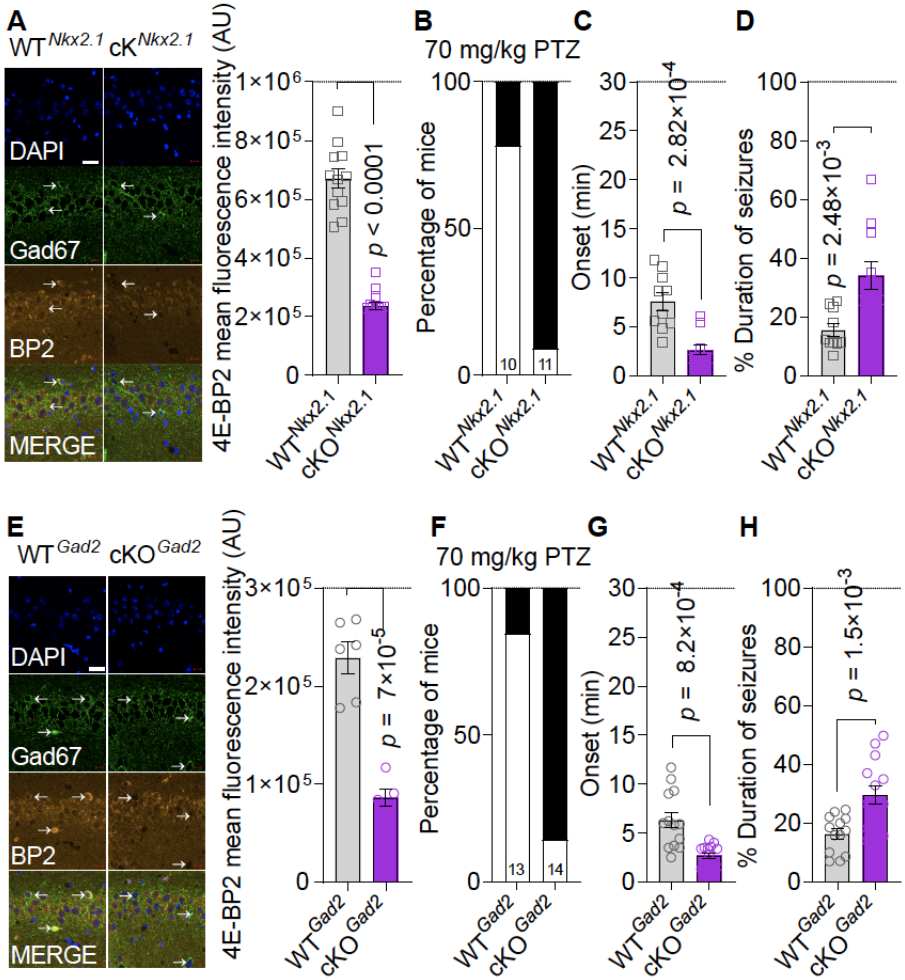

Figure 4. 3: Ablation of *Eif4Ebp2* in inhibitory neurons alters the susceptibility to PTZ-induced seizure.

A) Representative immunohistochemical co-staining of 4E-BP2 and Gad67 in the CA1 region of the hippocampus of *Eif4Ebp2*$^{flx/flx}$*; Nkx2.1-Cre*$^{+}$ mice. After perfusion, brain tissues were fixed and cut into 40 µm sections. Sections were incubated in blocking buffer followed by immunostaining of 4E-BP2 (1:400) and Gad67 (1:1000). DAPI (1:5000) was used to visualize cell nuclei. The pyramidal cell layer of the hippocampal CA1 region was used for immunofluorescence imaging and quantification. Quantitative analyses of 4E-BP2 mean fluorescence intensity are shown in the right panel. **B-D)** Mortality rates, seizure onsets, and cumulative duration of seizure of cKO$^{Nkx2.1}$ and WT$^{Nkx2.1}$ mice during 30 minutes after being injected with 70 mg/kg of PTZ. **E)** Representative immunohistochemical co-staining of 4E-BP2 and Gad67 in the CA1 region of the hippocampus of *Eif4Ebp2*$^{flx/flx}$*; Gad2-Cre*$^{+}$ mice. After perfusion, brain tissues were fixed and cut into 40 µm sections. Sections were incubated in blocking buffer and followed by immunostaining of 4E-BP2 and CAMK2α. DAPI was used to visualize cell nuclei. Quantitative analyses of 4E-BP2 mean fluorescence intensity are shown in the right panel. **F-H)** Mortality rates, seizure onsets, and cumulative duration of seizure of cKO^{Gad2} and WT^{Gad2} mice during 30 minutes after being injected with 70 mg/kg of PTZ. Scale bar = 20 µm. A two-tailed unpaired test with Welch's correction was used to compare the two groups. Quantitative data with mean ± SEM are shown (Sharma *et al.*, 2021).

4.3.2 4E-BP2 mediates epileptogenesis via Parvalbumin-expressing inhibitory interneurons

In order to further elucidate the function of 4E-BP2 in epileptogenesis, we then wanted to determine the specific inhibitory neuronal subtype in which the deletion of 4E-BP2 has a prominent impact. To do this, we bred *Eif4Ebp2*$^{flx/flx}$ mice with Cre^{+} transgenic lines to conditionally knockout 4E-BP2 in different subsets of inhibitory interneuron, including the somatostatin (SST^{+})-, vasoactive intestinal peptide (VIP^{+})- and parvalbumin (PVALB^{+})-expressing GABAergic inhibitory neurons (*Eif4Ebp2*$^{flx/flx}$*; Sst-Cre*$^{+}$ (cKO^{Sst}); *Eif4Ebp2*$^{flx/flx}$*; VIP-Cre*$^{+}$ (cKO^{VIP}); *Eif4Ebp2*$^{flx/flx}$*; Pvalb-Cre*$^{+}$ (cKO^{Pvalb})). Immunohistochemistry results of 4E-BP2 and cell-type specific marker co-staining confirmed the genetic deletion of 4E-BP2 in each of the three subsets of inhibitory neuron in the transgenic mice (cKO^{Sst} mice, $t_{9.532}$ = 5.011, $P = 6.12 \times 10^{-4}$, n = 6, 7, Figure 3.7 A; cKO^{VIP} mice, $t_{6.212}$ = 6.599, $P = 5.04 \times 10^{-4}$, n = 5, 5, Figure 3.7 E; cKO^{Pvalb} mice, $t_{6.378}$ = 4.743, $P = 2.7 \times 10^{-3}$, n = 7, 6, Figure 3.8A)

Seizure behavior in response to PTZ-induction were not altered in cKO^{Sst} mice or cKO^{VIP} mice as compared to their respective WT controls, *Eif4Ebp2*$^{+/+}$*; Sst-Cre*$^{+}$ (WT^{Sst}) and *Eif4Ebp2*$^{+/+}$*; VIP-Cre*$^{+}$ (WT^{VIP}) mice. 70 mg/kg of PTZ induction led to similar mortality rates (cKO^{Sst} mice, Figure 3.7 B; cKO^{VIP} mice, Figure 3.7 F), latency to first seizure (cKO^{Sst} mice, $t_{16.88}$ = 0.567, P = 0.578, n = 8, 11, Figure 3.7 C; cKO^{VIP} mice, $t_{12.31}$ = 0.095, P = 0.926, n = 8, 10, Figure 3.7 G), and also cumulative duration of seizures (cKO^{Sst} mice, $t_{15.78}$ = 0.167, P = 0.87, n = 8, 11, Figure 3.7 D; cKO^{VIP} mice, $t_{15.99}$ = 0.191, P = 0.851, n = 8, 10, Figure 3.7 H). These results showed that specific ablation of 4E-BP2 in SST^{+}- or VIP^{+}-expressing inhibitory interneuron does not affect the sensitivity or severity of PTZ-induced seizure.

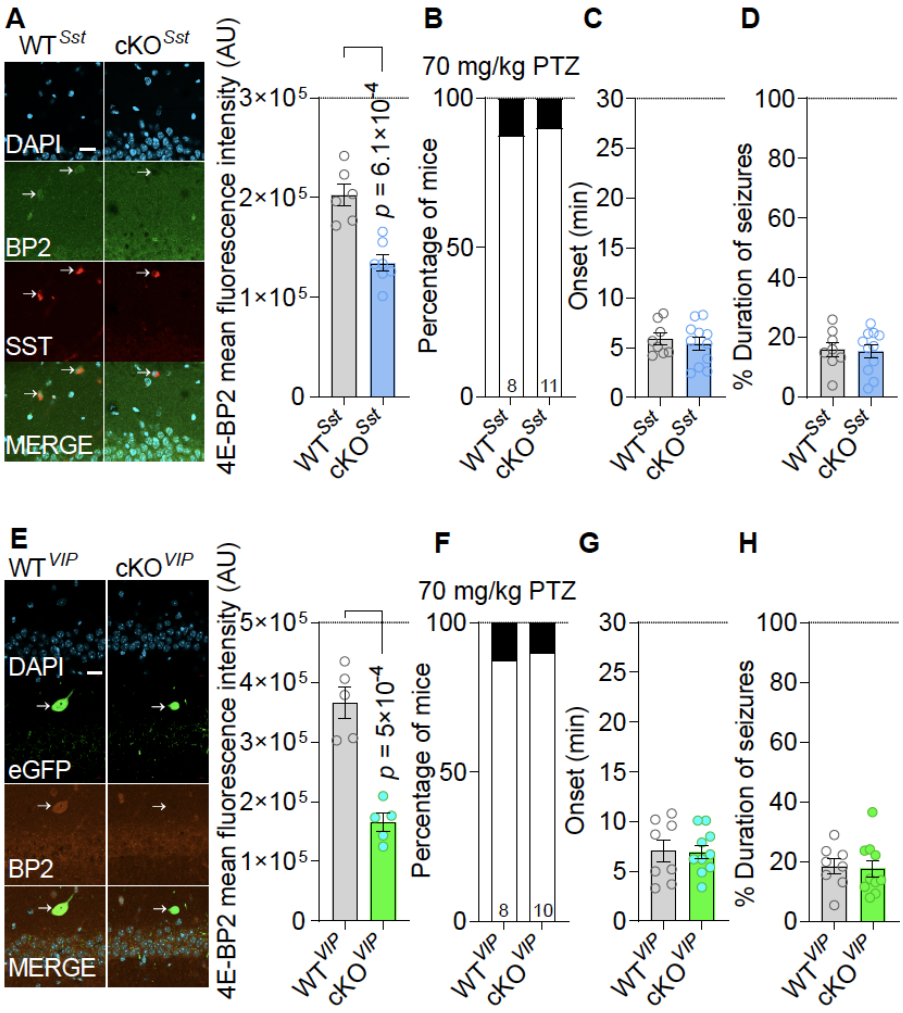

Figure 4. 4: Loss of *Eif4Ebp2* in SST^{+}- or VIP^{+}-expressing inhibitory neurons does not affect seizure behavior.

A) Representative immunohistochemical co-staining of 4E-BP2 and somatostatin in the CA1 region of the hippocampus of *Eif4Ebp2$^{flx/flx}$; Sst-Cre^{+}* mice. After perfusion, brain tissues were fixed and cut into 40 µm sections. Sections were incubated in blocking buffer followed by immunostaining of 4E-BP2 (1:400) and somatostatin (1:100). DAPI (1:5000) was used to visualize cell nuclei. The pyramidal cell layer of the hippocampal CA1 region was used for immunofluorescence imaging and quantification. Quantitative analyses of 4E-BP2 mean fluorescence intensity are shown in the right panel. **B-D)** Mortality rates, seizure onsets, and cumulative duration of seizure of cKO^{Sst} and WT^{Sst} mice during 30 minutes after injection with 70 mg/kg of PTZ. **E)** Representative immunohistochemical co-staining of 4E-BP2 and VIP in the CA1 region of the hippocampus of *Eif4Ebp2$^{flx/flx}$; VIP-Cre^{+}* mice. AAV9-EF1α-DIO-EYFP-WPRE-hGH was injected into the CA1 region of cKO^{VIP} and WT^{VIP} mice to label Cre-positive VIP-expressing neurons. After perfusion, brain tissues were fixed and cut into 40 µm sections. Sections were incubated in blocking buffer and followed by immunostaining of 4E-BP2. DAPI was used to visualize cell nuclei. Quantitative analyses of 4E-BP2 mean fluorescence intensity are shown in the right panel. **F-H)** Mortality rates, seizure onsets, and cumulative duration of seizure of cKO^{VIP} and WT^{VIP} mice 30 minutes after injection with 70 mg/kg of PTZ. Scale bar = 20 µm. A two-tailed unpaired *t*-test with Welch's correction was used to compare the two groups. Quantitative data with mean ± SEM are shown (Sharma *et al.*, 2021).

On the other hand, genetic deletion of 4E-BP2 in PVALB^{+}-expressing inhibitory neurons in mice significantly increased seizure severity upon PTZ-induction (70 mg/kg). cKO^{Pvalb} group had higher mortality rate compared to its corresponding WT control, *Eif4Ebp2*$^{+/+}$*; Pvalb-Cre*$^{+}$ (WT^{Pvalb}) (Figure 3.8 B). They also showed earlier onset of first seizures ($t_{14.64}$ = 3.99, P = 1.24 × 10^{-3}, n = 10, 12, Figure 3.8 C), and a generally longer cumulative duration of seizures ($t_{17.02}$ = 3.74, P = 1.6 × 10^{-3}, n = 10, 12, Figure 3.8 D). Therefore, we concluded that the deletion of 4E-BP2 in the PVALB^{+} inhibitory neurons could exacerbate epileptogenesis in the PTZ-induced seizure model.

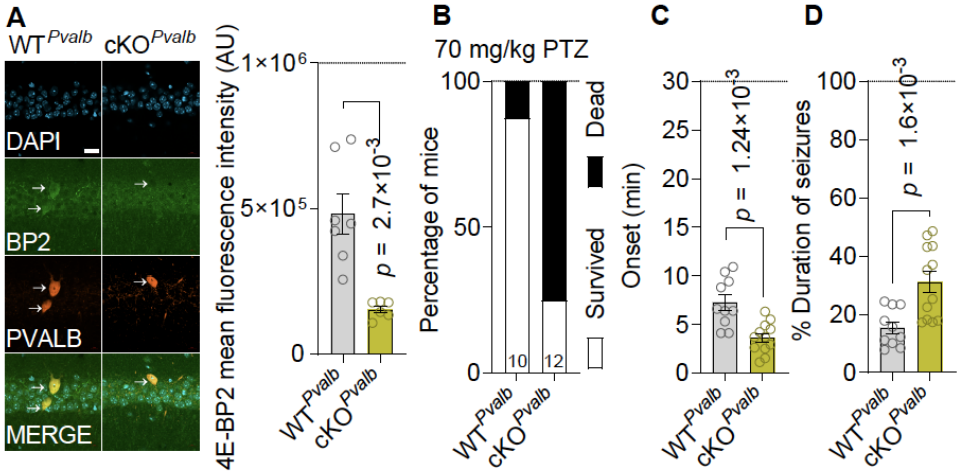

Figure 4. 5: Specific deletion of *Eif4Ebp2* in PVLAB^{+}-expressing inhibitory neurons influences the PTZ-induced seizure behavior.
A) Representative immunohistochemical co-staining of 4E-BP2 and parvalbumin in the CA1 region of the hippocampus of *Eif4Ebp2*$^{flx/flx}$*; Pvalb-Cre*$^{+}$ mice. After perfusion, brain tissues were fixed and cut into 40 µm sections. Sections were incubated in blocking buffer followed by immunostaining of 4E-BP2 (1:400) and parvalbumin (1:1000). DAPI (1:5000) was used to visualize cell nuclei. The pyramidal cell layer of the hippocampal CA1 region was used for immunofluorescence imaging and quantification. Quantitative analyses of 4E-BP2 mean fluorescence intensity are shown in the right panel. **B-D)** Mortality rates, seizure onsets, and cumulative duration of seizure of cKO^{Pvalb} and WT^{Pvalb} mice during 30 minutes after being injected with 70 mg/kg of PTZ. Scale bar = 20 µm. A two-tailed unpaired *t*-test with Welch's correction was used to compare the two groups. Quantitative data with mean ± SEM are shown (Sharma *et al.*, 2021).

To validate the importance of 4E-BP2 in PVALB^{+} neurons, we tested the responses of cKO^{Pvalb} and WT^{Pvalb} mice in the KA-induced epilepsy model. Within 30 minutes post-injection of 30 mg/kg of KA, cKO^{Pvalb} mice showed a significant earlier onset of first seizure (67.48 ± 3.51%, $t_{7.224}$ = 2.413, P = 0.0455, n = 8, 9; Figure 3.9 B) and an increase in total seizure duration (122.94 ± 24.85%, $t_{12.14}$ = 2.67, P = 0.02, n = 8, 9; Figure 3.9 C), comparing

to WT^{Pvalb} group. These results suggested that the deletion of 4E-BP2 in parvalbumin neurons also lowers the KA-induced seizure threshold.

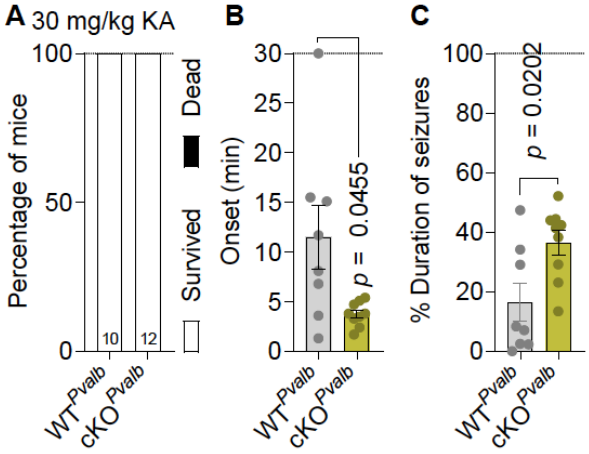

Figure 4. 6: *Eif4Ebp2*$^{flx/flx}$*; Pvalb-Cre*$^{+}$ mice showed severer responses in the kainic acid-induced epileptic model.
A-C) Mortality rates, seizure onsets, and cumulative duration of seizure of cKO^{Pvalb} and WT^{Pvalb} mice during 30 minutes after injection with 30 mg/kg of KA. A two-tailed unpaired test with Welch's correction was used to compare the two groups. Quantitative data with mean ± SEM are shown (Sharma *et al.*, 2021).

To provide insights into the neuronal circuits of cKO^{Pvalb} mice, we implanted a bipolar recording electrode into the CA3 region of the hippocampus and performed EEG recordings in cKO^{Pvalb} and WT^{Pvalb} mice after being injected with 50 mg/kg of PTZ (Figure 3.10 A). During the first 10 minutes post-injection, cKO^{Pvalb} mice had earlier onsets (61.74 ± 7.8%, $t_{13.17} = 5.29$, $P = 1.4 \times 10^{-4}$, $n = 7, 9$, Figure 3.10 C) and a longer duration of electrographic seizures (WT^{Pvalb}, 1.89 ± 1.12% and cKO^{Pvalb} 12.5 ± 3.92% seizure duration, $t_{9.27} = 2.61$, $P = 0.0277$, $n = 7, 9$, Figure 3.10 D), based on EEG signal analysis. Based on these observations, we concluded that the deletion of 4E-BP2 in PVALB^{+} neurons resulted in the hyperexcitability of hippocampal CA3 circuits and a lowered threshold for seizure induction.

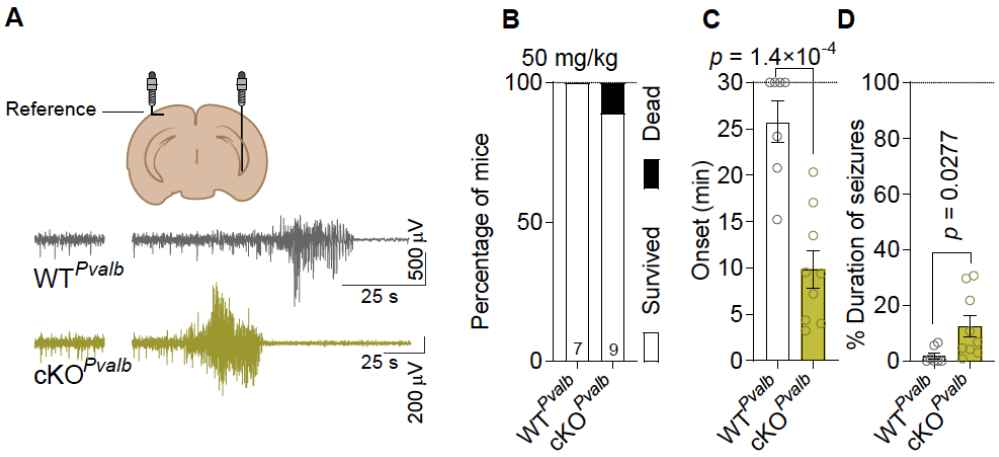

Figure 4. 7: Deletion of *Eif4Ebp2* in PVLAB$^+$ neurons enhanced EEG seizure activity upon PTZ induction.
A) Layout of electrode implantations and representative EEG traces of PTZ-induced seizure in cKO^{Pvalb} and WT^{Pvalb} mice. **B-D)** Mortality rates, seizure onsets, and cumulative duration of seizure of cKO^{Pvalb} and WT^{Pvalb} mice during 3 hours after being injected with 50 mg/kg of PTZ. A two-tailed unpaired test with Welch's correction was used to compare the two groups. Quantitative data with mean ± SEM are shown (Sharma *et al.*, 2021).

4.3.3 Conditional knock-in of human *Pik3ca^{H1047R}* mutation in PVALB$^+$ neurons increases seizure susceptibility

Our previous findings demonstrate the importance of mTORC1 signaling in PVALB$^+$ neurons in different drug-induced seizure models, and here we further investigated whether hyperactivation of PI3K, an upstream factor of the mTORC1 pathway, would have any effect on epileptogenesis. Therefore, we first generated mutant mice carrying heterozygous germline human *Pik3ca^{H1047R}* mutation in PVALB$^+$ neurons (*Pik3ca$^{H1047R\text{-}Pvalb}$*, Figure 3.11 A). The mutant PI3K protein has a hyperactivated catalytic p110α subunit, which would lead to the constitutive activation of mTORC1 via its subsequent signaling cascade (Sharma *et al.*, 2021). In PTZ-induced epilepsy model, *Pik3ca$^{H1047R\text{-}Pvalb}$* mice showed a higher mortality rate (Figure 3.11 B), a reduced latency to first seizure (28.21 ± 7.99%, $t_{25.07} = 2.185$, $P = 0.0384$, $n = 13, 19$, Figure 3.11 C), and an increase in the total duration of seizure within 30 minutes after injection of 70 mg/kg of PTZ (78.25 ± 24.02%, $t_{28.80} = 2.726$, $P = 0.0108$, $n = 13, 19$, Figure 3.11 D), as compared to WT control mice (*Pvalb-Cre*$^+$ (WT^{Pvalb}) mice). These data indicate that the susceptibility to PTZ-induced seizures is raised by hyperactivating PI3K in PVALB$^+$ neurons.

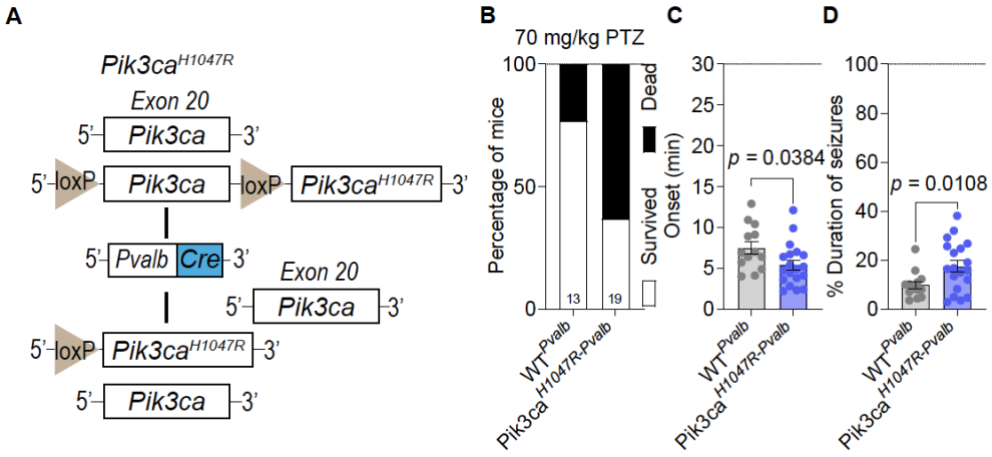

Figure 4. 8: Mice carrying a heterozygotic mutation of human *Pik3ca*^{H1047R} in PVALB^{+} neurons have a lower PTZ-induced seizure threshold.
A) Genetic design of PVALB^{+} neuron-specific heterozygotic knock-in of human *Pik3ca*^{H1047R} mutant. The exon 20 of one of the alleles of the *Pik3ca* gene is flanked by LoxP sites, followed by a mutant copy of exon 20. After crossing this transgenic line with mice expressing Cre recombinase under parvalbumin promoter, the offspring of this lineage express a hyperactivated form of PI3K protein. **B-D)** Mortality rates, seizure onsets, and cumulative seizure duration of *Pik3ca*$^{H1047R\text{-}Pvalb}$ and WT^{Pvalb} mice during 30 minutes after being injected with 70 mg/kg of PTZ. A two-tailed unpaired test with Welch's correction was used to compare the two groups. Quantitative data with mean ± SEM are shown (Sharma *et al.*, 2021).

4.3.4 The hyperactivation of PI3K results in an active mTORC1 pathway

To access the outcomes of enhanced PI3K kinase activity in PVALB^{+} neurons at the molecular level, we immunostained p-Akt at Ser473, a target of mTORC1, via positive feedback loop. Immunohistochemical analysis of the hippocampal slices showed that the intensity of p-Akt (Ser473) normalized to the intensity of total Akt was significantly elevated in the PVALB^{+} neurons of the *Pik3ca*$^{H1047R\text{-}Pvalb}$ mutant mice as compared to WT^{Pvalb} mice (26.14 ± 19.14%, $t_{8.53} = 2.813$, $P = 0.0389$, $n = 6, 6$, Figure 3.12A). We also examined the level of p-S6 (Ser240/244) as an indication of mTORC1 activity via its direct target S6K. The phosphorylation of S6 at Ser240/244 was also significantly increased in the PVALB^{+} neurons of the *Pik3ca*$^{H1047R\text{-}Pvalb}$ mutants (42.29 ± 18.38%, $t_{9.478} = 3.487$, $P = 0.0133$, $n = 6, 6$, Figure 3.12B). Confocal microscopy analysis showed that the level of p-Akt and p-S6 were constant in PVALB^{+} neurons of the cKO^{Pvalb} mice compared to WT^{Pvalb} mice (Figure 3.12). Therefore, it was concluded that hyperactivating PI3K in PVALB^{+} neurons increased mTORC1 kinase activity.

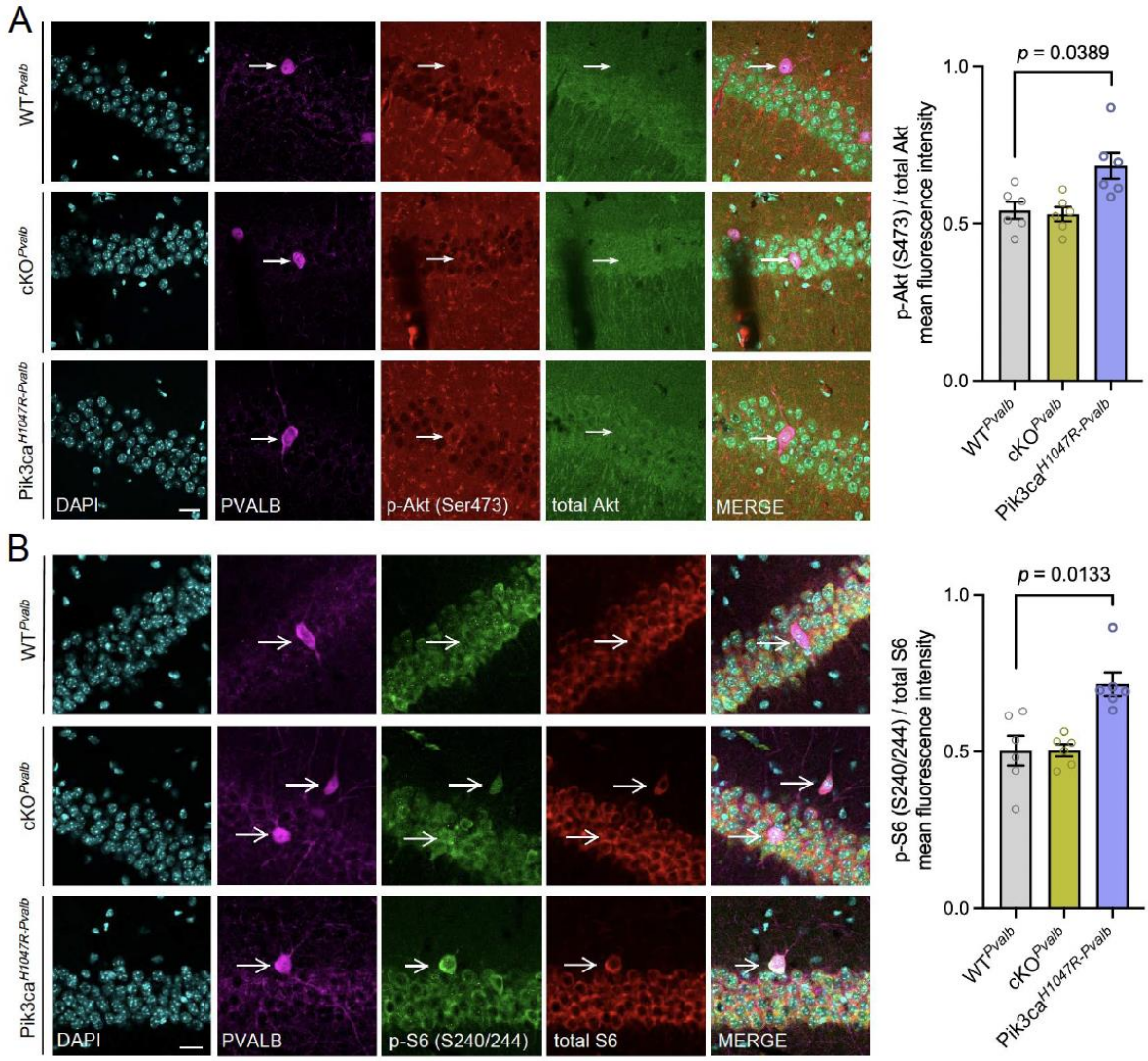

Figure 4. 9: Increased mTORC1 activity in PVALB^{+} neurons due to a PI3K hyperactivation mutation.

A) Representative immunohistochemical co-staining of p-Akt (S473), total Akt, and parvalbumin in the CA1 region of the hippocampus of WT^{Pvalb}, cKO^{Pvalb}, and *Pik3ca*$^{H1047R\text{-}Pvalb}$ mice. After perfusion, brain tissues were fixed and cut into 40 µm sections. Sections were incubated in blocking buffer and followed by immunostaining of p-Akt (S473) (1:400), Akt (1:400), and parvalbumin (1:1000). DAPI (1:5000) was used to visualize cell nuclei. The pyramidal cell layer of the hippocampal CA1 region was used for immunofluorescence imaging and quantification. Quantitative analyses of p-Akt (S473)/total Akt mean fluorescence intensity is shown in the right panel. **B)** Representative immunohistochemical co-staining of p-S6 (Ser240/244), total S6, and parvalbumin in the CA1 region of the hippocampus of WT^{Pvalb}, cKO^{Pvalb}, and *Pik3ca*$^{H1047R\text{-}Pvalb}$ mice. After perfusion, brain tissues were fixed and cut into 40 µm sections. Sections were incubated in blocking buffer and followed by immunostaining of p-S6 (S240/244) (1:400), S6 (1:500), and parvalbumin (1:1000). DAPI (1:5000) was used to visualize cell nuclei. The pyramidal cell layer of the hippocampal CA1 region was used for immunofluorescence imaging and quantification. Quantitative analyses of p-S6 (S240/244)/total S6 mean fluorescence intensity is shown in the right panel. Scale bar = 20 µm. One-way ANOVA followed by Dunnett's T3 multiple comparisons test was used. Quantitative data with mean ± SEM are shown.

In this chapter, we first showed that ablating 4E-BP2 in inhibitory neurons lowered the seizure threshold. And then, we determined that $PVALB^+$ neurons are the most important to mTORC1-related epileptogenesis among three major groups of inhibitory neurons. Moreover, $PVALB^+$ neuron-specific knockout of 4E-BP2 increased the severity of seizures in mice in PTZ- and KA-induced epilepsy models.

CHAPTER 5: Investigating the Cellular Changes in the Hippocampus due to Parvalbumin Neuron-Specific mTORC1 Hyperactivation

5.1 Introduction

Because mTORC1 signaling in CNS carefully regulates neurogenesis, cell growth, and renewal, a continuous neuronal mTORC1 dysregulation could lead to circuitry changes in the brain, which is one of the mechanisms that drive epileptogenesis (Lasarge and Danzer, 2014; Licausi and Hartman, 2018). Recent studies have demonstrated that hyperactivating the mTOR pathway in hippocampal granule cells would lead to recurrent circuits, interneuron loss, and epileptic seizures in those mutant mice (Lasarge *et al.*, 2021). Therefore, we aim to study the cellular phenotypic changes caused by the deletion of 4E-BP2 in $PVALB^+$ neurons, which may explain the lowered seizure threshold in mutant mice.

5.2 Experimental Aims

To gain further insights on how the enhanced mTORC1 activity in $PVALB^+$ neurons leads to a lowered seizure threshold, we set to determine whether there were any phenotypic changes at tissue and cellular levels. Using immunohistochemistry, we examined the population size of $PVALB^+$ neurons in the hippocampus and the expression of perineuronal nets which regulate the activity of $PVALB^+$ neurons. To study if hippocampal synaptic components were affected by the $PVALB^+$ neuron-specific mTORC1 hyperactivation, we examined the expression of different synaptic proteins in purified synaptic fractions from the mouse hippocampus.

5.3 Results and Conclusions

5.3.1 mTORC1 hyperactivity in parvalbumin neurons results in reduced CA1 $PVALB^+$ neuron population in adult mice

Previous immunostaining of $PVALB^+$ neurons in the hippocampal sections of adult WT^{Pvalb}, cKO^{Pvalb}, and $Pik3ca^{H1047R\text{-}Pvalb}$ mice suggested a reduction of the number of Wisteria floribunda agglutinin- (WFA-) positive $PVALB^+$ neurons specifically in the CA1 regions of the hippocampi of mutant mice as compared to WT control mice (cKO^{Pvalb}: 39.90 ± 4.81%, $t_{5.037} = 5.741$, $P = 0.0042$, $n = 5, 4$; $Pik3ca^{H1047R\text{-}Pvalb}$: 37.50 ± 12.41%, $t_{6.938} = 4.156$, $P =$

0.0081, n = 5, 4, Figure 3.13 A and B), while the CA2, CA3 and Dentate Gyrus (DG) population remain similar (Data not shown).

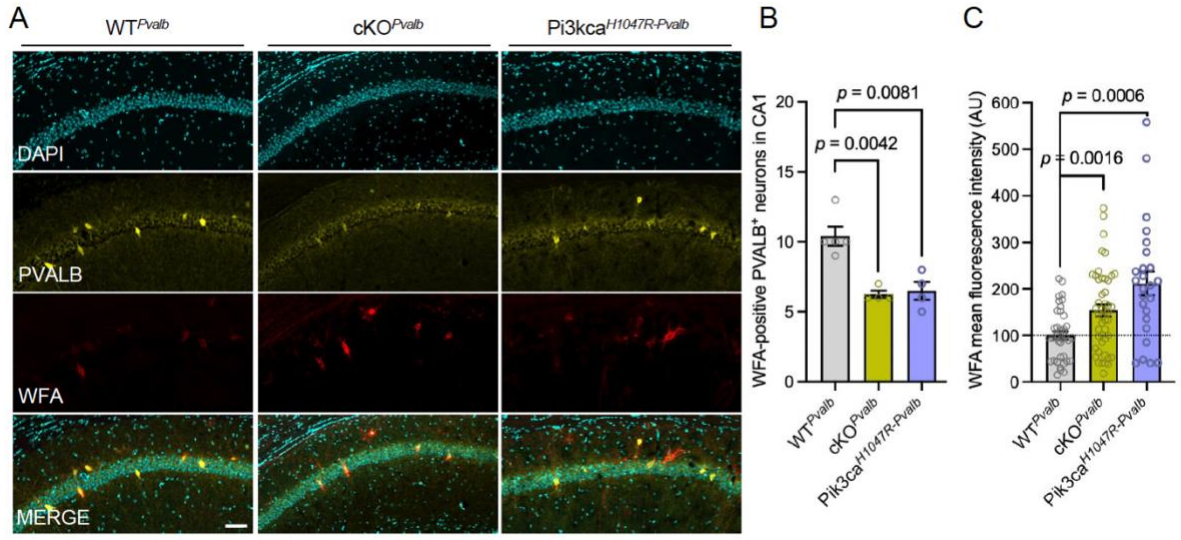

Figure 5. 1: Reduced PVALB$^+$ neurons and increased WFA intensity in the CA1 region due to mTORC1 hyperactivity.
A) Representative immunohistochemical co-staining of WFA and parvalbumin in the CA1 region of the hippocampus of WT^{Pvalb}, cKO^{Pvalb}, and *Pik3ca*$^{H1047R\text{-}Pvalb}$ mice. After perfusion, brain tissues were fixed and cut into 40 µm sections. Sections were incubated in blocking buffer, followed by WFA (1:500) and parvalbumin (1:1000) immunostaining. DAPI (1:5000) was used to visualize cell nuclei. **B)** Quantification of the number of WFA-positive PVALB$^+$ neurons in the CA1 region. **C)** Quantification of the WFA intensities of the WFA-positive PVALB$^+$ neurons in the CA1 region. One-way ANOVA followed by Dunnett's T3 multiple comparisons test was used. Mean ± SEM. Scale bar = 40 µm.

To examine the function of the remaining population, we immunofluorescence-labeled perineuronal nets (PNNs), which is a characteristic extracellular matrix structure surrounding PVALB$^+$ neurons and is responsible for controlling neuroplasticity (Carceller *et al.*, 2020). Using WFA to detect N-acetylgalactosamine β residues of the glycoproteins within PNNs (Hilbig *et al.*, 2001), we observed a drastic increment in the density of the PNNs around PVALB$^+$ neurons in the CA1 region in both cKO^{Pvalb} and *Pik3ca*$^{H1047R\text{-}Pvalb}$ groups as compared to the WT^{Pvalb} control group (cKO^{Pvalb}: 53.63 ± 86.83%, $t_{78.94}$ = 3.490, P = 0.0016, n = 40, 47; *Pik3ca*$^{H1047R\text{-}Pvalb}$: 111.41 ± 128.07%, $t_{29.62}$= 4.118, P = 0.0006, n = 40, 25, Figure 3.13 A and C). Based on these statistics, we concluded that PVALB$^+$ neuron-specific hyperactivation of the mTORC1 pathway reduced the number of PVALB$^+$ neurons and elevated the expression of PNNs in the hippocampal CA1 region.

5.3.2 Deletion of 4E-BP2 and PI3K hyperactivation in parvalbumin neurons alters hippocampal synaptic proteins' expression.

To testify if mTORC1 pathway hyperactivation in parvalbumin neurons could affect neuronal signal transduction at the level of synapses, we next performed synaptosome fractionations using hippocampal tissues from adults (6-8-week-old) WT^{Pvalb}, cKO^{Pvalb}, and $Pik3ca^{H1047R\text{-}Pvalb}$ mice. We ran western blots to probe for excitatory and inhibitory synaptic markers at pre- and post-synaptic terminals (Figure 3.14). Mutant mice showed significant higher expressions of postsynaptic density protein 95 (PSD-95, which is a postsynaptic scaffolding protein at excitatory synapses) (cKO^{Pvalb} mice, $P = 0.0059$, n = 5, 5; $Pik3ca^{H1047R\text{-}Pvalb}$ mice, $P = 0.0087$, n = 5, 5, Figure 3.14 B), gephyrin, a postsynaptic scaffolding protein at inhibitory synapses (cKO^{Pvalb} mice, $P = 0.0145$, n = 5, 5; $Pik3ca^{H1047R\text{-}Pvalb}$ mice, $P = 0.0103$, n = 5, 5, Figure 3.14 C), and synapsin, which is responsible for regulating the availability of synaptic vesicles at presynaptic terminals (cKO^{Pvalb} mice, $P = 0.0049$, n = 5, 5; $Pik3ca^{H1047R\text{-}Pvalb}$ mice, $P = 0.0019$, n = 5, 5, Figure 3.14 D). Whereas the levels of the vesicular GABA transporter (V-GAT), which loads GABA into synaptic vesicles in GABAergic neurons and synaptosomal-associated protein 25kDa (SNAP25), which functions in membrane fusion of the synaptic vesicles at presynaptic terminals, remain similar between mutants and WT control mice (Figure 3.14 E and F). These results suggest that the knockout of 4E-BP2 and activation of PI3K protein, therefore mTORC1 hyperactivity in $PVALB^{+}$ neurons may alter the expression of synaptic proteins in adult mouse hippocampus.

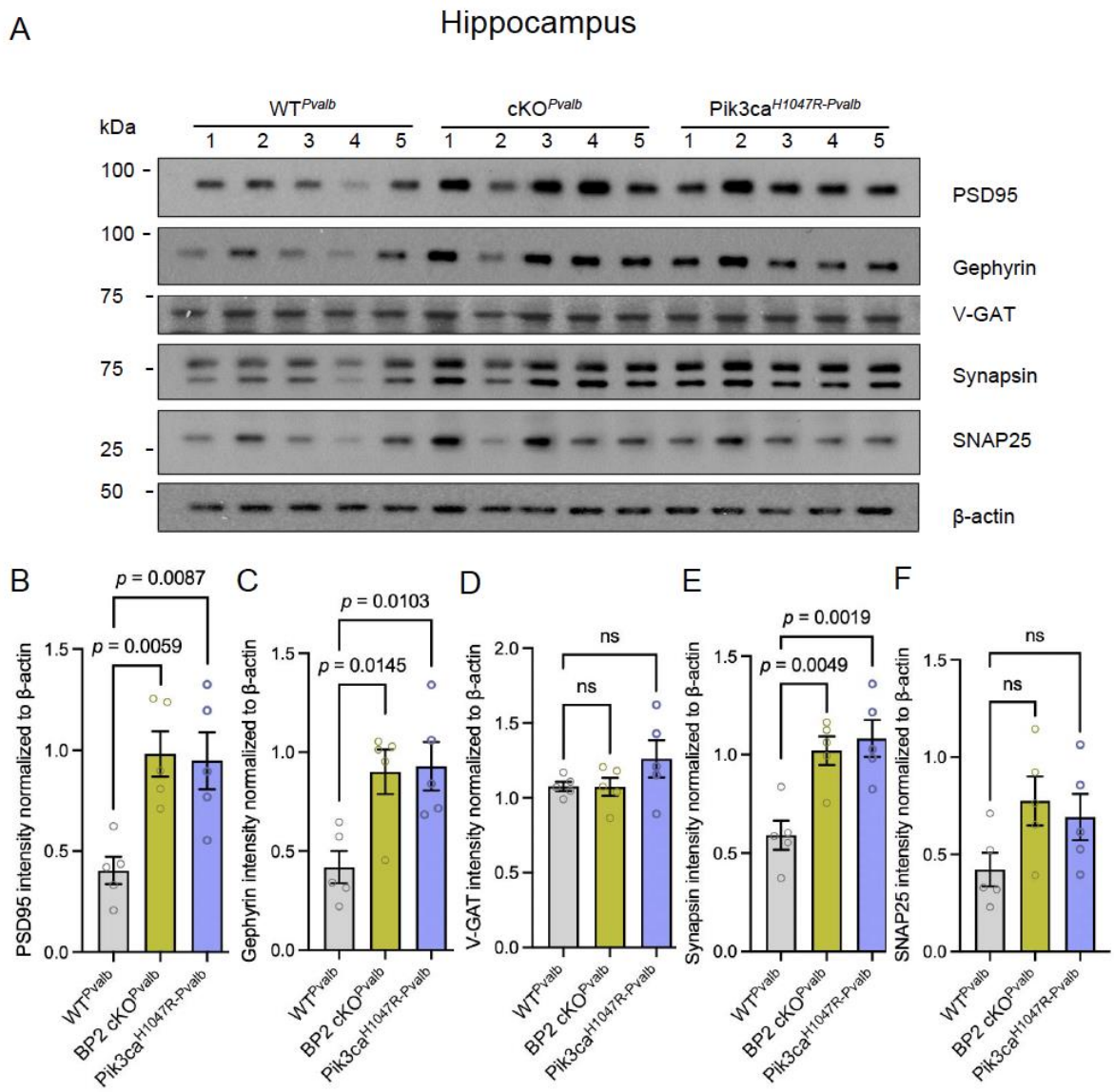

Figure 5. 2: mTORC1 hyperactivation in parvalbumin neurons change the expression level of critical synaptic proteins in the hippocampus.

A) Representative western blot of hippocampal tissue from adult WT^{Pvalb}, cKO^{Pvalb} and *Pik3ca*$^{H1047R\text{-}Pvalb}$ mice. Fresh hippocampi from mice were taken, and tissues from two animals were pooled and homogenized. Synaptosome fractions were isolated using Percoll gradient and ultracentrifugation and then analyzed by western blotting probing for PSD95 (95 kDa) and gephyrin (93 kDa), VGAT (55-60 kDa), synapsin (77 kDa), and SNAP25 (25 kDa). β-actin was used as a loading control at 42 kDa. Each sample represented 2 animals, and 5 samples were used in each group. **B-F)** Quantitative analyses of the intensities of PSD95, gephyrin, VGAT, synapsin, and SNAP25. The intensities were measured using ImageJ and normalized against the intensity of β-actin. One-way ANOVA with multiple comparisons. Quantitative data with mean ± SEM are shown.

In conclusion, in this section, we found that a hyperactive mTORC1 signaling pathway in PVALB^{+} neurons would lead to a reduced number of PVALB^{+} neurons in the hippocampus

and an increased expression of PNNs in the remaining population. It would also cause upregulated expression of synaptic markers, including PSD95, gephyrin, and synapsin.

CHAPTER 6: Discussion

The mTOR signaling is mediated by complexes, mTORC1, and mTORC2 (Chen *et al.*, 2019). mTORC1, as it integrates many cellular and environmental signals and controls the rate of mRNA translation via its downstream effectors, is crucial to maintaining cell and tissue homeostasis (Saxton and Sabatini, 2017). Dysfunction of the mTORC1 signaling pathway in the CNS affects learning and memory consolidation, underlies the molecular switch of addiction, and may lead to the progression of many neurodevelopmental and neurodegenerative diseases, including epilepsy (Costa-Mattioli and Monteggia, 2013; Graber *et al.*, 2013; Neasta *et al.*, 2014; Querfurth and Lee, 2021).

Over the past decades, an accumulative number of studies have revealed the implication of the mTORC1 signaling pathway in epilepsy and epileptogenesis (Cho, 2011). We demonstrated that upon pharmacological induction of seizures using PTZ (70 mg/kg), mice lacking the mTORC1 downstream effector 4E-BP (*Eif4ebp*$^{-/-}$) had, on average, an earlier onset of first seizure, prolonged cumulative duration of seizures, and a higher mortality rate, as compared to WT control mice (Figure 3.2 B-F). Translational dysregulations due to a brain somatic mTOR activation mutation is a known etiology of genetic epilepsy, and it has been proved that the inhibition of mRNA translation using eIF4E inhibitor metformin can alleviate intractable epilepsy symptoms (Kim *et al.*, 2019). A study using a standard epileptic animal model (Rheb^{CA}) has shown a positive correlation between the level of neuronal mTOR activity and the severity of epileptic seizures (Nguyen *et al.*, 2019). Genetic or pharmacological inhibition of eIF4E-dependent translation can partially rescue the behavioral deficits and prevent epileptogenesis in a mouse model for Fragile X syndrome (FXS) (Osterweil *et al.*, 2013; Gkogkas *et al.*, 2014). These results suggest that the disruption of the 4E-BPs' regulation of mRNA translation lowers the epileptic seizure threshold.

There are three isoforms of 4E-BPs in mammals, with different expression patterns in different tissues, among which 4E-BP2 is the most abundant isoform and 4E-BP3 is the least expressed isoform in the mammalian brain (Banko *et al.*, 2005; Bidinosti *et al.*, 2010; Sikalidis *et al.*, 2013) (Figure 3.2 A). It has been reported that the regulation of protein synthesis by mTORC1 via 4E-BP2 is crucial in brain disorders such as ASD (Gkogkas *et al.*, 2013). Mice lacking 4E-BP2 showed autism-related deficits, which could be rescued by inhibiting protein synthesis using an eIF4F inhibitor (Gkogkas *et al.*, 2013). Therefore, we

seek to determine whether the 4E-BP2-dependent translational regulation is also crucial in the progression of epilepsy. We observed that the general deletion of 4E-BP2 aggravated the epileptic seizure behaviors in all three assessed aspects (mortality rate, onset, and cumulative duration) in *Eif4ebp2*$^{-/-}$ mice upon PTZ-induction (Figure 3.3 F-H), whereas the loss of 4E-BP1 in *Eif4ebp1*$^{-/-}$ mice had no significant effect on epileptogenesis (Figure 3.3 B-D). These data indicate that the 4E-BP2 isoform is a specific target of mTORC1 that regulates epileptogenesis. Moreover, the full-body deletion of 4E-BP2 in mice resulted in an Excitation/Inhibition imbalance in the brain associated with neuronal hyperexcitability (Gkogkas *et al.*, 2013).

Neurons in the mammalian CNS are generally classified into two big groups: (excitatory) projection neurons and (inhibitory) interneurons (Masland, 2004; Sosulina *et al.*, 2006). Projection neurons exhibit a pyramidal shape and are glutamatergic, whereas interneurons are mainly inhibitory and GABAergic (Molyneaux *et al.*, 2007). A recent study showed that families of neurons are affected differentially by seizures at the level of transcriptomes, suggesting cell-type specific effects in the generation of seizure episodes (Pfisterer *et al.*, 2020). So far, there is a lack of understanding of whether there is a neuronal cell-type contribution of mTORC1/eIF4E signaling in epileptogenesis, which is essential for further uncovering the pathophysiology of epilepsy. Our data suggest that the deletion of 4E-BP2 in inhibitory interneurons increased the sensitivity to PTZ induction and the severity of induced seizures in both cKO$^{Nkx2.1}$ and cKO^{Gad2} mice (Figure 3.6). In contrast, 4E-BP2 cKO in excitatory neurons had no significant impact in response to PTZ-induction in neither cKO^{Emx1} nor cKO$^{Camk2\alpha}$ mice (Figure 3.5). These results reflect the importance of 4E-BP2 in inhibitory interneurons in regulating network excitability. By releasing GABA as the inhibitory neurotransmitter, inhibitory interneurons counterbalance the excitatory signals to maintain excitatory/inhibitory (E/I) balance in the brain (Khazipov, 2016). Furthermore, the loss of 4E-BP2 in inhibitory neurons, but not in excitatory neurons or astrocytes, could lead to autism-like behavior in rodents (Wiebe *et al.*, 2019). This is not surprising, considering the role of interneurons in maintaining excitatory and inhibitory neuronal properties in the brain (Castillo-Gomez *et al.*, 2016; Dehorter *et al.*, 2017). Our results are consistent with previous studies which discovered a causal link between abnormal GABAergic signaling and epilepsy (Treiman, 2001).

Inhibitory interneurons widely diversify in their physiological functions, and they are divided into different subtypes depending on the expression of characteristic calcium-binding proteins or neuropeptides (Markram *et al.*, 2004; Mayer *et al.*, 2018). There are three major GABAergic neuron subtypes, fast-spiking parvalbumin-expressing ($PVALB^+$) neurons, non-fast-spiking somatostatin-expressing (SST^+) neurons, and bipolar vasoactive intestinal peptide-expressing (VIP^+) neurons (Kelsom and Lu, 2013; Tang *et al.*, 2021). $PVALB^+$ neurons can form perisomatic synapses with pyramidal neurons, SST^+ neurons synapse onto distal dendrite of the pyramidal cells, and VIP^+ neurons target both $PVALB^+$ and SST^+ neurons to regulate their inhibition of excitatory neurons (Wamsley and Fishell, 2017; Tang *et al.*, 2021). We examined the outcomes of 4E-BP2 deletion in these three major groups of inhibitory interneurons in the brain. Our results indicated that deletion of 4E-BP2 in $PVALB^+$ neurons significantly lowered the threshold of PTZ-induced seizure in cKO^{Pvalb} mice (Figure 3.8). However, the deletion of 4EBP2 in the SST^+ or VIP^+ neurons could not promote epileptogenesis in cKO^{Sst} or cKO^{VIP} mice (Figure 3.7). In the mice with a heterozygous human $Pik3ca^{H1047R}$ mutation in $PVALB^+$ neurons, we also observed an increased mortality rate, reduced onset latency, and increased cumulative seizure duration, confirming the essential role of $PVALB^+$ neurons in epileptogenesis (Figure 3.11). $PVALB^+$ neurons account for around 40% of the total GABAergic interneuron population, and they are the major sources of GABA opposing the hyperactive neuronal networks due to their fast-spiking property (Cammarota *et al.*, 2013; Kelsom and Lu, 2013). The power of inhibition onto the excitatory pyramidal neurons is positively correlated to the firing frequencies of $PVALB^+$ neurons, as demonstrated in a model of focal epilepsy using cortical slices (Cammarota *et al.*, 2013). It has been revealed previously that dysfunctional $PVALB^+$ neurons are intricately related to epilepsy and epileptogenesis (Katsarou *et al.*, 2017). In a new mouse model with genetic epilepsy, the reduced inhibitory activities of $PVALB^+$ neurons have been found in the CA1 region of the hippocampus (Das *et al.*, 2021). Our results link the importance of the mTORC1/4E-BP2-dependent translational control and $PVALB^+$ neurons' function to the propagation of epileptic seizures.

Epilepsy is also characterized as interneuronopathy, because it is usually associated with impairments in the development or functions of interneurons (Katsarou *et al.*, 2017). There could be multiple mechanisms underlying the development of the dysfunctional GABAergic system (Chattopadhyaya and Cristo, 2012). In the *Fmr1 KO* mouse model of FXS, a defective GABAergic system has been noticed in the amygdala region, marked by attenuated

inhibitory post-synaptic currents and loss of inhibitory synapses (Olmos-Serrano *et al.*, 2010). As shown in post-mortem human epileptic brains, the number of hippocampal PVALB$^+$ neurons was significantly decreased (Sloviter, 1989). Studies illustrate that a defective PVALB$^+$ neuron specification or migration would lead to detrimental seizure outcomes in *Nkx2.1* and LIM homeobox protein 6 (*Lhx6*) mutant mice models (Butt *et al.*, 2008; Neves *et al.*, 2013; Jiang *et al.*, 2016). In accordance with the previous studies, we also found a reduced number of PVALB$^+$ neurons in the hippocampal CA1 regions of cKO^{Pvalb} and *Pik3ca*$^{H1047R\text{-}Pvalb}$ adult mice compared to WT^{Pvalb} control mice (Figure 3.13). Due to their fast-spiking property, PVALB$^+$ neurons have higher ATP requirements than other interneurons, making them vulnerable to different stresses, as evident in many neurological diseases (Kann *et al.*, 2014; Ruden *et al.*, 2021). Previous works using mice with direct mTORC1 hyperactivation in Purkinje cells revealed that a hyperactive mTORC1 signaling pathway could lead to decreased number of Purkinje cells, and this phenotype was reversed by rapamycin treatment to directly inhibit the mTOR function (Sakai *et al.*, 2019). Our results suggested that the loss of hippocampal PVALB$^+$ interneuron population is likely caused by uncontrolled mTORC1/eIF4E-dependent translation mechanisms, reducing the number of GABAergic interneurons in the adults might contribute to the E/I imbalance in the neuronal network and ultimately lowering the seizure threshold. Since all these immunohistochemical experiments were carried out using mice in their adult stages, it is important to determine whether the observed changes were due to altered neurogenesis during development or apoptosis, as the mTORC1 signaling pathway participates in both processes. Further investigations need to be done using mice at different developmental stages, such as adolescence and early childhood, to investigate the effect on neurogenesis by measuring the number of hippocampal PVALB$^+$ neurons at early stages. This could be helpful to understand the time window of the disease onset and provide early intervention for the disease.

In addition to alterations in the number of PVALB$^+$ neurons in the CA1 area, our immunohistochemical analysis using WFA staining also showed an increase in the density of the PNNs surrounding the PVALB$^+$ neurons in the cKO^{Pvalb} and *Pik3ca*$^{H1047R\text{-}Pvalb}$ groups as compared to WT control mice (Figure 3.13). PNNs function to organize ion channels at the membrane, regulate excitatory and inhibitory synapses formation on PVALB$^+$ neurons, and protect PVALB$^+$ neurons from detrimental oxidative stresses (Cabungcal *et al.*, 2013; Fawcett *et al.*, 2019). Drug-induced seizures often degrade PNN components and lead to altered excitability of PVALB$^+$ neurons (Rankin-Gee *et al.*, 2015; Wen *et al.*, 2018).

Moreover, the KO of matrix metalloproteinase 9, an enzyme responsible for PNNs breakdown during the seizure, partially reduced the seizure susceptibility in animal models of temporal lope epilepsy (Wilczynski *et al.*, 2008). Therefore, the observed changes in PNNs in cKO^{Pvalb} and *Pik3ca*$^{H1047R\text{-}Pvalb}$ mice might be one of the mechanisms by which 4E-BP2-dependent translation lowers the threshold for drug-induced seizures. As PNNs comprise multiple different proteoglycans, further investigations into which of its components are upregulated due to mTORC1 hyperactivity are required. Moreover, the functional status of the remaining hippocampal PVALB^{+} neurons is unclear. Thus, an electrophysiology study combined with optogenetics on the hippocampal sections will help to resolve this problem.

We then sought to determine whether synaptic protein expression was altered due to translational dysregulations in PVALB^{+} neurons. Indeed, we found that the expressions of synaptic markers such as PSD-95, gephyrin, and synapsin were all upregulated in the hippocampi of adult cKO^{Pvalb} and *Pik3ca*$^{H1047R\text{-}Pvalb}$ mice as compared to WT^{Pvalb} mice (Figure 3.14). First, PSD-95, which functions to anchor glutamate receptors on the postsynaptic membrane at excitatory synapses, has been increasingly co-assembled with NMDA receptor subunits in brain tissues resected from epileptic patients (Ying *et al.*, 2004; Keith and El-Husseini, 2008). Disruption of the interaction between PSD-95 and the NR2B subunit of NMDA receptor using a synthetic peptide has been proved neuroprotective in a rat status epilepticus model (Dykstra *et al.*, 2009). Therefore, the observed elevated expression of PSD-95 in mutant mice might result in excessive excitatory signals into the pyramidal neurons. Next, gephyrin is the crucial organizer that organizes and stabilizes the GABA receptors on postsynaptic terminals at inhibitory synapses (Choii and Ko, 2015). Dysfunctional gephyrin in the CA1 region of the hippocampus was found to cause instability of GABA receptors at the membranes, suggesting its potential to alter the excitability of the neuronal circuit (Gonzalez, 2013; Gonzalez *et al.*, 2013). On the other hand, increased expressions of gephyrin in newborn neurons following an insult have also been suggested to mitigate the hyperexcitability of the circuitry (Jackson *et al.*, 2012; Gonzalez, 2013). Thus, an increased expression of gephyrin could indicate the reduced inhibitory abilities of PVALB^{+} neurons. Synapsin acts at presynaptic terminals to control the release of neurotransmitters and, therefore, regulates the neuronal network's excitability (Chiappalone *et al.*, 2009; Cesca *et al.*, 2010). Nonsense synapsin I mutant has been identified from a family with hereditary epilepsy, indicating the involvement of synapsin in the disease (Garcia *et al.*, 2004). As revealed by previous studies KO of synapsin in mice showed a robust E/I imbalance with a

decreased basal inhibitory transmission, which might contribute to an epileptic phenotype (Casillas-Espinosa *et al.*, 2012; Farisello *et al.*, 2013; Ketzef and Gitler, 2014). Chiappalone *et al.* have found that KO of synapsin I reduced the amplitude of evoked inhibitory postsynaptic currents and raised the amplitude of evoked excitatory postsynaptic currents (Chiappalone *et al.*, 2009). Thus, the observed increased expression of synapsin in both cKO^{Pvalb} and *Pik3ca*$^{H1047R\text{-}Pvalb}$ mice might represent defective PVALB^{+} neurons, which fail to inhibit pyramidal neurons or prevent them from excessive firings. V-GAT belongs to the family of GABA transporters and is involved in GABA and glycine uptake into synaptic vesicles at the presynaptic terminals (Saito *et al.*, 2010). A recent whole-genome sequencing project from patients with Genetic Epilepsy with Febrile Seizures plus identified missense variants of V-GAT, whose affected transport abilities are detrimental to neuronal inhibition (Heron *et al.*, 2021). SNAP25 is responsible for the fusion of neurotransmitter-containing vesicles at the membranes in exocytosis (Pevsner *et al.*, 1994). A genetic variant has been identified in a patient with encephalopathy with severe generalized epilepsy (Rohena *et al.*, 2013). Indeed, our results showed an increasing trend in the level of expressions of both V-GAT and SNAP25 in both mutant groups, but the differences were not statistically significant. Changes at both pre- and postsynaptic terminals were observed, suggesting that ablation of 4E-BP2 and PI3K mutation in PVALB^{+} neurons would lead to the rewiring of the local circuitry. The observed changes are macroscopic at the tissue level, yet it remains to be elucidated which variations are manifested within PVALB^{+} neurons due to mTORC1 hyperactivation and which variations are manifested in the neighboring neurons as consequences of altered PVALB^{+} neuron functions. The translation profiling of hippocampal PVALB^{+} neurons will provide more accurate analysis.

In conclusion, in this present study, we have demonstrated that 4E-BP2, one of the mTORC1 direct targets, has an essential role specifically in PVALB^{+} interneurons in regulating the epileptic seizure susceptibility. Our adult 4E-BP2 cKO^{Pvalb} mice showed reduced seizure threshold and increased severity of drug-induced seizures. We also showed that the ablation of 4E-BP2 in PVALB^{+} neurons affects the hippocampal neuronal network, generating phenotypes including loss of CA1 PVALB^{+} neurons with increased PNNs' densities and dramatic changes in hippocampal synaptic transmissions. These phenotypes might contribute to the E/I imbalance in the brain, which is known to underly epilepsy and epileptogenesis. Further investigation into the detailed molecular changes taking place in the PVALB^{+} interneurons will be helpful for us to understand the disease. Our findings have proven the

potential of therapeutically targeting dysregulated mTORC1/eIF4E-dependent translation in the brain to treat epilepsy-related disorders. Moreover, efforts could be made to preferentially target $PVALB^{+}$ neurons in designing antiepileptic drugs for mTORC1-related epilepsies.

CHAPTER 7: Materials and Method

7.1 Reagents

- **Genotyping**: NaOH, ethylenediaminetetraacetic acid (EDTA) (BioShop EDT001.1), Trizma® hydrochloride (Tris-HCl, SIGMA T5941), AccuStart™ II GelTrack PCR SuperMix (Quantabio P/N 84228), Endotoxin-Free Ultra Pure Water (EMD Millipore TMS-011-A), 50X TAE buffer stock (50 mM EDTA, 2 M Tris, 1M Glacial acetic acid in deionized water), Agarose (Froggarose LE, FraggaBio A87), Ethidium Bromide (EtBr, Sigma-Aldrich), 100 bp DNA ladder RTU (FraggaBio DM001-R500F)

Table 7. 1 List of primers used in genotyping

Primer Name	Oligo Sequence (5' to 3')	Company
BP2 Flox-F	GTC GGT CTT CTG TAG ATT GTG AGT	IDT
BP2 Flox-R	GGC GAT CCC TAG AAA ATA AAG CCT	IDT
Cre F	GAT TGC TTA TAA CAC CCT GTT ACG	IDT
Cre R	GTA AAT CAA TCG ATG AGT TGC TTC A	IDT
PI3KCa 19F	TTG GTT CCA GCC TGA ATA AAG C	IDT
PI3KCa 20F	TCC ACA CCA TCA AGC AGC A	IDT
PI3KCa 20R	GTC CAA GGC TAG AGT CTT TCG G	IDT

- **Western Blotting**: Pierce™ BCA protein Assay Kit (ThermoScientific 23225), Sodium Dodecyl Sulfate (SDS, BioShop SDS999), Ponceau S solution (CEPHAM LIFE SCIENCE 10396), Western Lightening® Plus ECL (PerkinElmer 0RT2655), Bovine Serum Albumin (BSA, BioShop ALB001), Skim Milk Powder, 2X SDS-Sample Buffer (1M Tris-HCl pH 6.8, 10% SDS, 20% Glycerol, 5% β-mercaptoethanol, 1% Bromophenol Blue, Deionized water), 4-12% Bis-Tris Midi Gel (NuPAGE®, Invitrogen WG1403B0X), MOPS SDS Running Buffer (NuPAGE®, 20X, NOVEX™ NP0001), Transfer Buffer (25 mM Tris, 190 mM Glycine, 20% Methanol, Deionized water), Washing Buffer [Tris-HCl (Sigma-Aldrich T5941), NaCl, Tween-20 (BioShop TWN510), deionized water], Stripping Buffer [glycine, Tween-20, Dulbecco's Phosphate Buffered Saline (DPBS, 10X, Sigma-Aldrich, 59331C, deionized water)]

- **Seizure induction**: Kainic acid (KA, Tocris Biosciences UK-0222), pentylenetetrazol (PTZ, Sigma CAS-54-95-5), 0.9% NaCl (Saline, Baxter JB1323),

- **Immunohistochemistry**: DPBS (10X, Sigma-Aldrich 59331C), Phosphate-buffered 4% paraformaldehyde (FD NEURO TECHNOLOGIES INC., PF101), Sucrose (BioShop SUC507), sodium azide (NaN_3, BioShop SAZ001), O.C.T. Compound (Tissue-Tek®, SAKURA 4583), Normal Goat Serum (NGS, abcam ab7481), TRITON® X-100 (BioShop TRX506), 4',6-diamidino-2-phenylindole (DAPI, Invitrogen D1306), SlowFade™ Diamond Antifade Mountant (Invitrogen S36972)

- **Synaptosome fractionation**: Sucrose (BioShop SUC507), Tris-HCl (Sigma-Aldrich T5941), EDTA (BioShop EDT001.1), Percoll® (Sigma-Aldrich P4937), RIPA (Sigma-Aldrich R0278), Protease Inhibitor Cocktail Tablets (cOmplete Tablets, Roche 04 693 132 001), Phosphatase Inhibitor Cocktail 2 and 3 (Sigma-Aldrich, P5726 and P0044), Benzonase® Nuclease (E1014-5UK), Glucose, Na_2HPO_4, $MgCl_2$, $NaHCO_3$, KCl, NaCl

7.2 Animals and Environment

Mice (on a C57BL/6 background) carrying genetic mutations *Eif4ebp1/2/3* triple knockout (*Eif4ebp*$^{-/-/-}$), *Eif4ebp1* knockout (*Eif4ebp1*$^{-/-}$) or *Eif4ebp2* knockout (*Eif4ebp2*$^{-/-}$) were used in this study (Banko *et al.*, 2005; Pearl *et al.*, 2020). For cell-type specific deletion of *Eif4ebp2* in mice, *Eif4ebp2*$^{flx/flx}$ mice were bred with transgenic mice (on a C57BL/6 background) expressing Cre recombinase under different promoters (Exm1, Camk2α, Nkx2.1, Gad2, Pvalb, VIP or Sst promoters) (Wiebe *et al.*, 2019; Sharma *et al.*, 2021). Heterozygous *Pik3ca*$^{H1047R\text{-}Pvalb}$ (*Pvalb-Cre; Pik3ca*$^{H1047R/WT}$) mice were generated by breeding mice expressing *Pvalb-Cre*$^{+}$ and *Pik3ca*^{H1047R} mice (Kinross *et al.*, 2012; Sharma *et al.*, 2021). Mice expressing only Pvalb-Cre^{+} were used as controls in the experiments. Adult mice (6-12 weeks) were used for this research. Food and water were provided *ad libitum* to the mice, and the mice were kept at 12 hours light-dark cycles (07:00 AM to 07:00 PM light period). They were housed on ventilated racks under standard conditions (temperature: 20-21℃, humidity: ~55%) at the Goodman Cancer Institute (GCI), the Montreal Neurological Institute, and the University of Montréal animal facility. All experiments were carried out under the Canadian Council on Animal Care (CCAC) guidelines and were approved by McGill University.

7.3 Protocols

7.3.1 DNA extraction and Genotyping

Ear or tail samples from mice were collected in 1.5 mL Eppendorf tubes. 50 μL of Solution 1 (25 mM NaOH, 0.2 mM EDTA in deionized water) was added to each tube, and samples were incubated at 100℃ for 20 minutes. Samples were then centrifuged at 15,000 rpm for 30 seconds. 50 μL of Solution 2 (40 mM Tris in deionized water) was added to each sample to quench the reaction, and DNA extraction was completed. Extracted samples were stored at -20℃ for future analysis.

Primers were prepared as 5 mM aliquots. Reaction mixtures were made such that the ratio among PCR SuperMix, water, forward primer, reverse primer, and the extracted sample is 5:2:1:1:1 (each reaction mixture had a final volume of 10 μL). Then the polymerase chain reactions (PCRs) were run in a thermocycler (Mastercycler, Eppendorf) with different protocols according to the genes to be detected and the primers used for reactions.

Agarose gels were made with 1-1.5% (w/v) agarose in 1X TAE buffer (40 mM Tris, 20 mM Glacial acetic acid, 1 mM EDTA in deionized water). After the samples and DNA ladders (100 bp) were loaded, gels were run in a gel electrophoresis apparatus filled with 1X TAE buffer at different voltages for different amounts of time depending on the genes be detected. Gels were then read and imaged in AlphaImager as UV gels.

7.3.2 Synaptosome fractionation

Fresh brain from each mouse was dissected, and hippocampi were taken and placed in a pre-chilled homogenizer containing 1500 μL of ice-cold sucrose medium [1X SET: 320 mM sucrose, 5 mM Tris, 1 mM EDTA, protease inhibitor, a phosphatase inhibitor, benzoate nuclease (1:2000), pH 7.4] and the tissue was homogenized on ice. The homogenates were centrifuged at 1,000 g at 4℃ for 10 minutes, and the supernatant was transferred into a new 2 mL Eppendorf tube. The pellets were resuspended in 500 μL of ice-cold sucrose medium and centrifuged again at 1,000 g at 4℃ for 10 minutes. The supernatants were pooled, transferred into polycarbonate centrifuge tubes (Polyallomer, 331372), and ultracentrifuged at 21,000 g at 4℃ for 15 minutes with medium acceleration and medium deceleration. The pellets were resuspended in 500 mL of ice-cold 3% Percoll (v/v).

A discontinuous Percoll gradient was prepared with 5 mL of 24% Percoll (v/v) at the bottom of the polycarbonate centrifuge tube and 5 mL of 10% Percoll (v/v) above it. The resuspended pellet in 3% Percoll was added to the gradient. The column was then ultracentrifuged at 30,750 g at 4℃ for 16 minutes with low acceleration and no deceleration. Tissue materials were divided into three bands (from top to bottom): myelin and membrane fraction, synaptosome fraction, and mitochondrial fraction.

The synaptosome fraction was carefully collected into a 1.5 mL Eppendorf tube and centrifuged at 20,000 g at 4℃ for 15 minutes. Then the supernatant was discarded, and the pellet was eluted in ice-cold ionic media (20 mM HEPES, 10 mM Glucose, 1.2 mM Na_2HPO_4, 1 mM $MgCl_2$, 5 mM $NaHCO_3$, 5 mM KCl, 140 mM NaCl, pH 7.4) several times. The isolated synaptosome fraction was snap-frozen in liquid nitrogen and stored at -80 ℃ for future analysis.

Table 7. 2 Preparation of Percoll gradient

% (v/v)	**100% Percoll (mL)**	**5X SET (mL)**	**H_2O (mL)**
24%	48	40	112
10%	20	40	140
3%	6	40	154

7.3.3 Protein quantification and Western blotting

Hippocampus or isolated synaptosome fraction was lysed in RIPA buffer [50 mM Tris-HCl pH 7.4, 150 mM NaCl, 1% Nonidet P-40 (v/v), 0.1% sodium dodecyl sulfate (SDS) (w/v), 0.5% sodium deoxycholate (w/v), 5 mM EDTA pH 8.0, 1 mM ethylene glycol tetraacetic acid (EGTA) pH 8.0, 10 mM NaF, 1 mM β-glycerophosphate, 1 mM sodium orthovanadate)] with protease inhibitor and phosphatase inhibitor. Protein concentration in each sample was quantified using Pierce™ BCA Protein assay kit (ThermoFisher Scientific, 23225) and absorbance at λ_{562} by VARIOSKAN (Thermo ELECTRON CORPORATION). Samples were then prepared in SDS-sample buffer and heated at 100℃ for 5 minutes.

Proteins were then resolved in 4-12% Bis-Tris Midi Gel in 1X running buffer at 60 volts and then transferred overnight at 4℃ onto nitrocellulose membranes. The membranes were then incubated in blocking solution [3% bovine serum albumin (BSA) (w/v) in tris-buffered saline (20 mM Tris, 150 mM NaCl in deionized water) with 0.1% Tween-20 (TBST) (v/v)] at room

temperature for 1 hour. After being washed three times in TBST for 5 minutes, membranes were incubated in 4% BSA (w/v) in TBST containing primary antibodies at 4°C overnight.

After rinsing three times in TBST for 5 minutes, membranes were incubated in Horseradish peroxidase (HRP)-linked secondary antibodies in 4% BSA in TBST (1:5000) at room temperature for an hour. Then after washing three times in TBST, HRP on the immunoblots was detected by chemiluminescent activity using ECL substrate (PerkinElmer, Inc. Cat#0RT2655). Luminescence was then captured by a charge-coupled device (CCD) camera in ChemiDoc™ XRS+ (BIO-RAD) and the band intensities indicating protein concentrations were analyzed by ImageJ.

Prior to proceeding with re-staining, antibodies on the membranes were incubated in mild stripping buffer (1.5% glycine (w/v), 0.1% SDS (w/v), 1% Tween-20 (v/v) in deionized water, pH 2.2) for 10 minutes and washed in PBS 2 times for 10 minutes and then in TBST 2 times for 10 minutes. Then the membranes were ready for blocking.

Table 7. 3 List of antibodies for Western Blotting

Antibodies	**Company**	**Identifier**	**Dilution**
4E-BP1 (53H11)	Cell Signaling Technology	9644S	1: 1000
4E-BP2	Cell Signaling Technology	2845S	1: 1000
β-actin	Millipore	A1978	1: 1000
PSD95	abcam	ab76115	1: 5000
Gephyrin (G-6)	Santa Cruz	sc-25311	1: 1000
VGAT antibody	Synaptic systems	131011 C3	1: 1000
Synapsin antibody	Cell Signaling Technology	2312S	1: 1000
SNAP25 (SP-12)	Santa Cruz	sc-20038	1: 500
Peroxidase-conjugated AFFINPURE Goat Anti-Rabbit IgG (H+L)	Jackson ImmunoResearch	111-035-003	1:5000
Peroxidase-conjugated AFFINPURE Goat Anti-Mouse IgG (H+L)	Jackson ImmunoResearch	115-035-003	1:5000

7.3.4 Induction and analysis of seizure

Mice aged 2-4 months were injected intraperitoneally with different dosages of PTZ [50, 60, 70 mg/kg (Sigma CAS-54-95-5), dissolved in saline] or KA [10, 20, 30 mg/kg, (Tocris Biosciences UK-0222), dissolved in saline]. Mice were closely monitored after injections,

and videos were recorded for 30 minutes. Epileptic behaviors were scored based on the onset of the first seizure, the duration of total seizure events, and the mortality rates by an observer without knowing the treatments and the genotype of the mice. Mice were then sacrificed by standard euthanasia using carbon dioxide (CO_2), and cervical dislocations confirmed deaths according to CCAC guidelines.

7.3.5 Electrode implantation, EEG recordings, and Analysis

Adult mice, anesthetized using isoflurane, were implanted with a bipolar electrode (20 to 35 kO) into the CA3 region in one hemisphere (coordinates of CA3: anteroposterior, -2.85 mm; lateral, -3.0 mm; ventral, -4.0 mm relative to bregma, according to the Franklin and Paxinos atlas (Franklin and Paxinos, 2013)). An angled reference electrode (5 to 10 kO) was also implanted above the contralateral hemisphere cortex at the same time and sealed in place using dental acrylic cement. Chloramphenicol and lidocaine (5%; Odan) were administrated to the incision site after the surgery. Buprenorphine (0.1 mg/kg, diluted with saline), carprofen (20 mg/kg, diluted with saline), and enrofloxacin (5 mg/kg, diluted with saline) was administrated subcutaneously for perioperative pain relief. 7 days post-operation, the electrodes were connected to a multichannel cable and electrical swivel (Commutator SL 18C, HRS scientific). EEG activity was continuously recorded 24 hours before 3 hours after IP injection of 50 mg/kg of PTZ. EEGs were recorded and amplified by an interface kit (Mobile 36ch LTM ProAmp, Stellate) and low-pass filtered at 500 Hz with a 2,000-Hz sampling rate per channel. The data were collected using monitoring software (Harmonie, Stellate). Mice with decreased body weight 1-week post-implantation were not used for EEG recordings.

7.3.6 Stereotaxic surgery: microinjection of adeno-associated virus (AAV) into adult mouse brain

Mice were anesthetized with 2% isoflurane in oxygen, with their heads positioned in a stereotactic head frame. During the procedure and recovery, the mouse's body temperature was maintained at 37℃ using a temperature-controlled heating pad. 70% alcohol was used to disinfect the incision site before a small cut (< 1 cm) was made on the head skin. Excess blood was removed using hydrogen peroxide to expose the skull and visualize the bregma. A small hole was drilled using Ideal Micro Drill (CellPoint Scientific, 67-1200A) over the CA1 region of the hippocampus of each cerebral hemisphere [coordinates of CA1: anteroposterior,

-1.90 mm; lateral, ±1.00 mm; ventral, -1.50 mm relative to bregma, according to the Franklin and Paxinos atlas (Franklin and Paxinos, 2013)]. An amount of 0.5 μL of AAV9-EF1α-DIO-EYFP-WPRE-hGH ($3.3 \times e^{13}$ GC/mL; Addgene 27056-AAV9) was injected into each CA1 region at a rate of 50 nL per minute using a 5-μL Hamilton syringe with a 23G needle (HAMILTON) attached to the stereotactic infusion pump. The needle was kept in the injection site for 5 minutes before and after the surgery to minimize fluid retraction. The skin was sealed using tissue adhesive (3M Vetbond, No. 1469SB), followed by a suture (ETHICON VICRYL, J386). Carprofen (20 mg/kg, diluted with saline) was administrated subcutaneously for perioperative pain relief. Mice were monitored on the heating pad till they regained consciousness and in their home cages for the following 2-3 weeks before any experiments were conducted.

7.3.7 Transcardiac perfusion and immunohistochemistry

Mice were anesthetized with 2% isoflurane in oxygen and perfused transcardially using ice-cold 1X PBS followed by ice-cold 4% PFA. Brains were removed and fixed in 4% PFA at 4℃ overnight and then transferred into 30% sucrose with 0.03% NaN_3 in deionized water for cryoprotection at 4℃ for three days till the brains sank to the bottom of the tubes. Brains were then snap-frozen using liquid nitrogen, sectioned into 20-40-μm-thick slices using a cryostat, and stored in PBS with 0.03% NaN_3 at 4℃ for future analysis.

Prior to immunofluorescent staining, brain slices were washed in PBS 3 times for 5 minutes and blocked-in blocking solution [20% NGS (v/v), 0.1% TRITON X-100 (v/v) in PBS] at 37℃ for 1-3 hours. Slices were then incubated in primary antibodies in 2% NGS in PBS at 4℃ overnight. Sections were washed in PBS 3 times for 5 minutes and then incubated in secondary antibodies diluted 1:400 in PBS containing 2% NGS for 1-2 hours.

After being rinsed again in PBS 3 times for 5 minutes, the slices were stained with DAPI [1:5000 (v/v) in PBS] and then mounted onto adhesion microscope slides (Polysine slides, Epredia P4981-001) with SlowFade™ Diamond Antifade Mountant (Invitrogen, S36972) and covered by cover glasses (Fisher Scientific, 125485P).

Table 7. 4 List of antibodies for Immunohistochemistry

Antibodies	Company	Identifier	Dilution
4E-BP2	Cell Signaling Technology	2845S	1:400
Camk2α (Cba-2)	Invitrogen	13-730	1:1000
GAD67	Millipore	MAB5406	1:1000
Parvalbumin	Sigma-Aldrich	P3088	1:2000
Parvalbumin	Synaptic Systems	195004	1:1000
Parvalbumin	Synaptic Systems	195006	1:1000
Somatostatin	Millipore	MAB354	1:100
AKT (pan) (C67E7)	Cell Signaling Technology	4691S	1:400
Phospho-AKT (Ser473)	Proteintech	66444-1	1:400
Ribosomal Protein S6	Santa Cruz	sc-74459	1:500
Phospho-S6 Ribosomal Protein (Ser240/244)	Cell Signaling Technology	2215	1:400
WFA	Vector Labs B	1355	1:500
Alexa Fluor™ 488 goat anti-mouse IgG (H+L)	Invitrogen	A28175	1:400
Alexa Fluor™ 546 goat anti-mouse IgG (H+L)	Invitrogen	A11030	1:400
Alexa Fluor™ 647 goat anti-mouse IgG (H+L)	Invitrogen	A21235	1:400
Alexa Fluor™ 488 goat anti-rabbit IgG (H+L)	Invitrogen	A11008	1:400
Alexa Fluor™ 546 goat anti-rabbit IgG (H+L)	Invitrogen	A11035	1:400
Alexa Fluor™ 594 goat anti-rabbit IgG (H+L)	Invitrogen	A11012	1:400
Alexa Fluor™ 647 goat anti-rabbit IgG (H+L)	Invitrogen	A21245	1:400
Alexa Fluor™ 647 goat anti-guinea pig IgG (H+L)	Invitrogen	A21450	1:400
Alexa Fluor™ 647 goat anti-rat IgG (H+L)	Invitrogen	A21247	1:400
Alexa Fluor™ 647 goat anti-chicken IgY (H+L)	Invitrogen	A21449	1:400
Streptavidin, Alexa Fluor™ 647 conjugate	Invitrogen	S21374	1:400
Streptavidin, Alexa Fluor™ 488 conjugate	Invitrogen	S11223	1:400

7.3.8 Image analysis and statistical analysis

The brain slices were imaged using a confocal microscope (Zeiss LSM 880 with Airyscan), and the images were analyzed using ImageJ (NIH). GraphPad Prism 8.0-9.0 (GraphPad Prism Software Inc.) was used for statistical analysis. Statistic differences between the two groups were determined using a two-tailed unpaired Student's *t*-test with Welch's correction. The statistical significance differences at different time points were determined using a two-way repeated measure ANOVA or mixed-effects model (restricted maxi- mum likelihood [REML]). The post hoc test (Tukey's or Sidak's, α-level of 0.05 and $P < 0.05$) was used to compare individual groups. Quantitative data are presented as mean ± SEM.

References

ALBERT-GASCO, H. et al. MAP/ERK Signaling in Developing Cognitive and Emotional Function and Its Effect on Pathological and Neurodegenerative Processes. **Int J Mol Sci,** v. 21, n. 12, Jun 23 2020. ISSN 1422-0067 (Electronic)
1422-0067 (Linking). Available at: < https://www.ncbi.nlm.nih.gov/pubmed/32586047 >.

ALKALAEVA, E. Z. et al. In vitro reconstitution of eukaryotic translation reveals cooperativity between release factors eRF1 and eRF3. **Cell,** v. 125, n. 6, p. 1125-36, Jun 16 2006. ISSN 0092-8674 (Print)
0092-8674 (Linking). Available at: < https://www.ncbi.nlm.nih.gov/pubmed/16777602 >.

AMERICAN ASSOCIATION OF NEUROLOGICAL SURGEONS. Epilepsy. Avaialble at: < https://www.aans.org/en/Patients/Neurosurgical-Conditions-and-Treatments/Epilepsy >. Accessed on: December 6.

AMORIM, I. S.; LACH, G.; GKOGKAS, C. G. The Role of the Eukaryotic Translation Initiation Factor 4E (eIF4E) in Neuropsychiatric Disorders. **Front Genet,** v. 9, p. 561, 2018. ISSN 1664-8021 (Print)
1664-8021 (Linking). Available at: < https://www.ncbi.nlm.nih.gov/pubmed/30532767 >.

ANDERSON, M. P. DEPDC5 takes a second hit in familial focal epilepsy. **J Clin Invest,** v. 128, n. 6, p. 2194-2196, Jun 1 2018. ISSN 1558-8238 (Electronic)
0021-9738 (Linking). Available at: < https://www.ncbi.nlm.nih.gov/pubmed/29708509 >.

ANDREOU, A. Z.; KLOSTERMEIER, D. The DEAD-box helicase eIF4A: paradigm or the odd one out? **RNA Biol,** v. 10, n. 1, p. 19-32, Jan 2013. ISSN 1555-8584 (Electronic)
1547-6286 (Linking). Available at: < https://www.ncbi.nlm.nih.gov/pubmed/22995829 >.

ANTION, M. D. et al. mGluR-dependent long-term depression is associated with increased phosphorylation of S6 and synthesis of elongation factor 1A but remains expressed in S6K-deficient mice. **Mol Cell Biol,** v. 28, n. 9, p. 2996-3007, May 2008. ISSN 1098-5549 (Electronic)
0270-7306 (Linking). Available at: < https://www.ncbi.nlm.nih.gov/pubmed/18316404 >.

ANTION, M. D. et al. Removal of S6K1 and S6K2 leads to divergent alterations in learning, memory, and synaptic plasticity. **Learn Mem,** v. 15, n. 1, p. 29-38, Jan 2008. ISSN 1549-5485 (Electronic)
1072-0502 (Linking). Available at: < https://www.ncbi.nlm.nih.gov/pubmed/18174371 >.

ANTONIUK, S. A. et al. Sudden unexpected, unexplained death in epilepsy autopsied patients. **Arq Neuropsiquiatr,** v. 59, n. 1, p. 40-5, Mar 2001. ISSN 0004-282X (Print)
0004-282X (Linking). Available at: < https://www.ncbi.nlm.nih.gov/pubmed/11299429 >.

ARMIJO, J. A. et al. Ion channels and epilepsy. **Curr Pharm Des,** v. 11, n. 15, p. 1975-2003, 2005. ISSN 1381-6128 (Print)
1381-6128 (Linking). Available at: < https://www.ncbi.nlm.nih.gov/pubmed/15974971 >.

BABOO, S. et al. Most human proteins made in both nucleus and cytoplasm turn over within minutes. **PLoS One,** v. 9, n. 6, p. e99346, 2014. ISSN 1932-6203 (Electronic)
1932-6203 (Linking). Available at: < https://www.ncbi.nlm.nih.gov/pubmed/24911415 >.

BACKMAN, S. A. et al. Deletion of Pten in mouse brain causes seizures, ataxia and defects in soma size resembling Lhermitte-Duclos disease. **Nat Genet,** v. 29, n. 4, p. 396-403, Dec 2001. ISSN 1061-4036 (Print)
1061-4036 (Linking). Available at: < https://www.ncbi.nlm.nih.gov/pubmed/11726926 >.

BANKO, J. L. et al. The translation repressor 4E-BP2 is critical for eIF4F complex formation, synaptic plasticity, and memory in the hippocampus. **J Neurosci,** v. 25, n. 42, p. 9581-90, Oct 19 2005. ISSN 1529-2401 (Electronic)
0270-6474 (Linking). Available at: < https://www.ncbi.nlm.nih.gov/pubmed/16237163 >.

BAR-PELED, L.; SABATINI, D. M. Regulation of mTORC1 by amino acids. **Trends Cell Biol,** v. 24, n. 7, p. 400-6, Jul 2014. ISSN 1879-3088 (Electronic)
0962-8924 (Linking). Available at: < https://www.ncbi.nlm.nih.gov/pubmed/24698685 >.

BARKER-HALISKI, M.; WHITE, H. S. Glutamatergic Mechanisms Associated with Seizures and Epilepsy. **Cold Spring Harb Perspect Med,** v. 5, n. 8, p. a022863, Jun 22 2015. ISSN 2157-1422 (Electronic)
2157-1422 (Linking). Available at: < https://www.ncbi.nlm.nih.gov/pubmed/26101204 >.

BAULAC, S. et al. Familial focal epilepsy with focal cortical dysplasia due to DEPDC5 mutations. **Ann Neurol,** v. 77, n. 4, p. 675-83, Apr 2015. ISSN 1531-8249 (Electronic)
0364-5134 (Linking). Available at: < https://www.ncbi.nlm.nih.gov/pubmed/25623524 >.

BENBADIS, S. The differential diagnosis of epilepsy: a critical review. **Epilepsy Behav,** v. 15, n. 1, p. 15-21, May 2009. ISSN 1525-5069 (Electronic)
1525-5050 (Linking). Available at: < https://www.ncbi.nlm.nih.gov/pubmed/19236946 >.

BERG, A. T.; MILLICHAP, J. J. The 2010 revised classification of seizures and epilepsy. **Continuum (Minneap Minn),** v. 19, n. 3 Epilepsy, p. 571-97, Jun 2013. ISSN 1538-6899 (Electronic)
1080-2371 (Linking). Available at: < https://www.ncbi.nlm.nih.gov/pubmed/23739099 >.

BERKOVIC, S. F. et al. Human epilepsies: interaction of genetic and acquired factors. **Trends Neurosci,** v. 29, n. 7, p. 391-397, Jul 2006. ISSN 0166-2236 (Print)
0166-2236 (Linking). Available at: < https://www.ncbi.nlm.nih.gov/pubmed/16769131 >.

BIDINOSTI, M. et al. Postnatal deamidation of 4E-BP2 in brain enhances its association with raptor and alters kinetics of excitatory synaptic transmission. **Mol Cell,** v. 37, n. 6, p. 797-808, Mar 26 2010. ISSN 1097-4164 (Electronic)
1097-2765 (Linking). Available at: < https://www.ncbi.nlm.nih.gov/pubmed/20347422 >.

BLAUWBLOMME, T.; JIRUSKA, P.; HUBERFELD, G. Mechanisms of ictogenesis. **Int Rev Neurobiol,** v. 114, p. 155-85, 2014. ISSN 2162-5514 (Electronic)
0074-7742 (Linking). Available at: < https://www.ncbi.nlm.nih.gov/pubmed/25078502 >.

BOCKAERT, J.; MARIN, P. mTOR in Brain Physiology and Pathologies. **Physiol Rev,** v. 95, n. 4, p. 1157-87, Oct 2015. ISSN 1522-1210 (Electronic)
0031-9333 (Linking). Available at: < https://www.ncbi.nlm.nih.gov/pubmed/26269525 >.

BOLAND, B. et al. Autophagy induction and autophagosome clearance in neurons: relationship to autophagic pathology in Alzheimer's disease. **J Neurosci,** v. 28, n. 27, p. 6926-37, Jul 2 2008. ISSN 1529-2401 (Electronic)
0270-6474 (Linking). Available at: < https://www.ncbi.nlm.nih.gov/pubmed/18596167 >.

BOND, P. Regulation of mTORC1 by growth factors, energy status, amino acids and mechanical stimuli at a glance. **J Int Soc Sports Nutr,** v. 13, p. 8, 2016. ISSN 1550-2783 (Electronic)
1550-2783 (Linking). Available at: < https://www.ncbi.nlm.nih.gov/pubmed/26937223 >.

BOZZI, Y.; CASAROSA, S.; CALEO, M. Epilepsy as a neurodevelopmental disorder. **Front Psychiatry,** v. 3, p. 19, 2012. ISSN 1664-0640 (Electronic)
1664-0640 (Linking). Available at: < https://www.ncbi.nlm.nih.gov/pubmed/22457654 >.

BROWN, E. J. et al. A mammalian protein targeted by G1-arresting rapamycin-receptor complex. **Nature,** v. 369, n. 6483, p. 756-8, Jun 30 1994. ISSN 0028-0836 (Print)
0028-0836 (Linking). Available at: < https://www.ncbi.nlm.nih.gov/pubmed/8008069 >.

BUTT, S. J. et al. The requirement of Nkx2-1 in the temporal specification of cortical interneuron subtypes. **Neuron,** v. 59, n. 5, p. 722-32, Sep 11 2008. ISSN 1097-4199 (Electronic)
0896-6273 (Linking). Available at: < https://www.ncbi.nlm.nih.gov/pubmed/18786356 >.

CABUNGCAL, J. H. et al. Perineuronal nets protect fast-spiking interneurons against oxidative stress. **Proc Natl Acad Sci U S A,** v. 110, n. 22, p. 9130-5, May 28 2013. ISSN 1091-6490 (Electronic)
0027-8424 (Linking). Available at: < https://www.ncbi.nlm.nih.gov/pubmed/23671099 >.

CAMMAROTA, M. et al. Fast spiking interneuron control of seizure propagation in a cortical slice model of focal epilepsy. **J Physiol,** v. 591, n. 4, p. 807-22, Feb 15 2013. ISSN 1469-7793 (Electronic)
0022-3751 (Linking). Available at: < https://www.ncbi.nlm.nih.gov/pubmed/23207591 >.

CANTLEY, L. C. The phosphoinositide 3-kinase pathway. **Science,** v. 296, n. 5573, p. 1655-7, May 31 2002. ISSN 1095-9203 (Electronic)
0036-8075 (Linking). Available at: < https://www.ncbi.nlm.nih.gov/pubmed/12040186 >.

CARCELLER, H. et al. Perineuronal Nets Regulate the Inhibitory Perisomatic Input onto Parvalbumin Interneurons and gamma Activity in the Prefrontal Cortex. **J Neurosci,** v. 40, n. 26, p. 5008-5018, Jun 24 2020. ISSN 1529-2401 (Electronic)
0270-6474 (Linking). Available at: < https://www.ncbi.nlm.nih.gov/pubmed/32457072 >.

CASILLAS-ESPINOSA, P. M.; POWELL, K. L.; O'BRIEN, T. J. Regulators of synaptic transmission: roles in the pathogenesis and treatment of epilepsy. **Epilepsia,** v. 53 Suppl 9, p. 41-58, Dec 2012. ISSN 1528-1167 (Electronic)
0013-9580 (Linking). Available at: < https://www.ncbi.nlm.nih.gov/pubmed/23216578 >.

CASTELLANO, E.; DOWNWARD, J. RAS Interaction with PI3K: More Than Just Another Effector Pathway. **Genes Cancer,** v. 2, n. 3, p. 261-74, Mar 2011. ISSN 1947-6027 (Electronic)
1947-6019 (Linking). Available at: < https://www.ncbi.nlm.nih.gov/pubmed/21779497 >.

CASTILLO-GOMEZ, E. et al. Polysialic Acid Acute Depletion Induces Structural Plasticity in Interneurons and Impairs the Excitation/Inhibition Balance in Medial Prefrontal Cortex Organotypic Cultures. **Front Cell Neurosci,** v. 10, p. 170, 2016. ISSN 1662-5102 (Print)
1662-5102 (Linking). Available at: < https://www.ncbi.nlm.nih.gov/pubmed/27445697 >.

CESCA, F. et al. The synapsins: key actors of synapse function and plasticity. **Prog Neurobiol,** v. 91, n. 4, p. 313-48, Aug 2010. ISSN 1873-5118 (Electronic)
0301-0082 (Linking). Available at: < https://www.ncbi.nlm.nih.gov/pubmed/20438797 >.

CHANG, B. S.; LOWENSTEIN, D. H. Epilepsy. **N Engl J Med,** v. 349, n. 13, p. 1257-66, Sep 25 2003. ISSN 1533-4406 (Electronic)
0028-4793 (Linking). Available at: < https://www.ncbi.nlm.nih.gov/pubmed/14507951 >.

CHATTOPADHYAYA, B.; CRISTO, G. D. GABAergic circuit dysfunctions in neurodevelopmental disorders. **Front Psychiatry,** v. 3, p. 51, 2012. ISSN 1664-0640 (Electronic)
1664-0640 (Linking). Available at: < https://www.ncbi.nlm.nih.gov/pubmed/22666213 >.

CHAUVIN, C. et al. Ribosomal protein S6 kinase activity controls the ribosome biogenesis transcriptional program. **Oncogene,** v. 33, n. 4, p. 474-83, Jan 23 2014. ISSN 1476-5594 (Electronic)
0950-9232 (Linking). Available at: < https://www.ncbi.nlm.nih.gov/pubmed/23318442 >.

CHEN, C. J. et al. Therapeutic inhibition of mTORC2 rescues the behavioral and neurophysiological abnormalities associated with Pten-deficiency. **Nat Med,** v. 25, n. 11, p. 1684-1690, Nov 2019. ISSN 1546-170X (Electronic)
1078-8956 (Linking). Available at: < https://www.ncbi.nlm.nih.gov/pubmed/31636454 >.

CHEN, H. et al. Role of mammalian target of rapamycin in hypoxic or ischemic brain injury: potential neuroprotection and limitations. **Rev Neurosci,** v. 23, n. 3, p. 279-87, Apr 18 2012. ISSN 0334-1763 (Print)
0334-1763 (Linking). Available at: < https://www.ncbi.nlm.nih.gov/pubmed/22752785 >.

CHIANG, G. G.; ABRAHAM, R. T. Phosphorylation of mammalian target of rapamycin (mTOR) at Ser-2448 is mediated by p70S6 kinase. **J Biol Chem,** v. 280, n. 27, p. 25485-90, Jul 8 2005. ISSN 0021-9258 (Print)
0021-9258 (Linking). Available at: < https://www.ncbi.nlm.nih.gov/pubmed/15899889 >.

CHIAPPALONE, M. et al. Opposite changes in glutamatergic and GABAergic transmission underlie the diffuse hyperexcitability of synapsin I-deficient cortical networks. **Cereb Cortex,** v. 19, n. 6, p. 1422-39, Jun 2009. ISSN 1460-2199 (Electronic)
1047-3211 (Linking). Available at: < https://www.ncbi.nlm.nih.gov/pubmed/19020204 >.

CHO, C. H. Frontier of epilepsy research - mTOR signaling pathway. **Exp Mol Med,** v. 43, n. 5, p. 231-74, May 31 2011. ISSN 2092-6413 (Electronic)
1226-3613 (Linking). Available at: < https://www.ncbi.nlm.nih.gov/pubmed/21467839 >.

CHOI, D. W. Glutamate neurotoxicity and diseases of the nervous system. **Neuron,** v. 1, n. 8, p. 623-34, Oct 1988. ISSN 0896-6273 (Print)
0896-6273 (Linking). Available at: < https://www.ncbi.nlm.nih.gov/pubmed/2908446 >.

CHOII, G.; KO, J. Gephyrin: a central GABAergic synapse organizer. **Exp Mol Med,** v. 47, p. e158, Apr 17 2015. ISSN 2092-6413 (Electronic)
1226-3613 (Linking). Available at: < https://www.ncbi.nlm.nih.gov/pubmed/25882190 >.

CHU, Y. et al. Alterations in lysosomal and proteasomal markers in Parkinson's disease: relationship to alpha-synuclein inclusions. **Neurobiol Dis,** v. 35, n. 3, p. 385-98, Sep 2009. ISSN 1095-953X (Electronic)
0969-9961 (Linking). Available at: < https://www.ncbi.nlm.nih.gov/pubmed/19505575 >.

CLOETTA, D. et al. Inactivation of mTORC1 in the developing brain causes microcephaly and affects gliogenesis. **J Neurosci,** v. 33, n. 18, p. 7799-810, May 1 2013. ISSN 1529-2401 (Electronic)
0270-6474 (Linking). Available at: < https://www.ncbi.nlm.nih.gov/pubmed/23637172 >.

COSTA-MATTIOLI, M.; MONTEGGIA, L. M. mTOR complexes in neurodevelopmental and neuropsychiatric disorders. **Nat Neurosci,** v. 16, n. 11, p. 1537-43, Nov 2013. ISSN 1546-1726 (Electronic)
1097-6256 (Linking). Available at: < https://www.ncbi.nlm.nih.gov/pubmed/24165680 >.

CRINO, P. B. The mTOR signalling cascade: paving new roads to cure neurological disease. **Nat Rev Neurol,** v. 12, n. 7, p. 379-92, Jul 2016. ISSN 1759-4766 (Electronic)
1759-4758 (Linking). Available at: < https://www.ncbi.nlm.nih.gov/pubmed/27340022 >.

DAS, A. et al. Interneuron Dysfunction in a New Mouse Model of SCN1A GEFS. **eNeuro,** v. 8, n. 2, Mar-Apr 2021. ISSN 2373-2822 (Electronic)
2373-2822 (Linking). Available at: < https://www.ncbi.nlm.nih.gov/pubmed/33658306 >.

DAZERT, E.; HALL, M. N. mTOR signaling in disease. **Curr Opin Cell Biol,** v. 23, n. 6, p. 744-55, Dec 2011. ISSN 1879-0410 (Electronic)

0955-0674 (Linking). Available at: < https://www.ncbi.nlm.nih.gov/pubmed/21963299 >.

DE LANEROLLE, N. C.; LEE, T. S.; SPENCER, D. D. Histopathology of Human Epilepsy. In: TH;NOEBELS, J. L*., et al* (Ed.). **Jasper's Basic Mechanisms of the Epilepsies**. Bethesda (MD), 2012.

DEHORTER, N. et al. Tuning neural circuits by turning the interneuron knob. **Curr Opin Neurobiol,** v. 42, p. 144-151, Feb 2017. ISSN 1873-6882 (Electronic)
0959-4388 (Linking). Available at: < https://www.ncbi.nlm.nih.gov/pubmed/28088067 >.

DELORENZO, R. J.; SUN, D. A.; DESHPANDE, L. S. Cellular mechanisms underlying acquired epilepsy: the calcium hypothesis of the induction and maintainance of epilepsy. **Pharmacol Ther,** v. 105, n. 3, p. 229-66, Mar 2005. ISSN 0163-7258 (Print)
0163-7258 (Linking). Available at: < https://www.ncbi.nlm.nih.gov/pubmed/15737406 >.

DEVER, T. E.; DINMAN, J. D.; GREEN, R. Translation Elongation and Recoding in Eukaryotes. **Cold Spring Harb Perspect Biol,** v. 10, n. 8, Aug 1 2018. ISSN 1943-0264 (Electronic)
1943-0264 (Linking). Available at: < https://www.ncbi.nlm.nih.gov/pubmed/29610120 >.

DEVINSKY, O. et al. Epilepsy. **Nat Rev Dis Primers,** v. 4, p. 18024, May 3 2018. ISSN 2056-676X (Electronic)
2056-676X (Linking). Available at: < https://www.ncbi.nlm.nih.gov/pubmed/29722352 >.

DHIR, A. Pentylenetetrazol (PTZ) kindling model of epilepsy. **Curr Protoc Neurosci,** v. Chapter 9, p. Unit9 37, 2012. ISSN 1934-8576 (Electronic)
1934-8576 (Linking). Available at: < https://www.ncbi.nlm.nih.gov/pubmed/23042503 >.

DIBBENS, L. M. et al. Mutations in DEPDC5 cause familial focal epilepsy with variable foci. **Nat Genet,** v. 45, n. 5, p. 546-51, May 2013. ISSN 1546-1718 (Electronic)
1061-4036 (Linking). Available at: < https://www.ncbi.nlm.nih.gov/pubmed/23542697 >.

DON, A. S. et al. Targeting mTOR as a novel therapeutic strategy for traumatic CNS injuries. **Drug Discov Today,** v. 17, n. 15-16, p. 861-8, Aug 2012. ISSN 1878-5832 (Electronic)
1359-6446 (Linking). Available at: < https://www.ncbi.nlm.nih.gov/pubmed/22569182 >.

DYKSTRA, C. M.; RATNAM, M.; GURD, J. W. Neuroprotection after status epilepticus by targeting protein interactions with postsynaptic density protein 95. **J Neuropathol Exp Neurol,** v. 68, n. 7, p. 823-31, Jul 2009. ISSN 0022-3069 (Print)
0022-3069 (Linking). Available at: < https://www.ncbi.nlm.nih.gov/pubmed/19535989 >.

ELIA, M. et al. An atypical patient with Cowden syndrome and PTEN gene mutation presenting with cortical malformation and focal epilepsy. **Brain Dev,** v. 34, n. 10, p. 873-6, Nov 2012. ISSN 1872-7131 (Electronic)
0387-7604 (Linking). Available at: < https://www.ncbi.nlm.nih.gov/pubmed/22469695 >.

ENDERSBY, R.; BAKER, S. J. PTEN signaling in brain: neuropathology and tumorigenesis. **Oncogene,** v. 27, n. 41, p. 5416-30, Sep 18 2008. ISSN 1476-5594 (Electronic)

0950-9232 (Linking). Available at: < https://www.ncbi.nlm.nih.gov/pubmed/18794877 >.

ENGEL, J., JR. Surgical treatment for epilepsy: too little, too late? **JAMA,** v. 300, n. 21, p. 2548-50, Dec 3 2008. ISSN 1538-3598 (Electronic)
0098-7484 (Linking). Available at: < https://www.ncbi.nlm.nih.gov/pubmed/19050199 >.

FARISELLO, P. et al. Synaptic and extrasynaptic origin of the excitation/inhibition imbalance in the hippocampus of synapsin I/II/III knockout mice. **Cereb Cortex,** v. 23, n. 3, p. 581-93, Mar 2013. ISSN 1460-2199 (Electronic)
1047-3211 (Linking). Available at: < https://www.ncbi.nlm.nih.gov/pubmed/22368083 >.

FAWCETT, J. W.; OOHASHI, T.; PIZZORUSSO, T. The roles of perineuronal nets and the perinodal extracellular matrix in neuronal function. **Nat Rev Neurosci,** v. 20, n. 8, p. 451-465, Aug 2019. ISSN 1471-0048 (Electronic)
1471-003X (Linking). Available at: < https://www.ncbi.nlm.nih.gov/pubmed/31263252 >.

FISHER, R. S. Animal models of the epilepsies. **Brain Res Brain Res Rev,** v. 14, n. 3, p. 245-78, Jul-Sep 1989. Available at: < https://www.ncbi.nlm.nih.gov/pubmed/2679941 >.

FRANKLIN, K. B. J.; PAXINOS, G. **Paxinos and Franklin's The mouse brain in stereotaxic coordinates**. Fourth edition. Amsterdam: Academic Press, an imprint of Elsevier, 2013. 1 volume (unpaged) ISBN 9780123910578 (hardback).

FRANZ, D. N.; BISSLER, J. J.; MCCORMACK, F. X. Tuberous sclerosis complex: neurological, renal and pulmonary manifestations. **Neuropediatrics,** v. 41, n. 5, p. 199-208, Oct 2010. ISSN 1439-1899 (Electronic)
0174-304X (Linking). Available at: < https://www.ncbi.nlm.nih.gov/pubmed/21210335 >.

FRUMAN, D. A.; MEYERS, R. E.; CANTLEY, L. C. Phosphoinositide kinases. **Annu Rev Biochem,** v. 67, p. 481-507, 1998. ISSN 0066-4154 (Print)
0066-4154 (Linking). Available at: < https://www.ncbi.nlm.nih.gov/pubmed/9759495 >.

GARCIA, C. C. et al. Identification of a mutation in synapsin I, a synaptic vesicle protein, in a family with epilepsy. **J Med Genet,** v. 41, n. 3, p. 183-6, Mar 2004. ISSN 1468-6244 (Electronic)
0022-2593 (Linking). Available at: < https://www.ncbi.nlm.nih.gov/pubmed/14985377 >.

GARZA-LOMBO, C. et al. mTOR/AMPK signaling in the brain: Cell metabolism, proteostasis and survival. **Curr Opin Toxicol,** v. 8, p. 102-110, Apr 2018. ISSN 2468-2934 (Print)
2468-2020 (Linking). Available at: < https://www.ncbi.nlm.nih.gov/pubmed/30417160 >.

GAUTAM, V. et al. An insight into crosstalk among multiple signaling pathways contributing to epileptogenesis. **Eur J Pharmacol,** v. 910, p. 174469, Nov 5 2021. ISSN 1879-0712 (Electronic)
0014-2999 (Linking). Available at: < https://www.ncbi.nlm.nih.gov/pubmed/34478688 >.

GILMOUR, H.; RAMAGE-MORIN, P.; WONG, S. L. Epilepsy in Canada: Prevalence and impact. **Health Rep,** v. 27, n. 9, p. 24-30, Sep 21 2016. ISSN 1209-1367 (Electronic)
0840-6529 (Linking). Available at: < https://www.ncbi.nlm.nih.gov/pubmed/27655169 >.

GINGRAS, A. C. et al. Hierarchical phosphorylation of the translation inhibitor 4E-BP1. **Genes Dev,** v. 15, n. 21, p. 2852-64, Nov 1 2001. ISSN 0890-9369 (Print)
0890-9369 (Linking). Available at: < https://www.ncbi.nlm.nih.gov/pubmed/11691836 >.

GKOGKAS, C. G. et al. Pharmacogenetic inhibition of eIF4E-dependent Mmp9 mRNA translation reverses fragile X syndrome-like phenotypes. **Cell Rep,** v. 9, n. 5, p. 1742-1755, Dec 11 2014. ISSN 2211-1247 (Electronic). Available at: < https://www.ncbi.nlm.nih.gov/pubmed/25466251 >.

GKOGKAS, C. G. et al. Autism-related deficits via dysregulated eIF4E-dependent translational control. **Nature,** v. 493, n. 7432, p. 371-7, Jan 17 2013. ISSN 1476-4687 (Electronic)
0028-0836 (Linking). Available at: < https://www.ncbi.nlm.nih.gov/pubmed/23172145 >.

GOLDBERG, E. M.; COULTER, D. A. Mechanisms of epileptogenesis: a convergence on neural circuit dysfunction. **Nat Rev Neurosci,** v. 14, n. 5, p. 337-49, May 2013. ISSN 1471-0048 (Electronic)
1471-003X (Linking). Available at: < https://www.ncbi.nlm.nih.gov/pubmed/23595016 >.

GONG, X. et al. Activating the translational repressor 4E-BP or reducing S6K-GSK3beta activity prevents accelerated axon growth induced by hyperactive mTOR in vivo. **Hum Mol Genet,** v. 24, n. 20, p. 5746-58, Oct 15 2015. ISSN 1460-2083 (Electronic)
0964-6906 (Linking). Available at: < https://www.ncbi.nlm.nih.gov/pubmed/26220974 >.

GONZALEZ, M. I. The possible role of GABAA receptors and gephyrin in epileptogenesis. **Front Cell Neurosci,** v. 7, p. 113, 2013. ISSN 1662-5102 (Print)
1662-5102 (Linking). Available at: < https://www.ncbi.nlm.nih.gov/pubmed/23885234 >.

GONZALEZ, M. I.; CRUZ DEL ANGEL, Y.; BROOKS-KAYAL, A. Down-regulation of gephyrin and GABAA receptor subunits during epileptogenesis in the CA1 region of hippocampus. **Epilepsia,** v. 54, n. 4, p. 616-24, Apr 2013. ISSN 1528-1167 (Electronic)
0013-9580 (Linking). Available at: < https://www.ncbi.nlm.nih.gov/pubmed/23294024 >.

GRABER, T. E.; MCCAMPHILL, P. K.; SOSSIN, W. S. A recollection of mTOR signaling in learning and memory. **Learn Mem,** v. 20, n. 10, p. 518-30, Sep 16 2013. ISSN 1549-5485 (Electronic)
1072-0502 (Linking). Available at: < https://www.ncbi.nlm.nih.gov/pubmed/24042848 >.

GRIFFIN, R. J. et al. Activation of Akt/PKB, increased phosphorylation of Akt substrates and loss and altered distribution of Akt and PTEN are features of Alzheimer's disease pathology. **J Neurochem,** v. 93, n. 1, p. 105-17, Apr 2005. ISSN 0022-3042 (Print)
0022-3042 (Linking). Available at: < https://www.ncbi.nlm.nih.gov/pubmed/15773910 >.

GUERRINI, R. et al. Is Focal Cortical Dysplasia/Epilepsy Caused by Somatic MTOR Mutations Always a Unilateral Disorder? **Neurol Genet,** v. 7, n. 1, p. e540, Feb 2021. ISSN 2376-7839 (Print)
2376-7839 (Linking). Available at: < https://www.ncbi.nlm.nih.gov/pubmed/33542949 >.

GWINN, D. M. et al. AMPK phosphorylation of raptor mediates a metabolic checkpoint. **Mol Cell,** v. 30, n. 2, p. 214-26, Apr 25 2008. ISSN 1097-4164 (Electronic)
1097-2765 (Linking). Available at: < https://www.ncbi.nlm.nih.gov/pubmed/18439900 >.

HANAI, S. et al. Pathologic Active mTOR Mutation in Brain Malformation with Intractable Epilepsy Leads to Cell-Autonomous Migration Delay. **Am J Pathol,** v. 187, n. 5, p. 1177-1185, May 2017. ISSN 1525-2191 (Electronic)
0002-9440 (Linking). Available at: < https://www.ncbi.nlm.nih.gov/pubmed/28427592 >.

HANSEN, S. L.; SPERLING, B. B.; SANCHEZ, C. Anticonvulsant and antiepileptogenic effects of GABAA receptor ligands in pentylenetetrazole-kindled mice. **Prog Neuropsychopharmacol Biol Psychiatry,** v. 28, n. 1, p. 105-13, Jan 2004. ISSN 0278-5846 (Print)
0278-5846 (Linking). Available at: < https://www.ncbi.nlm.nih.gov/pubmed/14687864 >.

HARRISON, D. A. The Jak/STAT pathway. **Cold Spring Harb Perspect Biol,** v. 4, n. 3, Mar 1 2012. ISSN 1943-0264 (Electronic)
1943-0264 (Linking). Available at: < https://www.ncbi.nlm.nih.gov/pubmed/22383755 >.

HARTMAN, N. W. et al. mTORC1 targets the translational repressor 4E-BP2, but not S6 kinase 1/2, to regulate neural stem cell self-renewal in vivo. **Cell Rep,** v. 5, n. 2, p. 433-44, Oct 31 2013. ISSN 2211-1247 (Electronic). Available at: < https://www.ncbi.nlm.nih.gov/pubmed/24139800 >.

HAY, N.; SONENBERG, N. Upstream and downstream of mTOR. **Genes Dev,** v. 18, n. 16, p. 1926-45, Aug 15 2004. ISSN 0890-9369 (Print)
0890-9369 (Linking). Available at: < https://www.ncbi.nlm.nih.gov/pubmed/15314020 >.

HEARD, J. J. et al. Recent progress in the study of the Rheb family GTPases. **Cell Signal,** v. 26, n. 9, p. 1950-7, Sep 2014. ISSN 1873-3913 (Electronic)
0898-6568 (Linking). Available at: < https://www.ncbi.nlm.nih.gov/pubmed/24863881 >.

HELBIG, I. et al. Navigating the channels and beyond: unravelling the genetics of the epilepsies. **Lancet Neurol,** v. 7, n. 3, p. 231-45, Mar 2008. ISSN 1474-4422 (Print)
1474-4422 (Linking). Available at: < https://www.ncbi.nlm.nih.gov/pubmed/18275925 >.

HELLEN, C. U. T. Translation Termination and Ribosome Recycling in Eukaryotes. **Cold Spring Harb Perspect Biol,** v. 10, n. 10, Oct 1 2018. ISSN 1943-0264 (Electronic)
1943-0264 (Linking). Available at: < https://www.ncbi.nlm.nih.gov/pubmed/29735640 >.

HEMMINGS, B. A.; RESTUCCIA, D. F. The PI3K-PKB/Akt pathway. **Cold Spring Harb Perspect Biol,** v. 7, n. 4, Apr 1 2015. ISSN 1943-0264 (Electronic)
1943-0264 (Linking). Available at: < https://www.ncbi.nlm.nih.gov/pubmed/25833846 >.

HERON, S. E. et al. Association of SLC32A1 Missense Variants With Genetic Epilepsy With Febrile Seizures Plus. **Neurology,** v. 96, n. 18, p. e2251-e2260, May 4 2021. ISSN 1526-632X (Electronic)
0028-3878 (Linking). Available at: < https://www.ncbi.nlm.nih.gov/pubmed/34038384 >.

HILBIG, H. et al. Wisteria floribunda agglutinin labeling patterns in the human cortex: a tool for revealing areal borders and subdivisions in parallel with immunocytochemistry. **Anat Embryol (Berl),** v. 203, n. 1, p. 45-52, Jan 2001. ISSN 0340-2061 (Print)
0340-2061 (Linking). Available at: < https://www.ncbi.nlm.nih.gov/pubmed/11195088 >.

HINNEBUSCH, A. G.; LORSCH, J. R. The mechanism of eukaryotic translation initiation: new insights and challenges. **Cold Spring Harb Perspect Biol,** v. 4, n. 10, Oct 1 2012. ISSN 1943-0264 (Electronic)
1943-0264 (Linking). Available at: < https://www.ncbi.nlm.nih.gov/pubmed/22815232 >.

HOEFFER, C. A.; KLANN, E. mTOR signaling: at the crossroads of plasticity, memory and disease. **Trends Neurosci,** v. 33, n. 2, p. 67-75, Feb 2010. ISSN 1878-108X (Electronic)
0166-2236 (Linking). Available at: < https://www.ncbi.nlm.nih.gov/pubmed/19963289 >.

HOUSER, C. R. Do structural changes in GABA neurons give rise to the epileptic state? **Adv Exp Med Biol,** v. 813, p. 151-60, 2014. ISSN 0065-2598 (Print)
0065-2598 (Linking). Available at: < https://www.ncbi.nlm.nih.gov/pubmed/25012374 >.

HUANG, J.; MANNING, B. D. The TSC1-TSC2 complex: a molecular switchboard controlling cell growth. **Biochem J,** v. 412, n. 2, p. 179-90, Jun 1 2008. ISSN 1470-8728 (Electronic)
0264-6021 (Linking). Available at: < https://www.ncbi.nlm.nih.gov/pubmed/18466115 >.

HUANG, R. Q. et al. Pentylenetetrazole-induced inhibition of recombinant gamma-aminobutyric acid type A (GABA(A)) receptors: mechanism and site of action. **J Pharmacol Exp Ther,** v. 298, n. 3, p. 986-95, Sep 2001. ISSN 0022-3565 (Print)
0022-3565 (Linking). Available at: < https://www.ncbi.nlm.nih.gov/pubmed/11504794 >.

HUBER, K. M.; RODER, J. C.; BEAR, M. F. Chemical induction of mGluR5- and protein synthesis--dependent long-term depression in hippocampal area CA1. **J Neurophysiol,** v. 86, n. 1, p. 321-5, Jul 2001. ISSN 0022-3077 (Print)
0022-3077 (Linking). Available at: < https://www.ncbi.nlm.nih.gov/pubmed/11431513 >.

HUGHES, J. et al. Knockout of the epilepsy gene Depdc5 in mice causes severe embryonic dysmorphology with hyperactivity of mTORC1 signalling. **Sci Rep,** v. 7, n. 1, p. 12618, Oct 3 2017. ISSN 2045-2322 (Electronic)
2045-2322 (Linking). Available at: < https://www.ncbi.nlm.nih.gov/pubmed/28974734 >.

INOKI, K.; ZHU, T.; GUAN, K. L. TSC2 mediates cellular energy response to control cell growth and survival. **Cell,** v. 115, n. 5, p. 577-90, Nov 26 2003. ISSN 0092-8674 (Print)
0092-8674 (Linking). Available at: < https://www.ncbi.nlm.nih.gov/pubmed/14651849 >.

JACKSON, J. et al. Altered synaptic properties during integration of adult-born hippocampal neurons following a seizure insult. **PLoS One,** v. 7, n. 4, p. e35557, 2012. ISSN 1932-6203 (Electronic)
1932-6203 (Linking). Available at: < https://www.ncbi.nlm.nih.gov/pubmed/22539981 >.

JACKSON, R. J.; HELLEN, C. U.; PESTOVA, T. V. The mechanism of eukaryotic translation initiation and principles of its regulation. **Nat Rev Mol Cell Biol,** v. 11, n. 2, p. 113-27, Feb 2010. ISSN 1471-0080 (Electronic)
1471-0072 (Linking). Available at: < https://www.ncbi.nlm.nih.gov/pubmed/20094052 >.

JACOBS, M. P. et al. Future directions for epilepsy research. **Neurology,** v. 57, n. 9, p. 1536-42, Nov 13 2001. ISSN 0028-3878 (Print)
0028-3878 (Linking). Available at: < https://www.ncbi.nlm.nih.gov/pubmed/11706087 >.

JANSEN, L. A. et al. PI3K/AKT pathway mutations cause a spectrum of brain malformations from megalencephaly to focal cortical dysplasia. **Brain,** v. 138, n. Pt 6, p. 1613-28, Jun 2015. ISSN 1460-2156 (Electronic)
0006-8950 (Linking). Available at: < https://www.ncbi.nlm.nih.gov/pubmed/25722288 >.

JIANG, X.; LACHANCE, M.; ROSSIGNOL, E. Involvement of cortical fast-spiking parvalbumin-positive basket cells in epilepsy. **Prog Brain Res,** v. 226, p. 81-126, 2016. ISSN 1875-7855 (Electronic)
0079-6123 (Linking). Available at: < https://www.ncbi.nlm.nih.gov/pubmed/27323940 >.

JISHI, A.; QI, X.; MIRANDA, H. C. Implications of mRNA translation dysregulation for neurological disorders. **Semin Cell Dev Biol,** v. 114, p. 11-19, Jun 2021. ISSN 1096-3634 (Electronic)
1084-9521 (Linking). Available at: < https://www.ncbi.nlm.nih.gov/pubmed/34024497 >.

KANDRATAVICIUS, L. et al. Animal models of epilepsy: use and limitations. **Neuropsychiatr Dis Treat,** v. 10, p. 1693-705, 2014. ISSN 1176-6328 (Print)
1176-6328 (Linking). Available at: < https://www.ncbi.nlm.nih.gov/pubmed/25228809 >.

KANN, O.; PAPAGEORGIOU, I. E.; DRAGUHN, A. Highly energized inhibitory interneurons are a central element for information processing in cortical networks. **J Cereb Blood Flow Metab,** v. 34, n. 8, p. 1270-82, Aug 2014. ISSN 1559-7016 (Electronic)
0271-678X (Linking). Available at: < https://www.ncbi.nlm.nih.gov/pubmed/24896567 >.

KAPP, L. D.; LORSCH, J. R. The molecular mechanics of eukaryotic translation. **Annu Rev Biochem,** v. 73, p. 657-704, 2004. ISSN 0066-4154 (Print)
0066-4154 (Linking). Available at: < https://www.ncbi.nlm.nih.gov/pubmed/15189156 >.

KASSAI, H. et al. Selective activation of mTORC1 signaling recapitulates microcephaly, tuberous sclerosis, and neurodegenerative diseases. **Cell Rep,** v. 7, n. 5, p. 1626-1639, Jun 12 2014. ISSN 2211-1247 (Electronic). Available at: < https://www.ncbi.nlm.nih.gov/pubmed/24857653 >.

KATSAROU, A. M.; MOSHE, S. L.; GALANOPOULOU, A. S. Interneuronopathies and Their Role in Early Life Epilepsies and Neurodevelopmental Disorders. **Epilepsia Open,** v. 2, n. 3, p. 284-306, Sep 2017. ISSN 2470-9239 (Print)
2470-9239 (Linking). Available at: < https://www.ncbi.nlm.nih.gov/pubmed/29062978 >.

KAUL, G.; PATTAN, G.; RAFEEQUI, T. Eukaryotic elongation factor-2 (eEF2): its regulation and peptide chain elongation. **Cell Biochem Funct,** v. 29, n. 3, p. 227-34, Apr 2011. ISSN 1099-0844 (Electronic)
0263-6484 (Linking). Available at: < https://www.ncbi.nlm.nih.gov/pubmed/21394738 >.

KEEZER, M. R.; SISODIYA, S. M.; SANDER, J. W. Comorbidities of epilepsy: current concepts and future perspectives. **Lancet Neurol,** v. 15, n. 1, p. 106-15, Jan 2016. ISSN 1474-4465 (Electronic)
1474-4422 (Linking). Available at: < https://www.ncbi.nlm.nih.gov/pubmed/26549780 >.

KEITH, D.; EL-HUSSEINI, A. Excitation Control: Balancing PSD-95 Function at the Synapse. **Front Mol Neurosci,** v. 1, p. 4, 2008. ISSN 1662-5099 (Electronic)
1662-5099 (Linking). Available at: < https://www.ncbi.nlm.nih.gov/pubmed/18946537 >.

KELSOM, C.; LU, W. Development and specification of GABAergic cortical interneurons. **Cell Biosci,** v. 3, n. 1, p. 19, Apr 23 2013. ISSN 2045-3701 (Print)
2045-3701 (Linking). Available at: < https://www.ncbi.nlm.nih.gov/pubmed/23618463 >.

KEPECS, A.; FISHELL, G. Interneuron cell types are fit to function. **Nature,** v. 505, n. 7483, p. 318-26, Jan 16 2014. ISSN 1476-4687 (Electronic)
0028-0836 (Linking). Available at: < https://www.ncbi.nlm.nih.gov/pubmed/24429630 >.

KETZEF, M.; GITLER, D. Epileptic synapsin triple knockout mice exhibit progressive long-term aberrant plasticity in the entorhinal cortex. **Cereb Cortex,** v. 24, n. 4, p. 996-1008, Apr 2014. ISSN 1460-2199 (Electronic)
1047-3211 (Linking). Available at: < https://www.ncbi.nlm.nih.gov/pubmed/23236212 >.

KHAZIPOV, R. GABAergic Synchronization in Epilepsy. **Cold Spring Harb Perspect Med,** v. 6, n. 2, p. a022764, Jan 8 2016. ISSN 2157-1422 (Electronic)
2157-1422 (Linking). Available at: < https://www.ncbi.nlm.nih.gov/pubmed/26747834 >.

KIM, D. H. et al. mTOR interacts with raptor to form a nutrient-sensitive complex that signals to the cell growth machinery. **Cell,** v. 110, n. 2, p. 163-75, Jul 26 2002. ISSN 0092-8674 (Print)
0092-8674 (Linking). Available at: < https://www.ncbi.nlm.nih.gov/pubmed/12150925 >.

KIM, D. H. et al. GbetaL, a positive regulator of the rapamycin-sensitive pathway required for the nutrient-sensitive interaction between raptor and mTOR. **Mol Cell,** v. 11, n. 4, p. 895-904, Apr 2003. ISSN 1097-2765 (Print)
1097-2765 (Linking). Available at: < https://www.ncbi.nlm.nih.gov/pubmed/12718876 >.

KIM, J. K. et al. Brain somatic mutations in MTOR reveal translational dysregulations underlying intractable focal epilepsy. **J Clin Invest,** v. 129, n. 10, p. 4207-4223, Oct 1 2019. ISSN 1558-8238 (Electronic)
0021-9738 (Linking). Available at: < https://www.ncbi.nlm.nih.gov/pubmed/31483294 >.

KIM, L. C.; COOK, R. S.; CHEN, J. mTORC1 and mTORC2 in cancer and the tumor microenvironment. **Oncogene,** v. 36, n. 16, p. 2191-2201, Apr 20 2017. ISSN 1476-5594 (Electronic)
0950-9232 (Linking). Available at: < https://www.ncbi.nlm.nih.gov/pubmed/27748764 >.

KIMBALL, S. R. Eukaryotic initiation factor eIF2. **Int J Biochem Cell Biol,** v. 31, n. 1, p. 25-9, Jan 1999. ISSN 1357-2725 (Print)
1357-2725 (Linking). Available at: < https://www.ncbi.nlm.nih.gov/pubmed/10216940 >.

KINROSS, K. M. et al. An activating Pik3ca mutation coupled with Pten loss is sufficient to initiate ovarian tumorigenesis in mice. **J Clin Invest,** v. 122, n. 2, p. 553-7, Feb 2012. ISSN 1558-8238 (Electronic)
0021-9738 (Linking). Available at: < https://www.ncbi.nlm.nih.gov/pubmed/22214849 >.

KLOFAS, L. K. et al. Prevention of premature death and seizures in a Depdc5 mouse epilepsy model through inhibition of mTORC1. **Hum Mol Genet,** v. 29, n. 8, p. 1365-1377, May 28 2020. ISSN 1460-2083 (Electronic)
0964-6906 (Linking). Available at: < https://www.ncbi.nlm.nih.gov/pubmed/32280987 >.

KOBOLDT, D. C. et al. PTEN somatic mutations contribute to spectrum of cerebral overgrowth. **Brain,** v. 144, n. 10, p. 2971-2978, Nov 29 2021. ISSN 1460-2156 (Electronic)
0006-8950 (Linking). Available at: < https://www.ncbi.nlm.nih.gov/pubmed/34048549 >.

KOLITZ, S. E.; LORSCH, J. R. Eukaryotic initiator tRNA: finely tuned and ready for action. **FEBS Lett,** v. 584, n. 2, p. 396-404, Jan 21 2010. ISSN 1873-3468 (Electronic)
0014-5793 (Linking). Available at: < https://www.ncbi.nlm.nih.gov/pubmed/19925799 >.

LAPLANTE, M.; SABATINI, D. M. mTOR signaling at a glance. **J Cell Sci,** v. 122, n. Pt 20, p. 3589-94, Oct 15 2009. ISSN 1477-9137 (Electronic)
0021-9533 (Linking). Available at: < https://www.ncbi.nlm.nih.gov/pubmed/19812304 >.

LASARGE, C. L.; DANZER, S. C. Mechanisms regulating neuronal excitability and seizure development following mTOR pathway hyperactivation. **Front Mol Neurosci,** v. 7, p. 18, 2014. ISSN 1662-5099 (Print)
1662-5099 (Linking). Available at: < https://www.ncbi.nlm.nih.gov/pubmed/24672426 >.

LASARGE, C. L. et al. mTOR-driven neural circuit changes initiate an epileptogenic cascade. **Prog Neurobiol,** v. 200, p. 101974, May 2021. ISSN 1873-5118 (Electronic)
0301-0082 (Linking). Available at: < https://www.ncbi.nlm.nih.gov/pubmed/33309800 >.

LEE, J. H. et al. De novo somatic mutations in components of the PI3K-AKT3-mTOR pathway cause hemimegalencephaly. **Nat Genet,** v. 44, n. 8, p. 941-5, Jun 24 2012. ISSN 1546-1718 (Electronic)
1061-4036 (Linking). Available at: < https://www.ncbi.nlm.nih.gov/pubmed/22729223 >.

LEVENTER, R. J.; GUERRINI, R.; DOBYNS, W. B. Malformations of cortical development and epilepsy. **Dialogues Clin Neurosci,** v. 10, n. 1, p. 47-62, 2008. ISSN 1294-8322 (Print)
1294-8322 (Linking). Available at: < https://www.ncbi.nlm.nih.gov/pubmed/18472484 >.

LEVESQUE, M.; AVOLI, M. The kainic acid model of temporal lobe epilepsy. **Neurosci Biobehav Rev,** v. 37, n. 10 Pt 2, p. 2887-99, Dec 2013. ISSN 1873-7528 (Electronic)
0149-7634 (Linking). Available at: < https://www.ncbi.nlm.nih.gov/pubmed/24184743 >.

LEVINSON, J. N.; EL-HUSSEINI, A. Building excitatory and inhibitory synapses: balancing neuroligin partnerships. **Neuron,** v. 48, n. 2, p. 171-4, Oct 20 2005. ISSN 0896-6273 (Print)
0896-6273 (Linking). Available at: < https://www.ncbi.nlm.nih.gov/pubmed/16242398 >.

LICAUSI, F.; HARTMAN, N. W. Role of mTOR Complexes in Neurogenesis. **Int J Mol Sci,** v. 19, n. 5, May 22 2018. ISSN 1422-0067 (Electronic)
1422-0067 (Linking). Available at: < https://www.ncbi.nlm.nih.gov/pubmed/29789464 >.

LIM, J. S. et al. Somatic Mutations in TSC1 and TSC2 Cause Focal Cortical Dysplasia. **Am J Hum Genet,** v. 100, n. 3, p. 454-472, Mar 2 2017. ISSN 1537-6605 (Electronic)
0002-9297 (Linking). Available at: < https://www.ncbi.nlm.nih.gov/pubmed/28215400 >.

LIM, J. S. et al. Brain somatic mutations in MTOR cause focal cortical dysplasia type II leading to intractable epilepsy. **Nat Med,** v. 21, n. 4, p. 395-400, Apr 2015. ISSN 1546-170X (Electronic)
1078-8956 (Linking). Available at: < https://www.ncbi.nlm.nih.gov/pubmed/25799227 >.

LIM, L. et al. Development and Functional Diversification of Cortical Interneurons. **Neuron,** v. 100, n. 2, p. 294-313, Oct 24 2018. ISSN 1097-4199 (Electronic)
0896-6273 (Linking). Available at: < https://www.ncbi.nlm.nih.gov/pubmed/30359598 >.

LIU, Y. D. et al. Brain Proteomic Profiling in Intractable Epilepsy Caused by TSC1 Truncating Mutations: A Small Sample Study. **Front Neurol,** v. 11, p. 475, 2020. ISSN 1664-2295 (Print)
1664-2295 (Linking). Available at: < https://www.ncbi.nlm.nih.gov/pubmed/32655475 >.

LOMAKIN, I. B.; STEITZ, T. A. The initiation of mammalian protein synthesis and mRNA scanning mechanism. **Nature,** v. 500, n. 7462, p. 307-11, Aug 15 2013. ISSN 1476-4687 (Electronic)
0028-0836 (Linking). Available at: < https://www.ncbi.nlm.nih.gov/pubmed/23873042 >.

LUTTJOHANN, A.; FABENE, P. F.; VAN LUIJTELAAR, G. A revised Racine's scale for PTZ-induced seizures in rats. **Physiol Behav,** v. 98, n. 5, p. 579-86, Dec 7 2009. ISSN 1873-507X (Electronic)
0031-9384 (Linking). Available at: < https://www.ncbi.nlm.nih.gov/pubmed/19772866 >.

MA, X. M.; BLENIS, J. Molecular mechanisms of mTOR-mediated translational control. **Nat Rev Mol Cell Biol,** v. 10, n. 5, p. 307-18, May 2009. ISSN 1471-0080 (Electronic)
1471-0072 (Linking). Available at: < https://www.ncbi.nlm.nih.gov/pubmed/19339977 >.

MAGNUSON, B.; EKIM, B.; FINGAR, D. C. Regulation and function of ribosomal protein S6 kinase (S6K) within mTOR signalling networks. **Biochem J,** v. 441, n. 1, p. 1-21, Jan 1 2012. ISSN 1470-8728 (Electronic)
0264-6021 (Linking). Available at: < https://www.ncbi.nlm.nih.gov/pubmed/22168436 >.

MAGRI, L. et al. Sustained activation of mTOR pathway in embryonic neural stem cells leads to development of tuberous sclerosis complex-associated lesions. **Cell Stem Cell,** v. 9, n. 5, p. 447-62, Nov 4 2011. ISSN 1875-9777 (Electronic)
1875-9777 (Linking). Available at: < https://www.ncbi.nlm.nih.gov/pubmed/22056141 >.

MAHONEY, C. et al. Switching on mTORC1 induces neurogenesis but not proliferation in neural stem cells of young mice. **Neurosci Lett,** v. 614, p. 112-8, Feb 12 2016. ISSN 1872-7972 (Electronic)
0304-3940 (Linking). Available at: < https://www.ncbi.nlm.nih.gov/pubmed/26812181 >.

MARCHESE, M. et al. Autism-epilepsy phenotype with macrocephaly suggests PTEN, but not GLIALCAM, genetic screening. **BMC Med Genet,** v. 15, p. 26, Feb 27 2014. ISSN 1471-2350 (Electronic)
1471-2350 (Linking). Available at: < https://www.ncbi.nlm.nih.gov/pubmed/24580998 >.

MARKRAM, H. et al. Interneurons of the neocortical inhibitory system. **Nat Rev Neurosci,** v. 5, n. 10, p. 793-807, Oct 2004. ISSN 1471-003X (Print)
1471-003X (Linking). Available at: < https://www.ncbi.nlm.nih.gov/pubmed/15378039 >.

MASLAND, R. H. Neuronal cell types. **Curr Biol,** v. 14, n. 13, p. R497-500, Jul 13 2004. ISSN 0960-9822 (Print)
0960-9822 (Linking). Available at: < https://www.ncbi.nlm.nih.gov/pubmed/15242626 >.

MAYER, C. et al. Developmental diversification of cortical inhibitory interneurons. **Nature,** v. 555, n. 7697, p. 457-462, Mar 22 2018. ISSN 1476-4687 (Electronic)
0028-0836 (Linking). Available at: < https://www.ncbi.nlm.nih.gov/pubmed/29513653 >.

MEIKLE, L. et al. A mouse model of tuberous sclerosis: neuronal loss of Tsc1 causes dysplastic and ectopic neurons, reduced myelination, seizure activity, and limited survival. **J Neurosci,** v. 27, n. 21, p. 5546-58, May 23 2007. ISSN 1529-2401 (Electronic)
0270-6474 (Linking). Available at: < https://www.ncbi.nlm.nih.gov/pubmed/17522300 >.

MENDOZA, M. C.; ER, E. E.; BLENIS, J. The Ras-ERK and PI3K-mTOR pathways: cross-talk and compensation. **Trends Biochem Sci,** v. 36, n. 6, p. 320-8, Jun 2011. ISSN 0968-0004 (Print)
0968-0004 (Linking). Available at: < https://www.ncbi.nlm.nih.gov/pubmed/21531565 >.

MENG, X. F. et al. Role of the mTOR signaling pathway in epilepsy. **J Neurol Sci,** v. 332, n. 1-2, p. 4-15, Sep 15 2013. ISSN 1878-5883 (Electronic)
0022-510X (Linking). Available at: < https://www.ncbi.nlm.nih.gov/pubmed/23773767 >.

MIAO, L. et al. mTORC1 is necessary but mTORC2 and GSK3beta are inhibitory for AKT3-induced axon regeneration in the central nervous system. **Elife,** v. 5, p. e14908, Mar 30 2016. ISSN 2050-084X (Electronic)
2050-084X (Linking). Available at: < https://www.ncbi.nlm.nih.gov/pubmed/27026523 >.

MIHAYLOVA, M. M.; SHAW, R. J. The AMPK signalling pathway coordinates cell growth, autophagy and metabolism. **Nat Cell Biol,** v. 13, n. 9, p. 1016-23, Sep 2 2011. ISSN 1476-4679 (Electronic)
1465-7392 (Linking). Available at: < https://www.ncbi.nlm.nih.gov/pubmed/21892142 >.

MOHAN, M. et al. The long-term outcomes of epilepsy surgery. **PLoS One,** v. 13, n. 5, p. e0196274, 2018. ISSN 1932-6203 (Electronic)
1932-6203 (Linking). Available at: < https://www.ncbi.nlm.nih.gov/pubmed/29768433 >.

MOLLER, R. S. et al. Germline and somatic mutations in the MTOR gene in focal cortical dysplasia and epilepsy. **Neurol Genet,** v. 2, n. 6, p. e118, Dec 2016. ISSN 2376-7839 (Print)
2376-7839 (Linking). Available at: < https://www.ncbi.nlm.nih.gov/pubmed/27830187 >.

MOLONEY, P. B.; CAVALLERI, G. L.; DELANTY, N. Epilepsy in the mTORopathies: opportunities for precision medicine. **Brain Commun,** v. 3, n. 4, p. fcab222, 2021. ISSN 2632-1297 (Electronic)
2632-1297 (Linking). Available at: < https://www.ncbi.nlm.nih.gov/pubmed/34632383 >.

MOLYNEAUX, B. J. et al. Neuronal subtype specification in the cerebral cortex. **Nat Rev Neurosci,** v. 8, n. 6, p. 427-37, Jun 2007. ISSN 1471-003X (Print)
1471-003X (Linking). Available at: < https://www.ncbi.nlm.nih.gov/pubmed/17514196 >.

MUSA, J. et al. Eukaryotic initiation factor 4E-binding protein 1 (4E-BP1): a master regulator of mRNA translation involved in tumorigenesis. **Oncogene,** v. 35, n. 36, p. 4675-88, Sep 8 2016. ISSN 1476-5594 (Electronic)
0950-9232 (Linking). Available at: < https://www.ncbi.nlm.nih.gov/pubmed/26829052 >.

NADLER, J. V. Minireview. Kainic acid as a tool for the study of temporal lobe epilepsy. **Life Sci,** v. 29, n. 20, p. 2031-42, Nov 16 1981. ISSN 0024-3205 (Print)
0024-3205 (Linking). Available at: < https://www.ncbi.nlm.nih.gov/pubmed/7031398 >.

NADLER, J. V.; PERRY, B. W.; COTMAN, C. W. Intraventricular kainic acid preferentially destroys hippocampal pyramidal cells. **Nature,** v. 271, n. 5646, p. 676-7, Feb 16 1978. ISSN 0028-0836 (Print)
0028-0836 (Linking). Available at: < https://www.ncbi.nlm.nih.gov/pubmed/625338 >.

NANDAGOPAL, N.; ROUX, P. P. Regulation of global and specific mRNA translation by the mTOR signaling pathway. **Translation (Austin),** v. 3, n. 1, p. e983402, Jan-Jun 2015. ISSN 2169-074X (Print)
2169-0731 (Linking). Available at: < https://www.ncbi.nlm.nih.gov/pubmed/26779414 >.

NEASTA, J. et al. mTOR complex 1: a key player in neuroadaptations induced by drugs of abuse. **J Neurochem,** v. 130, n. 2, p. 172-84, Jul 2014. ISSN 1471-4159 (Electronic)
0022-3042 (Linking). Available at: < https://www.ncbi.nlm.nih.gov/pubmed/24666346 >.

NEVES, G. et al. The LIM homeodomain protein Lhx6 regulates maturation of interneurons and network excitability in the mammalian cortex. **Cereb Cortex,** v. 23, n. 8, p. 1811-23, Aug 2013. ISSN 1460-2199 (Electronic)
1047-3211 (Linking). Available at: < https://www.ncbi.nlm.nih.gov/pubmed/22710612 >.

NEW, D. C.; WONG, Y. H. Molecular mechanisms mediating the G protein-coupled receptor regulation of cell cycle progression. **J Mol Signal,** v. 2, p. 2, Feb 26 2007. ISSN 1750-2187 (Electronic)
1750-2187 (Linking). Available at: < https://www.ncbi.nlm.nih.gov/pubmed/17319972 >.

NGUYEN, L. H.; MAHADEO, T.; BORDEY, A. mTOR Hyperactivity Levels Influence the Severity of Epilepsy and Associated Neuropathology in an Experimental Model of Tuberous Sclerosis Complex and Focal Cortical Dysplasia. **J Neurosci,** v. 39, n. 14, p. 2762-2773, Apr 3 2019. ISSN 1529-2401 (Electronic)
0270-6474 (Linking). Available at: < https://www.ncbi.nlm.nih.gov/pubmed/30700531 >.

NICHOLSON, K. M.; ANDERSON, N. G. The protein kinase B/Akt signalling pathway in human malignancy. **Cell Signal,** v. 14, n. 5, p. 381-95, May 2002. ISSN 0898-6568 (Print)
0898-6568 (Linking). Available at: < https://www.ncbi.nlm.nih.gov/pubmed/11882383 >.

NICOLAS, C. S. et al. The role of JAK-STAT signaling within the CNS. **JAKSTAT,** v. 2, n. 1, p. e22925, Jan 1 2013. ISSN 2162-3988 (Print)
2162-3988 (Linking). Available at: < https://www.ncbi.nlm.nih.gov/pubmed/24058789 >.

NOACHTAR, S.; BORGGRAEFE, I. Epilepsy surgery: a critical review. **Epilepsy Behav,** v. 15, n. 1, p. 66-72, May 2009. ISSN 1525-5069 (Electronic)
1525-5050 (Linking). Available at: < https://www.ncbi.nlm.nih.gov/pubmed/19236942 >.

NUNES, V. D. et al. Diagnosis and management of the epilepsies in adults and children: summary of updated NICE guidance. **BMJ,** v. 344, p. e281, Jan 26 2012. ISSN 1756-1833 (Electronic)
0959-8138 (Linking). Available at: < https://www.ncbi.nlm.nih.gov/pubmed/22282528 >.

OH, W. J.; JACINTO, E. mTOR complex 2 signaling and functions. **Cell Cycle,** v. 10, n. 14, p. 2305-16, Jul 15 2011. ISSN 1551-4005 (Electronic)
1551-4005 (Linking). Available at: < https://www.ncbi.nlm.nih.gov/pubmed/21670596 >.

OLMOS-SERRANO, J. L. et al. Defective GABAergic neurotransmission and pharmacological rescue of neuronal hyperexcitability in the amygdala in a mouse model of fragile X syndrome. **J Neurosci,** v. 30, n. 29, p. 9929-38, Jul 21 2010. ISSN 1529-2401 (Electronic) 0270-6474 (Linking). Available at: < https://www.ncbi.nlm.nih.gov/pubmed/20660275 >.

OSHIRO, N. et al. Dissociation of raptor from mTOR is a mechanism of rapamycin-induced inhibition of mTOR function. **Genes Cells,** v. 9, n. 4, p. 359-66, Apr 2004. ISSN 1356-9597 (Print)
1356-9597 (Linking). Available at: < https://www.ncbi.nlm.nih.gov/pubmed/15066126 >.

OSTENDORF, A. P.; WONG, M. mTOR inhibition in epilepsy: rationale and clinical perspectives. **CNS Drugs,** v. 29, n. 2, p. 91-9, Feb 2015. ISSN 1179-1934 (Electronic) 1172-7047 (Linking). Available at: < https://www.ncbi.nlm.nih.gov/pubmed/25633849 >.

OSTERWEIL, E. K. et al. Lovastatin corrects excess protein synthesis and prevents epileptogenesis in a mouse model of fragile X syndrome. **Neuron,** v. 77, n. 2, p. 243-50, Jan 23 2013. ISSN 1097-4199 (Electronic)
0896-6273 (Linking). Available at: < https://www.ncbi.nlm.nih.gov/pubmed/23352161 >.

OYRER, J. et al. Ion Channels in Genetic Epilepsy: From Genes and Mechanisms to Disease-Targeted Therapies. **Pharmacol Rev,** v. 70, n. 1, p. 142-173, Jan 2018. ISSN 1521-0081 (Electronic)
0031-6997 (Linking). Available at: < https://www.ncbi.nlm.nih.gov/pubmed/29263209 >.

PANDOLFO, M. Genetics of epilepsy. **Semin Neurol,** v. 31, n. 5, p. 506-18, Nov 2011. ISSN 1098-9021 (Electronic)
0271-8235 (Linking). Available at: < https://www.ncbi.nlm.nih.gov/pubmed/22266888 >.

PARENT, J. M. et al. Dentate granule cell neurogenesis is increased by seizures and contributes to aberrant network reorganization in the adult rat hippocampus. **J Neurosci,** v. 17, n. 10, p. 3727-38, May 15 1997. ISSN 0270-6474 (Print)
0270-6474 (Linking). Available at: < https://www.ncbi.nlm.nih.gov/pubmed/9133393 >.

PEARL, D. et al. 4E-BP-Dependent Translational Control of Irf8 Mediates Adipose Tissue Macrophage Inflammatory Response. **J Immunol,** v. 204, n. 9, p. 2392-2400, May 1 2020. ISSN 1550-6606 (Electronic)
0022-1767 (Linking). Available at: < https://www.ncbi.nlm.nih.gov/pubmed/32213561 >.

PERNICE, H. F. et al. mTOR and MAPK: from localized translation control to epilepsy. **BMC Neurosci,** v. 17, n. 1, p. 73, Nov 17 2016. ISSN 1471-2202 (Electronic)
1471-2202 (Linking). Available at: < https://www.ncbi.nlm.nih.gov/pubmed/27855659 >.

PESTOVA, T. V. et al. Molecular mechanisms of translation initiation in eukaryotes. **Proc Natl Acad Sci U S A,** v. 98, n. 13, p. 7029-36, Jun 19 2001. ISSN 0027-8424 (Print)
0027-8424 (Linking). Available at: < https://www.ncbi.nlm.nih.gov/pubmed/11416183 >.

PETERSON, T. R. et al. DEPTOR is an mTOR inhibitor frequently overexpressed in multiple myeloma cells and required for their survival. **Cell,** v. 137, n. 5, p. 873-86, May 29 2009. ISSN 1097-4172 (Electronic)
0092-8674 (Linking). Available at: < https://www.ncbi.nlm.nih.gov/pubmed/19446321 >.

PEVSNER, J. et al. Specificity and regulation of a synaptic vesicle docking complex. **Neuron,** v. 13, n. 2, p. 353-61, Aug 1994. ISSN 0896-6273 (Print)
0896-6273 (Linking). Available at: < https://www.ncbi.nlm.nih.gov/pubmed/8060616 >.

PFISTERER, U. et al. Identification of epilepsy-associated neuronal subtypes and gene expression underlying epileptogenesis. **Nat Commun,** v. 11, n. 1, p. 5038, Oct 7 2020. ISSN 2041-1723 (Electronic)
2041-1723 (Linking). Available at: < https://www.ncbi.nlm.nih.gov/pubmed/33028830 >.

PIROZZI, F. et al. Analysis of common PI3K-AKT-MTOR mutations in pediatric surgical epilepsy by droplet digital PCR reveals novel clinical and molecular insights. **medRxiv**, p. 2021.06.09.21257462, 2021. Available at: < https://www.medrxiv.org/content/medrxiv/early/2021/06/20/2021.06.09.21257462.full.pdf >.

PITKANEN, A.; SUTULA, T. P. Is epilepsy a progressive disorder? Prospects for new therapeutic approaches in temporal-lobe epilepsy. **Lancet Neurol,** v. 1, n. 3, p. 173-81, Jul 2002. ISSN 1474-4422 (Print)
1474-4422 (Linking). Available at: < https://www.ncbi.nlm.nih.gov/pubmed/12849486 >.

PODURI, A.; LOWENSTEIN, D. Epilepsy genetics--past, present, and future. **Curr Opin Genet Dev,** v. 21, n. 3, p. 325-32, Jun 2011. ISSN 1879-0380 (Electronic)
0959-437X (Linking). Available at: < https://www.ncbi.nlm.nih.gov/pubmed/21277190 >.

PREVOT, D.; DARLIX, J. L.; OHLMANN, T. Conducting the initiation of protein synthesis: the role of eIF4G. **Biol Cell,** v. 95, n. 3-4, p. 141-56, May-Jun 2003. ISSN 0248-4900 (Print)
0248-4900 (Linking). Available at: < https://www.ncbi.nlm.nih.gov/pubmed/12867079 >.

QUERFURTH, H.; LEE, H. K. Mammalian/mechanistic target of rapamycin (mTOR) complexes in neurodegeneration. **Mol Neurodegener,** v. 16, n. 1, p. 44, Jul 2 2021. ISSN 1750-1326 (Electronic)
1750-1326 (Linking). Available at: < https://www.ncbi.nlm.nih.gov/pubmed/34215308 >.

RAMANJANEYULU, R.; TICKU, M. K. Interactions of pentamethylenetetrazole and tetrazole analogues with the picrotoxinin site of the benzodiazepine-GABA receptor-ionophore complex. **Eur J Pharmacol,** v. 98, n. 3-4, p. 337-45, Mar 2 1984. ISSN 0014-2999 (Print)
0014-2999 (Linking). Available at: < https://www.ncbi.nlm.nih.gov/pubmed/6327331 >.

RANKIN-GEE, E. K. et al. Perineuronal net degradation in epilepsy. **Epilepsia,** v. 56, n. 7, p. 1124-33, Jul 2015. ISSN 1528-1167 (Electronic)
0013-9580 (Linking). Available at: < https://www.ncbi.nlm.nih.gov/pubmed/26032766 >.

REIJNDERS, M. R. F. et al. Variation in a range of mTOR-related genes associates with intracranial volume and intellectual disability. **Nat Commun,** v. 8, n. 1, p. 1052, Oct 20 2017. ISSN 2041-1723 (Electronic)
2041-1723 (Linking). Available at: < https://www.ncbi.nlm.nih.gov/pubmed/29051493 >.

RICOS, M. G. et al. Mutations in the mammalian target of rapamycin pathway regulators NPRL2 and NPRL3 cause focal epilepsy. **Ann Neurol,** v. 79, n. 1, p. 120-31, Jan 2016. ISSN 1531-8249 (Electronic)
0364-5134 (Linking). Available at: < https://www.ncbi.nlm.nih.gov/pubmed/26505888 >.

ROGAWSKI, M. A.; LOSCHER, W. The neurobiology of antiepileptic drugs. **Nat Rev Neurosci,** v. 5, n. 7, p. 553-64, Jul 2004. ISSN 1471-003X (Print)
1471-003X (Linking). Available at: < https://www.ncbi.nlm.nih.gov/pubmed/15208697 >.

ROHENA, L. et al. Mutation in SNAP25 as a novel genetic cause of epilepsy and intellectual disability. **Rare Dis,** v. 1, p. e26314, 2013. ISSN 2167-5511 (Print)
2167-5511 (Linking). Available at: < https://www.ncbi.nlm.nih.gov/pubmed/25003006 >.

ROY, A. et al. Mouse models of human PIK3CA-related brain overgrowth have acutely treatable epilepsy. **Elife,** v. 4, Dec 3 2015. ISSN 2050-084X (Electronic)
2050-084X (Linking). Available at: < https://www.ncbi.nlm.nih.gov/pubmed/26633882 >.

RUDEN, J. B.; DUGAN, L. L.; KONRADI, C. Parvalbumin interneuron vulnerability and brain disorders. **Neuropsychopharmacology,** v. 46, n. 2, p. 279-287, Jan 2021. ISSN 1740-634X (Electronic)
0893-133X (Linking). Available at: < https://www.ncbi.nlm.nih.gov/pubmed/32722660 >.

RUSSO, E. et al. The mTOR signaling pathway in the brain: focus on epilepsy and epileptogenesis. **Mol Neurobiol,** v. 46, n. 3, p. 662-81, Dec 2012. ISSN 1559-1182 (Electronic)
0893-7648 (Linking). Available at: < https://www.ncbi.nlm.nih.gov/pubmed/22825882 >.

RYTHER, R. C.; WONG, M. Mammalian target of rapamycin (mTOR) inhibition: potential for antiseizure, antiepileptogenic, and epileptostatic therapy. **Curr Neurol Neurosci Rep,** v. 12, n. 4, p. 410-8, Aug 2012. ISSN 1534-6293 (Electronic)
1528-4042 (Linking). Available at: < https://www.ncbi.nlm.nih.gov/pubmed/22544534 >.

SABATINI, D. M. et al. RAFT1: a mammalian protein that binds to FKBP12 in a rapamycin-dependent fashion and is homologous to yeast TORs. **Cell,** v. 78, n. 1, p. 35-43, Jul 15 1994. ISSN 0092-8674 (Print)
0092-8674 (Linking). Available at: < https://www.ncbi.nlm.nih.gov/pubmed/7518356 >.

SAITO, K. et al. The physiological roles of vesicular GABA transporter during embryonic development: a study using knockout mice. **Mol Brain,** v. 3, p. 40, Dec 30 2010. ISSN 1756-6606 (Electronic)
1756-6606 (Linking). Available at: < https://www.ncbi.nlm.nih.gov/pubmed/21190592 >.

SAKAI, Y. et al. Hyperactivation of mTORC1 disrupts cellular homeostasis in cerebellar Purkinje cells. **Sci Rep,** v. 9, n. 1, p. 2799, Feb 26 2019. ISSN 2045-2322 (Electronic) 2045-2322 (Linking). Available at: < https://www.ncbi.nlm.nih.gov/pubmed/30808980 >.

SALINAS, V. et al. Identification of a somatic mutation in the RHEB gene through high depth and ultra-high depth next generation sequencing in a patient with Hemimegalencephaly and drug resistant Epilepsy. **Eur J Med Genet,** v. 62, n. 11, p. 103571, Nov 2019. ISSN 1878-0849 (Electronic)
1769-7212 (Linking). Available at: < https://www.ncbi.nlm.nih.gov/pubmed/30414531 >.

SANCAK, Y. et al. The Rag GTPases bind raptor and mediate amino acid signaling to mTORC1. **Science,** v. 320, n. 5882, p. 1496-501, Jun 13 2008. ISSN 1095-9203 (Electronic) 0036-8075 (Linking). Available at: < https://www.ncbi.nlm.nih.gov/pubmed/18497260 >.

SANCHEZ-ALEGRIA, K. et al. PI3K Signaling in Neurons: A Central Node for the Control of Multiple Functions. **Int J Mol Sci,** v. 19, n. 12, Nov 23 2018. ISSN 1422-0067 (Electronic) 1422-0067 (Linking). Available at: < https://www.ncbi.nlm.nih.gov/pubmed/30477115 >.

SAXTON, R. A.; SABATINI, D. M. mTOR Signaling in Growth, Metabolism, and Disease. **Cell,** v. 168, n. 6, p. 960-976, Mar 9 2017. ISSN 1097-4172 (Electronic)
0092-8674 (Linking). Available at: < https://www.ncbi.nlm.nih.gov/pubmed/28283069 >.

SCHMIDT, D. Drug treatment of epilepsy: options and limitations. **Epilepsy Behav,** v. 15, n. 1, p. 56-65, May 2009. ISSN 1525-5069 (Electronic)
1525-5050 (Linking). Available at: < https://www.ncbi.nlm.nih.gov/pubmed/19236951 >.

SCHULLER, A. P. et al. eIF5A Functions Globally in Translation Elongation and Termination. **Mol Cell,** v. 66, n. 2, p. 194-205 e5, Apr 20 2017. ISSN 1097-4164 (Electronic)
1097-2765 (Linking). Available at: < https://www.ncbi.nlm.nih.gov/pubmed/28392174 >.

SETO, B. Rapamycin and mTOR: a serendipitous discovery and implications for breast cancer. **Clin Transl Med,** v. 1, n. 1, p. 29, Nov 15 2012. ISSN 2001-1326 (Print) 2001-1326 (Linking). Available at: < https://www.ncbi.nlm.nih.gov/pubmed/23369283 >.

SHARMA, A. et al. Dysregulation of mTOR signaling in fragile X syndrome. **J Neurosci,** v. 30, n. 2, p. 694-702, Jan 13 2010. ISSN 1529-2401 (Electronic)
0270-6474 (Linking). Available at: < https://www.ncbi.nlm.nih.gov/pubmed/20071534 >.

SHARMA, V. et al. 4E-BP2-dependent translation in parvalbumin neurons controls epileptic seizure threshold. **Proc Natl Acad Sci U S A,** v. 118, n. 15, Apr 13 2021. ISSN 1091-6490 (Electronic)
0027-8424 (Linking). Available at: < https://www.ncbi.nlm.nih.gov/pubmed/33876772 >.

SHIMADA, T.; YAMAGATA, K. Pentylenetetrazole-Induced Kindling Mouse Model. **J Vis Exp**, n. 136, Jun 12 2018. ISSN 1940-087X (Electronic)
1940-087X (Linking). Available at: < https://www.ncbi.nlm.nih.gov/pubmed/29985308 >.

SHIROKIKH, N. E.; PREISS, T. Translation initiation by cap-dependent ribosome recruitment: Recent insights and open questions. **Wiley Interdiscip Rev RNA,** v. 9, n. 4, p. e1473, Jul 2018. ISSN 1757-7012 (Electronic)
1757-7004 (Linking). Available at: < https://www.ncbi.nlm.nih.gov/pubmed/29624880 >.

SHORVON, S.; PERUCCA, E.; ENGEL JR, J. **The treatment of epilepsy**. John Wiley & Sons, 2015. ISBN 1118936981.

SIKALIDIS, A. K. et al. Total 4EBP1 Is Elevated in Liver of Rats in Response to Low Sulfur Amino Acid Intake. **J Amino Acids,** v. 2013, p. 864757, 2013. ISSN 2090-0104 (Print)
2090-0112 (Linking). Available at: < https://www.ncbi.nlm.nih.gov/pubmed/24089634 >.

SINGH, T.; MISHRA, A.; GOEL, R. K. PTZ kindling model for epileptogenesis, refractory epilepsy, and associated comorbidities: relevance and reliability. **Metab Brain Dis,** v. 36, n. 7, p. 1573-1590, Oct 2021. ISSN 1573-7365 (Electronic)
0885-7490 (Linking). Available at: < https://www.ncbi.nlm.nih.gov/pubmed/34427842 >.

SLOVITER, R. S. Calcium-binding protein (calbindin-D28k) and parvalbumin immunocytochemistry: localization in the rat hippocampus with specific reference to the selective vulnerability of hippocampal neurons to seizure activity. **J Comp Neurol,** v. 280, n. 2, p. 183-96, Feb 8 1989. ISSN 0021-9967 (Print)
0021-9967 (Linking). Available at: < https://www.ncbi.nlm.nih.gov/pubmed/2925892 >.

SOLIMAN, G. A. et al. mTOR Ser-2481 autophosphorylation monitors mTORC-specific catalytic activity and clarifies rapamycin mechanism of action. **J Biol Chem,** v. 285, n. 11, p. 7866-79, Mar 12 2010. ISSN 1083-351X (Electronic)
0021-9258 (Linking). Available at: < https://www.ncbi.nlm.nih.gov/pubmed/20022946 >.

SONENBERG, N.; HINNEBUSCH, A. G. Regulation of translation initiation in eukaryotes: mechanisms and biological targets. **Cell,** v. 136, n. 4, p. 731-45, Feb 20 2009. ISSN 1097-4172 (Electronic)
0092-8674 (Linking). Available at: < https://www.ncbi.nlm.nih.gov/pubmed/19239892 >.

SOSULINA, L. et al. Classification of projection neurons and interneurons in the rat lateral amygdala based upon cluster analysis. **Mol Cell Neurosci,** v. 33, n. 1, p. 57-67, Sep 2006. ISSN 1044-7431 (Print)
1044-7431 (Linking). Available at: < https://www.ncbi.nlm.nih.gov/pubmed/16861000 >.

SPERK, G. et al. Kainic acid induced seizures: neurochemical and histopathological changes. **Neuroscience,** v. 10, n. 4, p. 1301-15, Dec 1983. ISSN 0306-4522 (Print)
0306-4522 (Linking). Available at: < https://www.ncbi.nlm.nih.gov/pubmed/6141539 >.

SRIDHARAN, S.; BASU, A. Distinct Roles of mTOR Targets S6K1 and S6K2 in Breast Cancer. **Int J Mol Sci,** v. 21, n. 4, Feb 11 2020. ISSN 1422-0067 (Electronic)
1422-0067 (Linking). Available at: < https://www.ncbi.nlm.nih.gov/pubmed/32054043 >.

STAFSTROM, C. E.; CARMANT, L. Seizures and epilepsy: an overview for neuroscientists. **Cold Spring Harb Perspect Med,** v. 5, n. 6, Jun 1 2015. ISSN 2157-1422 (Electronic)
2157-1422 (Linking). Available at: < https://www.ncbi.nlm.nih.gov/pubmed/26033084 >.

STARK, H. et al. Ribosome interactions of aminoacyl-tRNA and elongation factor Tu in the codon-recognition complex. **Nat Struct Biol,** v. 9, n. 11, p. 849-54, Nov 2002. ISSN 1072-8368 (Print)
1072-8368 (Linking). Available at: < https://www.ncbi.nlm.nih.gov/pubmed/12379845 >.

SUN, Y. et al. Signaling pathway of MAPK/ERK in cell proliferation, differentiation, migration, senescence and apoptosis. **J Recept Signal Transduct Res,** v. 35, n. 6, p. 600-4, 2015. ISSN 1532-4281 (Electronic)
1079-9893 (Linking). Available at: < https://www.ncbi.nlm.nih.gov/pubmed/26096166 >.

SUZUKI, T.; INOKI, K. Spatial regulation of the mTORC1 system in amino acids sensing pathway. **Acta Biochim Biophys Sin (Shanghai),** v. 43, n. 9, p. 671-9, Sep 2011. ISSN 1745-7270 (Electronic)
1672-9145 (Linking). Available at: < https://www.ncbi.nlm.nih.gov/pubmed/21785113 >.

SWITON, K. et al. Molecular neurobiology of mTOR. **Neuroscience,** v. 341, p. 112-153, Jan 26 2017. ISSN 1873-7544 (Electronic)
0306-4522 (Linking). Available at: < https://www.ncbi.nlm.nih.gov/pubmed/27889578 >.

TAKEI, N.; NAWA, H. mTOR signaling and its roles in normal and abnormal brain development. **Front Mol Neurosci,** v. 7, p. 28, 2014. ISSN 1662-5099 (Print)
1662-5099 (Linking). Available at: < https://www.ncbi.nlm.nih.gov/pubmed/24795562 >.

TAN, V. P.; MIYAMOTO, S. Nutrient-sensing mTORC1: Integration of metabolic and autophagic signals. **J Mol Cell Cardiol,** v. 95, p. 31-41, Jun 2016. ISSN 1095-8584 (Electronic)
0022-2828 (Linking). Available at: < https://www.ncbi.nlm.nih.gov/pubmed/26773603 >.

TANG, S. J.; SCHUMAN, E. M. Protein synthesis in the dendrite. **Philos Trans R Soc Lond B Biol Sci,** v. 357, n. 1420, p. 521-9, Apr 29 2002. ISSN 0962-8436 (Print)
0962-8436 (Linking). Available at: < https://www.ncbi.nlm.nih.gov/pubmed/12028789 >.

TANG, X.; JAENISCH, R.; SUR, M. The role of GABAergic signalling in neurodevelopmental disorders. **Nat Rev Neurosci,** v. 22, n. 5, p. 290-307, May 2021. ISSN 1471-0048 (Electronic)
1471-003X (Linking). Available at: < https://www.ncbi.nlm.nih.gov/pubmed/33772226 >.

TERENZIO, M. et al. Locally translated mTOR controls axonal local translation in nerve injury. **Science,** v. 359, n. 6382, p. 1416-1421, Mar 23 2018. ISSN 1095-9203 (Electronic)
0036-8075 (Linking). Available at: < https://www.ncbi.nlm.nih.gov/pubmed/29567716 >.

TREIMAN, D. M. GABAergic mechanisms in epilepsy. **Epilepsia,** v. 42 Suppl 3, p. 8-12, 2001. ISSN 0013-9580 (Print)
0013-9580 (Linking). Available at: < https://www.ncbi.nlm.nih.gov/pubmed/11520315 >.

TREMBLAY, R.; LEE, S.; RUDY, B. GABAergic Interneurons in the Neocortex: From Cellular Properties to Circuits. **Neuron,** v. 91, n. 2, p. 260-92, Jul 20 2016. ISSN 1097-4199 (Electronic)
0896-6273 (Linking). Available at: < https://www.ncbi.nlm.nih.gov/pubmed/27477017 >.

WAHL, S. E. et al. Mammalian target of rapamycin promotes oligodendrocyte differentiation, initiation and extent of CNS myelination. **J Neurosci,** v. 34, n. 13, p. 4453-65, Mar 26 2014. ISSN 1529-2401 (Electronic)
0270-6474 (Linking). Available at: < https://www.ncbi.nlm.nih.gov/pubmed/24671992 >.

WALSH, S. et al. A systematic review of the risks factors associated with the onset and natural progression of epilepsy. **Neurotoxicology,** v. 61, p. 64-77, Jul 2017. ISSN 1872-9711 (Electronic)
0161-813X (Linking). Available at: < https://www.ncbi.nlm.nih.gov/pubmed/27000515 >.

WAMSLEY, B.; FISHELL, G. Genetic and activity-dependent mechanisms underlying interneuron diversity. **Nat Rev Neurosci,** v. 18, n. 5, p. 299-309, May 2017. ISSN 1471-0048 (Electronic)
1471-003X (Linking). Available at: < https://www.ncbi.nlm.nih.gov/pubmed/28381833 >.

WANG, H. et al. An in vitro single-molecule assay for eukaryotic cap-dependent translation initiation kinetics. **Nucleic Acids Res,** v. 48, n. 1, p. e6, Jan 10 2020. ISSN 1362-4962 (Electronic)
0305-1048 (Linking). Available at: < https://www.ncbi.nlm.nih.gov/pubmed/31722415 >.

WANG, J. et al. Epilepsy-associated genes. **Seizure,** v. 44, p. 11-20, Jan 2017. ISSN 1532-2688 (Electronic)
1059-1311 (Linking). Available at: < https://www.ncbi.nlm.nih.gov/pubmed/28007376 >.

WAUDBY, C. A.; DOBSON, C. M.; CHRISTODOULOU, J. Nature and Regulation of Protein Folding on the Ribosome. **Trends Biochem Sci,** v. 44, n. 11, p. 914-926, Nov 2019. ISSN 0968-0004 (Print)
0968-0004 (Linking). Available at: < https://www.ncbi.nlm.nih.gov/pubmed/31301980 >.

WEK, R. C. Role of eIF2alpha Kinases in Translational Control and Adaptation to Cellular Stress. **Cold Spring Harb Perspect Biol,** v. 10, n. 7, Jul 2 2018. ISSN 1943-0264 (Electronic)
1943-0264 (Linking). Available at: < https://www.ncbi.nlm.nih.gov/pubmed/29440070 >.

WELLS, S. E. et al. Circularization of mRNA by eukaryotic translation initiation factors. **Mol Cell,** v. 2, n. 1, p. 135-40, Jul 1998. ISSN 1097-2765 (Print)
1097-2765 (Linking). Available at: < https://www.ncbi.nlm.nih.gov/pubmed/9702200 >.

WEN, T. H. et al. The Perineuronal 'Safety' Net? Perineuronal Net Abnormalities in Neurological Disorders. **Front Mol Neurosci,** v. 11, p. 270, 2018. ISSN 1662-5099 (Print)
1662-5099 (Linking). Available at: < https://www.ncbi.nlm.nih.gov/pubmed/30123106 >.

WHO, W. H. O. **Epilepsy: A public health imperative: summary**. Geneva: World Health Organization, 2019. 171 ISBN 978-92-4-151593-1. Available at: < https://www.who.int/publications/i/item/epilepsy-a-public-health-imperative >.

WIEBE, S. et al. Inhibitory interneurons mediate autism-associated behaviors via 4E-BP2. **Proc Natl Acad Sci U S A,** v. 116, n. 36, p. 18060-18067, Sep 3 2019. ISSN 1091-6490 (Electronic)
0027-8424 (Linking). Available at: < https://www.ncbi.nlm.nih.gov/pubmed/31427534 >.

WILCZYNSKI, G. M. et al. Important role of matrix metalloproteinase 9 in epileptogenesis. **J Cell Biol,** v. 180, n. 5, p. 1021-35, Mar 10 2008. ISSN 1540-8140 (Electronic)
0021-9525 (Linking). Available at: < https://www.ncbi.nlm.nih.gov/pubmed/18332222 >.

WIZA, C.; NASCIMENTO, E. B.; OUWENS, D. M. Role of PRAS40 in Akt and mTOR signaling in health and disease. **Am J Physiol Endocrinol Metab,** v. 302, n. 12, p. E1453-60, Jun 15 2012. ISSN 1522-1555 (Electronic)
0193-1849 (Linking). Available at: < https://www.ncbi.nlm.nih.gov/pubmed/22354785 >.

YANG, L. et al. The mTORC1 effectors S6K1 and 4E-BP play different roles in CNS axon regeneration. **Nat Commun,** v. 5, p. 5416, Nov 10 2014. ISSN 2041-1723 (Electronic)
2041-1723 (Linking). Available at: < https://www.ncbi.nlm.nih.gov/pubmed/25382660 >.

YANG, Y.; WANG, Z. IRES-mediated cap-independent translation, a path leading to hidden proteome. **J Mol Cell Biol,** v. 11, n. 10, p. 911-919, Oct 25 2019. ISSN 1759-4685 (Electronic)
1759-4685 (Linking). Available at: < https://www.ncbi.nlm.nih.gov/pubmed/31504667 >.

YING, Z.; BINGAMAN, W.; NAJM, I. M. Increased numbers of coassembled PSD-95 to NMDA-receptor subunits NR2B and NR1 in human epileptic cortical dysplasia. **Epilepsia,** v. 45, n. 4, p. 314-21, Apr 2004. ISSN 0013-9580 (Print)
0013-9580 (Linking). Available at: < https://www.ncbi.nlm.nih.gov/pubmed/15030493 >.

YU, W. et al. A clinical and pathological study in patients with sudden unexpected death in Epilepsy. **Acta Epileptologica,** v. 1, n. 1, p. 7, 2019/11/13 2019. ISSN 2524-4434. Available at: < https://doi.org/10.1186/s42494-019-0007-5 >.

ZENG, L. H. et al. Tsc2 gene inactivation causes a more severe epilepsy phenotype than Tsc1 inactivation in a mouse model of tuberous sclerosis complex. **Hum Mol Genet,** v. 20, n. 3, p. 445-54, Feb 1 2011. ISSN 1460-2083 (Electronic)
0964-6906 (Linking). Available at: < https://www.ncbi.nlm.nih.gov/pubmed/21062901 >.

ZHAO, S. et al. A brain somatic RHEB doublet mutation causes focal cortical dysplasia type II. **Exp Mol Med,** v. 51, n. 7, p. 1-11, Jul 23 2019. ISSN 2092-6413 (Electronic)
1226-3613 (Linking). Available at: < https://www.ncbi.nlm.nih.gov/pubmed/31337748 >.

ZHOU, J.; PARADA, L. F. PTEN signaling in autism spectrum disorders. **Curr Opin Neurobiol,** v. 22, n. 5, p. 873-9, Oct 2012. ISSN 1873-6882 (Electronic)
0959-4388 (Linking). Available at: < https://www.ncbi.nlm.nih.gov/pubmed/22664040 >.

ZHOU, Y.; DANBOLT, N. C. Glutamate as a neurotransmitter in the healthy brain. **J Neural Transm (Vienna),** v. 121, n. 8, p. 799-817, Aug 2014. ISSN 1435-1463 (Electronic) 0300-9564 (Linking). Available at: < https://www.ncbi.nlm.nih.gov/pubmed/24578174 >.